R006-01
C 会場 ：11/5　PM1 （13:45-15:30）
13:45〜14:00

#海老原　祐輔 [1)], 田中　高史 [2)]
([1 京大生存圏,([2 九大

Region 1 field-aligned current and energy transfer from solar wind to polar ionosphere

#Yusuke Ebihara[1)], Takashi Tanaka[2)]
([1RISH, Kyoto Univ.,([2REPPU code Institute

The ultimate source of the electromagnetic energy consumed in the ionosphere is the solar wind and interplanetary magnetic field (IMF), but the pathway of the energy transfer is not well known. According to global magnetohydrodynamics (MHD) simulation, the integral curve of the Poynting flux (S-curve) in the magnetosphere shows a spiral with its center moving toward the Earth (Ebihara and Tanaka, 2017). The spiral shape probably implies that the magnetic energy is transferred to the perpendicular direction, which may be an alternative view of the magnetospheric convection. The earthward shift of the center probably implies the transport of the magnetic energy toward the Earth along the magnetic field lines. The shape of the S-curve is reasonably understood to be the presence of the large-scale field-aligned currents, known as the Region 1 current, which twist Earth's magnetic field lines. In that sense, the magnetospheric convection and the Region 1 field-aligned current (FAC) are tied to each other. By tracing "packets" that are supposed to carry perturbations associated with FACs backward in time from the ionosphere in a reference frame of the plasma bulk flow, we identified the generation region of the Region 1 current to be the flank (low-latitude) magnetopause, in which the solar wind-originated plasma pulls Earth's magnetic field lines to excite the Alfven waves (Ebihara and Tanaka, 2022). We overview the relationship between the Region 1 FACs and the global energy transfer, and possible pathway of the energy from interplanetary space to the ionosphere as well as energy conversion processes taking place during the substorms and interplanetary shocks.

R006-02
C 会場 ：11/5　PM1 （13:45-15:30）
14:00〜14:15

#中溝　葵 [1)], 吉川　顕正 [2,3)], 中田　裕之 [4)], 深沢　圭一郎 [5)], 田中　高史 [3)]
([1]NICT,[(2] 九大・理学研究院,[(3] 九大・国際宇宙惑星環境研究センター,[(4] 千葉大・工,[(5] 京大・メディアセンター

Evolution of electrostatic potential in magnetosphere-ionospheric system as simulated by global MHD model with Alfvenic-coupling

#Aoi Nakamizo[1)], Akimasa Yoshikawa[2,3)], Hiroyuki Nakata[4)], Keiichiro Fukazawa[5)], Takashi Tanaka[3)]
([1]NICT,[(2]Fac. of Sci., Kyushu Univ.,[(3]i-SPES, Kyushu Univ.,[(4]Grad. School of Eng., Chiba Univ.,[(5]ACCMS, Kyoto Univ.

By using the Polarization Field Separation method [Nakamizo and Yoshikawa, 2019] and a global MHD model [Tanaka, 2015], we have shown that the ionosphere plays an active role in the configuration and dynamics of the global magnetosphere due to its non-uniform conductance distribution. The feedback process from the ionosphere to the magnetosphere in the current global MHD simulations can be described as follows; (1) The ionospheric conductance non-uniformity generates polarization fields, thereby deforming the ionospheric electric potential pattern. (2) The information of deformation is reflected in the magnetospheric bulk velocity updated by the potential mapped back to the magnetospheric inner boundary. (3) The updated velocity disturbances propagate the magnetosphere, modifying the force and energy balance of MHD field. (4) The FAC distribution at the next time step is calculated in the magnetosphere updated in this way and is inputted again to the ionosphere, generating the ionospheric potential of the next time step. (5) Thus, the effect of ionospheric polarization fields is accumulatively included in the development of the magnetosphere − ionosphere system.

In order to investigate precisely the role of ionosphere, we implement Alfvenic-coupling scheme proposed by Yoshikawa et al. [2010] in the MHD code. In the Alfvenic-coupling scheme, both FACs and potential are mapped between the magnetosphere and ionosphere in terms of the incident and reflection process of shear Alfven waves, therefore the continuities of physical quantities and the conservations of momentum and energy are ensured.

As an implementation test, we investigate how the reflected FACs, reflected potential, and total (M-I coupled) potential change depending on the ratio of Pedersen conductance and Alfven conductance. It is found that the total potential becomes larger and its distribution is more deformed as ratio of Pedersen conductance and Alfven conductance increases. The result is consistent with theoretical prediction [Yoshikawa & Fujii, 2018]. We also compare the total FACs, total potential, and velocity perturbations around the inner boundary obtained by the normal coupling and Alfvenic-coupling.

R006-03
C 会場 ：11/5　PM1 （13:45-15:30）
14:15〜14:30

高緯度帯での Alfvén 波を介した M-I 結合系の記述；分極、誘導効果、伝導度発展による複合効果の探査

#森澤　将 [1)], 吉川　顕正 [2,3)]
[(1] 九州大学理学府地球惑星科学科,[(2] 九州大学理学研究院地球惑星科学部門,[(3] 国際宇宙環境研究センター

M-I Coupling at High Latitude via Alfven Waves; Combined Effects through Polarization, Induction and Conductance Evolution

#MASARU MORISAWA[1)], Akimasa Yoshikawa[2,3)]
[(1]Department of Earth and Planetary Sciences, Graduate School of Science, Kyushu University,[(2]Department of Earth and Planetary Sciences, Kyushu University,[(3]International Research center for Space and Planetary Environmental Science

In this study, we evaluate the polarization, the induction effects and the time evolution of the electrical conductance in the high latitude ionosphere. There is a strong non-uniformity of electrical conductivity there, especially on the boundary of the auroral region. Because of this inhomogeneity, the polarization is very important. The polarization is a physical theory that explains the recently reviewed the Cowling effect [Yoshikawa et al. 2013a, b], which was originally reported in Glasmeier, [1983, 1984]. It was shown that the Pedersen and Hall current in the ionosphere occurs to satisfy the continuity between them, with the Pedersen current causing the acceleration of the background convection and the Hall current causing the distortion of the background convection, and the importance of the divergence of the Hall current, which has been ignored in the previous study. On the other hand, the induction effect in the incident and the reflection of Alfven waves is the following effect when a uniform electrical conductance is assumed. The Hall effect is induced by the diverging electric field carried by field aligned currents, which induces a rotational Hall current. If it changes with time, the poloidal magnetic field also changes with time, producing an induced (rotating) electric field. Due to this field, the divergent Hall current flows and closes with the field aligned currents. This consideration, however, is made under uniformity of electrical conductivity [e.g., Yoshikawa and Itonaga, 1996, 2000]. As shown above, the inductive effect can be explained by the renormalization of the multi-step Hall effect to the M-I coupling, which is essential if the divergent and rotational current system including the Hall current is to be fully described [Yoshikawa, 2002]. In addition to the polarization due to the non-uniform conductance and the induction effect on the time evolution, in this study, we also consider the time evolution of the electrical conductance. In early papers, only the effect of the precipitating electrons associated with the field aligned current is considered [e.g., Sato, 1978], but in our model, we also consider the effect of advection in the direction perpendicular to the magnetic field lines [Yoshikawa et al., 2011]. By incorporating these effects, a theory of magnetospheric-ionospheric coupling systems that takes into account ‘polarization’, ‘induction effect’ and ‘conductance evolution’ is developed, and we will develop a general discussion using this theory.

As a first step, we have performed simulations assuming a situation in which FACs are incident from the magnetosphere into a conductivity inhomogeneous region (auroral zone) in the high latitude ionosphere. In this presentation, we show the initial results.

本研究では、高緯度電離圏における分極および誘導効果、それと電気伝導度の時間発展の評価を行った。高緯度電離圏でも特にオーロラ帯の境界上では電気伝導度の強い非一様性が存在する。この非一様性ゆえに重要となるのが分極である。この効果は、電離圏を流れる電離層電流の連続性を満たすために発生する分極電場生成に由来する一連の物理効果の事である。Glaßmeier, [1983, 1984] により磁気圏電離圏結合系における重要性が初めて議論され、Yoshikawa et al., [2013a, b] により、Pedersen 電流による分極効果は背景対流の加減速を、Hall 電流による分極効果が背景対流の歪曲を引き起こすこと等が定式化された。一方、電離圏での Alfvén 波の入反射において誘導効果は以下のような考察がされた [e.g., Yoshikawa and Itonaga, 1996, 2000]。磁気圏から入射する沿磁力線電流が発散電場を運んでくるが、これによってホール効果が誘起された結果、回転性 Hall 電流が発生する。それの時間変化に伴い、ポロイダル磁場も時間変化して誘導 (回転) 性電場が生じる。この電場により流れる発散性 Hall 電流が沿磁力線電流と閉じる。ただし、この考察は電気伝導度一様性の下で行われている [e.g., Yoshikawa and Itonaga, 1996, 2000]。このように誘導効果は M-I 結合への多段階 Hall 効果の繰り込みで説明でき、ホール電流を含む発散性・回転性電流系を完全に記述するのであれば、必須の効果と言える [Yoshikawa, 2002]。以上のような電気伝導度非一様性による分極効果や時間発展に対する誘導効果に加えて本研究では、電気伝導度の時間発展も考慮している。従来電気伝導度の時間発展方程式には沿磁力線電流に伴う降り込み電子の効果のみを考慮したもの [e.g., Sato, 1978] が多いが、本研究ではさらに、磁力線に垂直方向の移流の効果 [Yoshikawa et al., 2011] も考慮した。これらを取り入れることで、「分極」、「誘導効果」、「伝導度発展」を考慮した磁気圏電離圏結合系の理論構築を図り、それを用いた一般的な議論を展開する。

その第一歩として、高緯度電離圏の電気伝導度非一様領域に磁気圏から FAC を入射させた状況を想定して数値計算を行った。本発表では、その初期結果を示す。

R006-04
C 会場 ：11/5　PM1 （13:45-15:30）
14:30〜14:45

2017 年 9 月 8 日の磁気嵐中のサブストーム開始時のオーロラのあらせ衛星による観測

#Chen　Liwei[1)], 塩川　和夫 [2)], 三好　由純 [3)], 大山　伸一郎 [3)], 田　采祐 [4)], 小川　泰信 [5)], 細川　敬祐 [6)], 風間　洋一 [7)],Wang　S.-Y.[8)],Tam　S. W. Y.[9)],Chang　T. F.[9)],Wang　B.-J.[10)], 浅村　和史 [11)], 笠原　慧 [12)], 横田　勝一郎 [13)], 堀　智昭 [3)], 桂華　邦裕 [14)], 笠羽　康正 [15)], 熊本　篤志 [16)], 土屋　史紀 [16)], 小路　真史 [3)], 笠原　禎也 [17)], 松岡　彩子 [18)], 篠原　育 [19)], 今城　峻 [20)]
[1 宇地研,[2 名大宇地研,[3 名大 ISEE,[4 名大 ISEE 研,[5 極地研,[6 電通大,[7 中央研究院天文・宇宙物理学研究所,[8 台湾・中央研究院,[9 台湾・國立成功大学,[10ASIAA, Taiwan,[11 宇宙研,[12 東京大学,[13 大阪大,[14 東大・理,[15 東北大・理,[16 東北大・理・惑星プラズマ大気,[17 金沢大,[18 京都大学,[19 宇宙研／宇宙機構,[20 京大・地磁気センター

Observation of a substorm onset poleward expansion aurora by the Arase satellite during the geomagnetic storm of September 8, 2017

#Liwei Chen[1)], Kazuo Shiokawa[2)], Yoshizumi Miyoshi[3)], Shin ichiro Oyama[3)], ChaeWoo Jun[4)], Yasunobu Ogawa[5)], Keisuke Hosokawa[6)], Yoichi Kazama[7)], S.-Y. Wang[8)], S. W. Y. Tam[9)], T. F. Chang[9)], B.-J. Wang[10)], Kazushi Asamura[11)], Satoshi Kasahara[12)], Shoichiro Yokota[13)], Tomoaki Hori[3)], Kunihiro Keika[14)], Yasumasa Kasaba[15)], Atsushi Kumamoto[16)], Fuminori Tsuchiya[16)], Masafumi Shoji[3)], Yoshiya Kasahara[17)], Ayako Matsuoka[18)], Iku Shinohara[19)], Shun Imajo[20)]
[1ISEE,[2ISEE, Nagoya Univ.,[3ISEE, Nagoya Univ.,[4ISEE, Nagoya Univ.,[5NIPR,[6UEC,[7Institute of Astronomy and Astrophysics, Academia Sinica, Taiwan,[8ASIAA, Taiwan,[9PSSC, NCKU, Taiwan,[10ASIAA, Taiwan,[11ISAS/JAXA,[12The University of Tokyo,[13Osaka Univ.,[14University of Tokyo,[15Tohoku Univ.,[16Planet. Plasma Atmos. Res. Cent., Tohoku Univ.,[17Kanazawa Univ.,[18Kyoto University,[19ISAS/JAXA,[20WDC for Geomagnetism, Kyoto, Kyoto University

Since the plasma and electromagnetic conditions can be very different with quiet time during geomagnetic storm, there will be differences between substorms that occur during geomagnetic quiet time and storm time. In this presentation, we show a unique auroral substorm study during a geomagnetic storm using a ground-based all-sky camera and the Arase satellite at L~6. The auroral arcs of interest were observed on September 8, 2017, at Tromsoe, Norway (69.6N, 19.2E, in geographic coordinate; 66.7N in geomagnetic coordinate). The ground-based electron-multiplying charge-coupled device (EMCCD) camera observed that the substorm auroral arcs in the south edge of FOV that started poleward expansion at ~2040 UT, while the footprint of the Arase satellite was moving southeastward and crossed the brightening arc at the southwestern edge of FOV at ~2043 UT. The Dst index indicates that this substorm occurred during the recovery phase of a geomagnetic storm with a minimum Dst of -122 nT at 0200 UT on September 8. The ion and electron omnidirectional energy spectra from the Arase measurements show clear signatures of plasma sheet stretch (satellite got into the lobe) and subsequent ion and electron flux enhancements at the timing of the footprint crossing of the poleward expanding aurora. A series of field-aligned Poynting flux enhancements were found to appear simultaneously with the plasma sheet flux enhancement. The electric field also significantly deviated from the quiet level in the lobe. We will discuss these results with previous conjugate observations of substorm auroral brightening during a geomagnetically quiet time that occurred at L~6.

R006-05
C 会場 ：11/5　PM1 （13:45-15:30）
14:45〜15:00

#中村　るみ [1)], ホスナー　マーティン [1)]
[(1] オーストリア宇宙研

Current sheet thinning associated with the dipolarization front

#Rumi Nakamura[1)], Martin Hosner[1)]
[(1]IWF/OEAW

We discuss on the transient deformation of the ambient current sheet associated with the dipolarization front. Recent multi-scale multipoint measurements by MMS and Cluster in the near Earth magnetotail during a unique conjugate observation of localized fast flows (Nakamura et al., 2021) showed that combination of the two multi-point missions enabled to determine the change in the overall flow and the current sheet changes while monitoring the detailed structure of the thin current sheet. It is shown that dipolarization front of a localized flow can lead to an additional thinning of the current sheet behind the front. Intense perpendicular and parallel currents in the off-equatorial region was detected mainly during this interval of the current sheet thinning. Another conjugate observations of the dipolarization front showed a strong magnetic shear region developed locally at dusk-side of the front. This region has been identified as an electron diffusion region of an X-line based on the non-magnetized signature of the electron distribution function (Marshall et al. 2020) and the geometry of the current sheet (Hosner et al., 2022). These observations indicate that the near-Earth flow braking processes accompany also complex localized current sheet restructuring. We also discuss potential mechanism how these transient thin current sheet can be created in the near-Earth magnetotail and the role of these current sheets in the energy conversion processes in the magnetotail.

Reference
Hosner, M., et al. (2022) Fall AGU Meeting
Marshal A. et al. (2020) J. Geophys. Res., doi:10.1029/2019JA027296
Nakamura, R. et al.(2021) J. Geophys. Res., doi:10.1029/2021JA029518

R006-06
C 会場 ：11/5　PM1 （13:45-15:30）
15:00〜15:15

MMS 衛星の観測による地球バウショックでの電子加速における高周波ホイッスラー波強度の重要性

#増田　未希 [1)], 天野　孝伸 [2)], 岡　光夫 [3)], 北村　成寿 [4)]
([1] 東京大学　地球惑星科学専攻,[2] 東大・理,[3] カリフォルニア大学バークレー校・宇宙科学,[4] 名大・宇地研

MMS observation of importance of high-frequency whistler waves intensity for electron acceleration at Earth's bow shock

#Miki Masuda[1)], Takanobu Amano[2)], Mitsuo Oka[3)], Naritoshi Kitamura[4)]
([1]Department of Earth and Planetary Science, Univers,[2]University of Tokyo,[3]SSL, UC Berkeley,[4]ISEE, Nagoya University,

Non-thermal high-energy particles are frequently observed in space, and collisionless shock waves are one of the sources of these particles. Particle acceleration in the vicinity of shock waves has been observed, but the specific process has not been understood clearly. Although shock drift acceleration is candidate mechanism for the acceleration process, some problems remain yet. For example, in these mechanism, low-energy electrons cannot be accelerated or accelerated electrons' energy is not sufficient. To solve these problems, Katou & Amano (2019) proposed stochastic shock drift acceleration. In this mechanism, low-energy electrons are trapped in the transition layer by cyclotron resonant scattering with high-frequency waves. The most promising candidate for the scattering agent is whistler waves with frequencies ranging from 10% to 50% of the electron cyclotron frequency. On the other hand, Oka et al. (2006) showed statistically that the electron acceleration occurs efficiently only when the shock is super-critical with respect to the whistler critical Mach number. This result suggested that the whistler waves play important roles to accelerate electrons in the layer, but the specific mechanism has yet been not understood. Katou & Amano (2019) and Amano et al. (2020) predicted that the electron acceleration occurs only when the intensity of the whistler waves exceeds a certain theoretical threshold, which comes from the condition that electrons need to be trapped sufficiently in the layer. The theoretical threshold is proportional to $(M_A \cos\theta_{Bn})^{-2}$ and may be consistent with Oka et al. (2006) in the statistical sense. However, since the intensity of the whistler waves may vary in each event, more detailed analysis is needed.

In this study, we use the data of the Earth's bow shock crossing events observed by the Magnetospheric Multiscale (MMS) spacecraft in the burst mode. We investigate statistically the relation between the intensity of whistler waves and some shock parameters (M_A, θ_{Bn}, β_e), as well as efficiency of electron acceleration. We select events where the upstream and the downstream are stable during 2017 to 2018 performed a detailed analysis of the transition layer where the electron acceleration occurs efficiently. We define the time when the magnetic field strength increased by a factor of more than 1.2 relative to the upstream magnetic field as the transition layer. First, by using Search Coil Magnetometers (SCM), we calculated the power spectrum of magnetic fluctuations with a time resolution 1s. We determine the wave intensity for each frequency normalized by the electron cyclotron frequency and correlate with each shock parameter. As the result, we find the positive correlation between the intensity of the high-frequency whistler wave and $M_A/M_{crit}{}^{w}$. Furthermore, we investigate the relation between the shock parameters and the energy density of high-energy electron in the downstream normalized to the flow kinetic energy of the upstream plasma, or the electron pressure in the downstream for each event. Based on these results, we discuss the relation between the electron acceleration efficiency and the property of whistler waves.

宇宙空間にはベキ型のスペクトルを持つ非熱的な高エネルギー荷電粒子が存在し、無衝突衝撃波はこれらの粒子の生成源として考えられている。実際に衝撃波近傍での粒子加速は観測されているが、その具体的な過程は明らかになっていない。これまで加速過程の候補として一次フェルミ加速や衝撃波ドリフト加速などが挙げられているが、低エネルギー電子の加速ができないことや、十分な加速ができないという課題が残っている。この課題に対して、低エネルギー電子の加速メカニズムの候補として統計的衝撃波ドリフト加速が提唱された（Katou & Amano, 2019）。このメカニズムでは電子と高周波の波動とのサイクロトロン共鳴散乱により電子を遷移層内に捕獲することで低エネルギー電子の十分な加速が可能であると考える。そしてこの散乱体の有力候補と考えられているものが電子のサイクロトロン周波数の 10% から 50% 程度の周波数を持つ高周波ホイッスラー波である。一方で、Oka et al. (2006) では観測のデータを元に衝撃波アルフベンマッハ数 (M_A) がホイッスラー臨界マッハ数 ($M_{crit}{}^{w}$) に比べて超臨界の時にのみ電子加速が効率的になるということを統計的に明らかにした。この結果からホイッスラー波が電子加速に重要な役割を担っていることが示唆されるが、その具体的なメカニズムは明らかになっていない。Katou & Amano (2019) や Amano et al. (2020) は遷移層内に電子が十分に加速されるという条件からホイッスラー波の強度についての閾値を導き、それよりも大きい時にのみ電子加速が起こることを予言した。衝撃波面の法線方向と上流の磁場のなす角を θ_{Bn} とするとこの閾値は $(M_A / \cos\theta_{Bn})^{-2}$ に比例するため、定性的には Oka et al. (2006) と整合的であるが、ホイッスラー波の強度はイベントごとに異なるため、各イベントに対しての調査が必要である。

本研究では Magnetospheric Multiscale (MMS) 衛星による地球バウショックの burst mode 観測のデータを用いる。各イベントごとのホイッスラー波強度とマッハ数や θ_{Bn}、電子ベータなどの衝撃波パラメータ、エネルギー密度の関係を

統計的に調べ、電子加速とホイッスラー波強度の関係を調べた。イベントは 2017 年から 2018 年の観測のうち衝撃波上流と下流が安定しているものを用い、電子加速が効率的に働いている遷移層の範囲を詳細に解析した。このとき、上流の磁場に対し磁場強度が 1.2 倍以上に増加している時間帯を遷移層と定義した。まず、Search Coil Magnetometers(SCM) のデータを用い、1s 間隔の磁場のパワースペクトルの平均を計算し、サイクロトロン周波数で規格化した周波数ごとに波動強度を求め、衝撃波の各パラメータとの相関を調べた。その結果、特に高周波ホイッスラー波強度と $\mathrm{M}_A/\mathrm{M}_{crit}{}^w$ に正の相関を得ることができた。さらに、各イベントに対し下流の高エネルギー電子のエネルギー密度と衝撃波上流の運動エネルギーや下流圧力の比をとることで衝撃波エネルギーから高エネルギー電子へのエネルギー分配率を算出し、加速が効率的になる場合の条件を調べる。以上の結果を元に、地球バウショックにおける電子加速とホイッスラー波との関係性を議論する。

R006-07
C 会場 ：11/5　PM1 （13:45-15:30）
15:15〜15:30

#北村　成寿 [1)], 天野　孝伸 [2)], 大村　善治 [3)],Boardsen　Scott[4,5)], 北原　理弘 [7)], 三好　由純 [1)], 中村　紗都子 [6)], 小路　真史 [1)], 加藤　雄人 [7)], 小嶋　浩嗣 [8)],Lee　Sun-Hee[9)],Gershman　Daniel J.[4)], 齋藤　義文 [10)], 平原　聖文 [11)], 横田　勝一郎 [12)],Giles　Barbara L.[4)],Paterson　William R.[4)],Pollock　Craig J.[13)],Le Contel　Olivier[14)],Russell　Christopher[15)],Strangeway　Robert J.[16)],Lindqvist　Per-Arne[17)],Ergun　Robert E.[18)],Burch　James L.[19)]
([1 名大・宇地研,([2 東大・理,([3 京大・生存圏,([4NASA/GSFC,([5 メリーランド大学ボルチモア郡校 惑星太陽圏研,([6 名大・IAR&ISEE,([7 東北大・理・地球物理,([8 京大・生存圏,([9 カトリック大学アメリカ・物理天体,([10 宇宙研,([11 名大・宇地研,([12 大阪大,([13Denali Scientific,([14CNRS・プラズマ物理学研究ユニット,([15UCLA・EPSS,([16UCLA・EPSS,([17 スウェーデン王立工科大学,([18 コロラド大学ボルダー校・LASP,([19Southwest Research Institute

Observational evidence of nonlinear growth of whistler-mode waves around quasi-perpendicular bow shocks

#Naritoshi Kitamura[1)], Takanobu Amano[2)], Yoshiharu Omura[3)], Scott Boardsen[4,5)], Masahiro Kitahara[7)], Yoshizumi Miyoshi[1)], Satoko Nakamura[6)], Masafumi Shoji[1)], Yuto Katoh[7)], Hirotsugu Kojima[8)], Sun-Hee Lee[9)], Daniel J. Gershman[4)], Yoshifumi Saito[10)], Masafumi Hirahara[11)], Shoichiro Yokota[12)], Barbara L. Giles[4)], William R. Paterson[4)], Craig J. Pollock[13)], Olivier Le Contel[14)], Christopher Russell[15)], Robert J. Strangeway[16)], Per-Arne Lindqvist[17)], Robert E. Ergun[18)], James L. Burch[19)]
([1ISEE, Nagoya Univ.,([2University of Tokyo,([3RISH, Kyoto Univ.,([4NASA/GSFC,([5Goddard Planet. Heliophys. Inst., Univ. of Maryland in Baltimore,([6IAR&ISEE, Nagoya University,([7Dept. Geophys., Grad. Sch. Sci., Tohoku Univ.,([8RISH, Kyoto Univ.,([9Inst. of Astrophys. and Computational Sci., Catholic Univ. of America,([10ISAS,([11ISEE, Nagoya Univ.,([12Osaka Univ.,([13Denali Scientific,([14LPP, CNRS,([15EPSS, UCLA,([16EPSS, UCLA,([17Royal Institute of Technology, Sweden,([18LASP, Univ. of Colorado, Boulder,([19Southwest Research Institute

In this presentation, we show observational results of nongyrotropic electrons close to the cyclotron resonance velocity, which is a key feature of nonlinear growth of whistler-mode waves, using data obtained by the Magnetospheric Multiscale (MMS) spacecraft around quasi-perpendicular bow shocks. Interaction between the electromagnetic field and charged particles is central for the collisionless plasma dynamics in space. Whistler-mode waves are one of the electromagnetic plasma waves, which play important roles in efficient pitch-angle scattering and acceleration of electrons in solar wind, collisionless shock waves as well as planetary magnetospheres. The nonlinear wave-particle interaction theory for coherent large amplitude waves predicts that resonant electrons exhibit nongyrotropy due to phase trapping motion around resonance velocities in the presence of an appropriate inhomogeneity. The nongyrotropic electrons exchange energy and momentum with waves efficiently. While the nonlinear wave growth has been discussed mainly for wave growth in the magnetosphere, it has rarely been discussed for whistler-mode waves in other regions. Here we show examples of nongyrotropic electrons close to the cyclotron resonance velocity during whistler-mode wave events around three quasi-perpendicular bow shock crossings as the observational evidence of nonlinear wave growth. Using measurements by the Fast Plasma Investigation Dual Electron Spectrometer (FPI-DES) and the search-coil magnetometer (SCM), we identified electron flux hole events that induce wave growth; a hole at an appropriate relative phase angle to the whistler-mode wave magnetic field appeared only close to the cyclotron resonance velocity. The magnitudes of the gradient of the magnetic field intensity along the magnetic field line during such time intervals are consistent with an appropriate magnitude to cause phase trapping of resonant electrons. This result provides strong evidence of nonlinear growth of whistler-mode waves around quasi-perpendicular bow shocks. The nonlinear wave growth of whistler-mode waves due to phase trapping, which has been discussed mainly for wave growth in the magnetosphere, probably plays a role in broader applications in space if the appropriate condition is satisfied.

R006-08
C 会場 ：11/5　PM2 （15:45-18:15）
16:00〜16:15

#田口　聡 [1)], 長房　勇之介 [1)], 大井川　智一 [1)], 小川　泰信 [2)], 細川　敬祐 [3)], 品川　裕之 [4)]
([1] 京大理,[2] 極地研,[3] 電通大,[4] 情報通信研究機構

Smooth expansion of cusp aurora and expansion accompanied with mesoscale auroral detachment during plasma flow burst

#Satoshi Taguchi[1)], Yunosuke Nagafusa[1)], Tomokazu Oigawa[1)], Yasunobu Ogawa[2)], Keisuke Hosokawa[3)], Hiroyuki Shinagawa[4)]
([1]Grad school of Science, Kyoto Univ.,[2]NIPR,[3]UEC,[4]NICT,

Previous studies have shown that a moving mesoscale cusp aurora, which is separated by regions devoid of aurora, is accompanied by fast plasma flow nearby. The purpose of this study is to determine if a moving mesoscale cusp aurora actually appears whenever very fast plasma flow occurs. First, we identified approximately 77 hours from five winter seasons as the period of the simultaneous observation of the dayside 630-nm aurora from an all-sky imager at Svalbard and the EISCAT Svalbard Radar (ESR) at 76 MLAT. Using ESR data from that period, we examined the ion temperatures, which reflect plasma flow burst, and confirmed that the ion temperatures in the F-region above 2000 K at 76 MLAT in daytime sector represent very fast plasma flow in the cusp. A detailed analysis of a representative case of such high ion temperatures observed repeatedly on December 8, 2016 revealed that the smooth poleward expansion of the main cusp emission is a clear phenomenon that occurs simultaneously with the plasma flow burst. This indicates that the formation of a moving mesoscale cusp aurora is not directly related to whether the plasma flow is fast or not in the cusp. The analysis also showed that expansion accompanied with mesoscale auroral detachment tends to occur with the motion of auroras with relatively large longitudinal speed. We also found from two-dimensional local simulation that the F-region ion temperatures tend to increase more on the poleward side of the main cusp emission than within it although the ion temperatures generally reflect the plasma flow well.

R006-09
C 会場 ：11/5　PM2 （15:45-18:15）
16:15〜16:30

#八島　和輝 [1)], 田口　聡 [1)], 細川　敬祐 [2)]
([1] 京大理,[2] 電通大

Characteristics of temporal evolution of the 2-D distribution of soft electron precipitation near the nightside polar cap boundary

#Kazuki Yashima[1)], Satoshi Taguchi[1)], Keisuke Hosokawa[2)]
([1]Grad school of Science, Kyoto Univ.,[2]UEC

Strong low-energy electron precipitation often occurs near the polar cap boundary on the night side. This is believed to be related to Alfvenic electron acceleration, which is also known to produce tall red auroras. Satellite observations have revealed the detailed energy distribution of that low-energy electron precipitation and its spatial characteristics. However, how the low-energy component of the electron precipitation grows and decays near the nightside polar cap boundary is still unknown. To understand the temporal characteristics of the low-energy electron flux near the nightside polar cap boundary, we devised an automated method to determine the 2-D distributions of low-energy electron flux by comparing 630-nm auroral image data from an all-sky imager (located at Longyearbyen, Svalbard) with 630-nm emission distributions calculated by the Global Airglow model. We also validated the usefulness of this automated method based on simultaneous observations by the DMSP satellite and the all-sky imager. We have applied this method to a number of 630-nm auroral image data obtained near the polar cap boundary on the night side. We report on the characteristics of the temporal evolution of the horizontal 2-D distribution of low-energy electron flux, especially focusing on the speed at which high flux areas move, and discuss how these characteristics are produced.

R006-10
C 会場 ：11/5　PM2 （15:45-18:15）
16:30〜16:45

#橋本　翼 [1)], 吉川　顕正 [2)], 田中　高史 [3)]
([1] 九大・理・地惑,([2] 九大/理学研究院,([3] 九大・国際宇宙天気科学教育センター

How is stacked northward IMF removed from the dayside magnetosheath region due to the southward IMF reversal?

#Tsubasa Hashimoto[1)], Akimasa Yoshikawa[2)], Takashi Tanaka[3)]
([1]Earth and Planetary Sciences,Kyushu Univ.,([2]Kyushu Univ.,([3]REPPU code Institute

When the IMF is northward, the reconnection occurs where the antiparallel magnetic field line structure between northward IMF and lobe magnetic field lines at high latitudes poleward of the Earth's magnetospheric cusp, but in the dayside magnetopause, these field lines are stacked. According to previous model and observation, when the southward IMF reaches the stacked northward IMF region, the disruption of this region starts via the reconnection between northward and southward IMF. We reproduced IMF's reconnection to use the Reproduce Plasma Universe (REPPU) code (Tanaka, 2015). As the results, starting point of IMF's reconnection is the bow shock and reconnection point moves the dayside magnetopause gradually. Then, the reconnection between southward IMF and closed magnetic field line starts after stacked northward IMF disrupted completely. Varying solar wind speed, density and magnetic field strength of southward IMF also resulted in different time to completely disrupt this stacked northward IMF. In this presentation, we discuss which of some factors contribute to disruption time by reproducing the change in Vy, Vz, Lorentz force, and so on.

IMF が北向きのとき、高緯度カスプ領域で北向き IMF とローブ磁力線がリコネクションを起こすが、昼側の magnetopause では、北向き IMF が積み重なっている状態である。観測やモデルの先行研究では、積み重なった北向き IMF の領域に南向き IMF が到達すると、IMF 同士のリコネクションによりその領域は破壊されると示唆された。そこで我々は、IMF 同士のリコネクションを REPPU コードを用いて再現した。すると、IMF 同士のリコネクションは bow shock 付近から始まり、リコネクションポイントは magnetopause の方へ移動していった。積み重なった北向き IMF が完全になくなったのち、magnetopause で南向き IMF と地球の closed 磁力線のリコネクションが始まる。また、南向き IMF における Vsw や Bz を変化させると、この stacked northward IMF を完全に破壊するまでの時間が異なることが分かった。本発表では、この時間を変動させうる要因としてどのようなものがあるのか、Vy や Vz や J × B などを可視化することで議論する。

R006-11
C 会場 ：11/5　PM2 （15:45-18:15）
16:45〜17:00

#小池　春人 [1)], 田口　聡 [1)]
([1] 京大理

Outflow jets from lobe reconnection and their relationship to shear flow

#Haruto Koike[1)], Satoshi Taguchi[1)]
([1]Grad school of Science, Kyoto Univ.

One of the key parameters of magnetic reconnection is shear flow which is parallel to the reconnecting field. Several simulation studies have suggested that shear flow can reduce the reconnection rate and the outflow jet speed. On the other hand, another simulation indicates that the reconnection rate is not necessarily affected by the increase in shear flow. Further studies need to be done from observations to understand the role of shear flow in reconnection deeply. In reconnection at the high-latitude magnetopause during northward IMF, the magnetosheath flow in the tailward direction acts as shear flow. In this study, we took the lobe reconnection events from the observation by the Cluster satellites, and examined the relationships of the ion outflow jet to the magnetosheath tailward flow. In order to evaluate the role of shear flow quantitatively, we determined the velocity of shear flow and outflow jet, using data from the ion velocity distribution function. The result from the analysis has shown that there is a tendency for the ion outflow jet to increase as the speed of the magnetosheath flow tangential to the magnetopause current sheet increases. This indicates that ions are more greatly accelerated through the lobe reconnection as shear flow streams faster. This tendency seems to be inconsistent with the result of the previous simulation studies. We will discuss this discrepancy in terms of additional acceleration by the Hall electric field in the ion diffusion region.

R006-12
C 会場 ：11/5　PM2 （15:45-18:15）
17:00〜17:15

#浅村　和史 [1)], 三好　由純 [2)], 細川　敬祐 [3)], 滑川　拓 [4)], 三谷　烈史 [1)], 坂野井　健 [5)], 川村　美季 [6)], 能勢　正仁 [7)], 野村　麗子 [8)], 寺本　万里子 [9)]
([1] 宇宙研,[2] 名大 ISEE,[3] 電通大,[4] 東大・理・地惑,[5] 東北大・理・PPARC,[6] 東北大学,[7] 名大・宇地研,[8]JAXA,[9] 九工大

The LAMP sounding rocket mission; in-situ observations of microburst electron precipitations associated with pulsating aurorae

#Kazushi Asamura[1)], Yoshizumi Miyoshi[2)], Keisuke Hosokawa[3)], Taku Namekawa[4)], Takefumi Mitani[1)], Takeshi Sakanoi[5)], Miki Kawamura[6)], Masahito Nose[7)], Reiko Nomura[8)], Mariko Teramoto[9)]
([1]ISAS/JAXA,[2]ISEE, Nagoya Univ.,[3]UEC,[4]Earth and Planetary Science, Tokyo Univ.,[5]PPARC, Grad. School of Science, Tohoku Univ.,[6]TU,[7]ISEE, Nagoya Univ.,[8]JAXA,[9]Kyutech

On March 5th, 2022, NASA's LAMP (Loss through Auroral Microburst Pulsations) sounding rocket was launched from Poker Flat Research Range (PFRR), Alaska, USA. One of the scientific objectives of LAMP is to reveal a relationship between the microburst of relativistic energy electrons precipitating into the ionosphere and modulations of optical auroral emissions in the pulsating aurora. We, Japanese team, provided the PARM2 (Pulsating AuroRa and Microburst 2) instrument suite for LAMP as onboard scientific hardware. PARM2 consists of four instruments; HEP (SSD based high-energy electron detector), MIM (a magnetometer using the magneto-impedance effect), and AIC1/AIC2 (two auroral imaging cameras installed on a despun table which cancels spinning motion of the rocket). We also provided ground-based supporting observations at three sites; Venetie, Fort Yukon, and PFRR, which contained several high-speed auroral imaging systems including operations at the site. By using these ground-based supporting observations, LAMP successfully hit the pulsating auroral patches. And then, HEP detected the microburst electron precipitations in 100 keV range in conjunction with intensification of auroral emissions at geomagnetic footprint. AIC captured pulsating auroral patches with sub-second modulations. And MIM detected magnetic field fluctuations which might be due to auroral current system. In this presentation, we will report on an overview of the LAMP mission and its observations.

R006-13
C 会場 ：11/5　PM2 （15:45-18:15）
17:15〜17:30

LAMP ロケット搭載多波長オーロラカメラ AIC2 による脈動オーロラの観測

#坂野井　健 [1)], 浅村　和史 [2)], 三好　由純 [3)], 細川　敬祐 [4)], 滑川　拓 [2)], 三谷　烈史 [2)], 能勢　正仁 [3)], 野村　麗子 [5)], 寺本　万里子 [6)],Lessard　Marc[7)],Halford　Alexa[8)]
([1] 東北大学・理・PPARC,[(2]JAXA 宇宙研,[(3] 名古屋大学 ISEE,[(4] 電気通信大学,[(5]JAXA 国際宇宙探査センター,[(6] 九州工業大学,[(7] ニューハンプシャー大学,[(8]NASA ゴダード宇宙飛行センター

Observation of pulsating auroras with a multi-spectral auroral camera AIC2 on the LAMP rocket

#Takeshi Sakanoi[1)], Kazushi Asamura[2)], Yoshizumi Miyoshi[3)], Keisuke Hosokawa[4)], Taku Namekawa[2)], Takefumi Mitani[2)], Masahito Nose[3)], Reiko Nomura[5)], Mariko Teramoto[6)], Marc Lessard[7)], Alexa Halford[8)]
([1]PPARC, Grad. School of Science, Tohoku Univ.,[(2]ISAS/JAXA,[(3]ISEE, Nagoya Univ.,[(4]The University of Electro-Communications,[(5]JAXA Space Exploration Center,[(6]Kyushu Institute of Technology,[(7]University of New Hampshire,[(8]NASA/GSFC

We report the results of a multi-spectral auroral camera AIC2 installed on the LAMP rocket which was successfully launched from Poker Flat at 11:27:30 UT on March 5, 2022. We also give the results on coordinated observation between AIC2 and other instruments on the rocket and ground-based all-sky imagers. The purpose of the LAMP rocket mission is to clarify the relationship between pulsating aurora (PsA) and microbursts with simultaneous particle, magnetic field, and and imaging measurements. AIC2 is one of the Japanese PARM2 instrument package. AIC2 measures two auroral emissions mainly in the E-region at 670 nm (N2 1PG) and in the F-region at 844.6 nm (OI) using 2 CMOS cameras called AIC-S1 and AIC-S2. AIC2 is characterized by a low noise (1.6 e-RMS) and wide dynamic range sampling capability (16-bit ADC) using the consumer CMOS sensors. Two cameras take images simultaneously with a time resolution of ˜10 frame/s. AIC-S1 is pointed to the magnetic footprint with a FOV of 29 deg x 29 deg which covered 180 km x 180 km with a resolution of 3 km x 3 km at the apex altitude (˜430 km altitude). FOV of AIC-S2 is 106 deg diameter circle which covered the wide range from the nadir to the limb of the Earth. AIC2 is mounted on the despun table to cancel the rocket spin and obtain stable line-of-sight directions of FOVs. The dynamic ranges of AIC-S1 and S2 are 1.1 - 860 kR, and 0.4 - 5800 kR, respectively. Two set of NanoPi M4V2 board computer and FPGA are used to handle a large amount of image data generated in two cameras. Total weight and power of AIC2 are 3.0 kg and 20 W, respectively.

At ˜10:30 UT on March 5, 2022, a typical auroral break up with a negative excursion of geomagnetic east-west component of ˜500 nT (Kp=4-) happened at Poker Flat, and afterward significant pulsating auroral patches with several Hz internal modulations appeared in the northward sky of Pokar Flat. The LAMP rocket was successfully launched into and flew over the pulsating auroral patches. AIC2 worked satisfactorily as expected throughout the flight. For the flight time after the launch from ˜90 s to the end of flight (˜620 s), the despun table worked correctly and small-scale auroral images were continuously obtained by AIC2 above the auroral emission layer for the first time. On the other hand, AIC-S1 and S2 observed the in-situ auroral intensities when the rocket was in the emission layers in E- and F-region, respectively. The auroral image data taken by AIC2 were analyzed as follows: 1) subtraction of background count using a dark frame, 2) field flattering applying the image data of integrating sphere obtained at ground testing, 3) unit conversion from count to Rayleigh using calibration data obtained at ground testing. From AIC-S1 data, we found significant pulsating auroral patches with sub-second modulations during the period of flight time of ˜160-200 s, ˜450-500s, and black arcs at 600s. From AIC-S2 data, we identified the limb and large-scale 844.6 nm auroral emission in the equatorward of auroral oval. Other PARM instruments and ground-based high-speed imagers at Poker Flat, Venetie, and Fort Yukon succeeded to observe during the flight. We compared auroral images taken by AIC2 with high-energy electrons (>100keV), low-energy electrons (several to 10 keV) and ground auroral images and found that they showed good correspondence on the main pulsating aurora (˜5s) and even on the sub-second variations which is probably microbursts.

R006-14
C 会場 ：11/5　PM2 （15:45-18:15）
17:30〜17:45

ホイッスラー波動強度が脈動オーロラ発光強度に与える影響

#高橋　一輝[1)], 齊藤　慎司[2)], 三好　由純[3)], 浅村　和史[4)], 細川　敬祐[5)]
([1 名古屋大学宇宙地球環境研究所,([2 情報通信研究機構,([3 名大 ISEE,([4 宇宙研,([5 電通大

Wave amplitude dependence of the pulsating aurora emissions

#Kazuteru Takahashi[1)], Shinji Saito[2)], Yoshizumi Miyoshi[3)], Kazushi Asamura[4)], Keisuke Hosokawa[5)]
([1ISEE, Nagoya University,([2NICT,([3ISEE, Nagoya Univ.,([4ISAS/JAXA,([5UEC

The Pulsating aurora is a type of diffuse aurora, and pulsation periods are several seconds - several tens of seconds. The amplitudes of the optical emissions should be proportional to the downward energy flux inside the loss cone, so it is natural to consider that that optical emission increases when the wave amplitudes increase if we consider the quasi-liner process. Recent observations indicated that the non-linear wave-particle interactions are essential to cause the pulsating aurora, and it is expected that the relationship between the optical emissions and wave amplitude is not simple as expected from the quasi-linear theory. For example, the phase-trapping effect may suppress the precipitation flux if the wave amplitudes increase. In order to investigate how the precipitation flux changes with the wave amplitudes, we conduct a test-particle simulation about chorus wave-particle interactions using GEMSIS-RBW (Saito+, 2012). Besides non-linear wave-particle interaction processes, stochastic differential equations that is equivalent to the Fokker-Planck equation are included to realize stable precipitations as like the quasi-linear process. Using the simulated precipitating electron flux from the test-particle simulation, we calculate the optical emissions at different wavelength at the ionospheric altitudes. From the simulations, we found that both the intermittent precipitations by chorus wave particle interactions and steady precipitations by quasi-linear process are suppressed when chorus amplitude increases, which are not expected from the quasi-linear process.

R006-15
C 会場 ：11/5　PM2 （15:45-18:15）
17:45〜18:00

AI とジンバルを用いたアクティブなオーロラ観測システムの開発と運用

#南條　壮汰 [1)],Braendstroem Urban[2)], 津田　卓雄 [1)], 青木　猛 [1)], 細川　敬祐 [1)]
([1] 電通大,[2] スウェーデン王立宇宙科学研究所

Development and operation of an active aurora observation system using AI and gimbal

#Sota Nanjo[1)], Urban Braendstroem[2)], Takuo Tsuda[1)], Takeshi Aoki[1)], Keisuke Hosokawa[1)]
([1]UEC,[2]Swedish Institute of Space Physics（IRF)

Intense auroras are observed over a wide area in the polar regions when a magnetic storm occurs. During such occasions, many images and videos of the auroras captured by digital cameras and smartphones are uploaded to social networking services. Most of these images and videos are captured by wide-angle lenses with an angle of view (AoV) of 70 – 80 degrees. In contrast, most scientific auroral observations often employ fisheye lenses with an AoV of 180 degrees. The all-sky observation has the advantage of recording all the auroras seen from the observatory. However, since the entire sky is imaged with a limited sensor size, the spatial resolution is not as good as the observation by a digital camera. In addition, images and videos from digital cameras and smartphones are recorded with three RGB channels, whereas most scientific optical observations are monochromatic. Since the bandwidth of the RGB channels is wide (FWHM ˜100 nm), digital cameras and smartphones are not proper multi-wavelength optical instruments. However, Nanjo et al. (2021) suggest that the ratio of the B and G channels can be used to estimate the average energy of pulsating aurora electrons, which is a significant advantage of digital camera observations. Thus, it is important to use images and videos by digital cameras and smartphones for scientific research. However, it is still unclear how accurately the recorded RGB values reflect the intensity of an aurora. Therefore, it is necessary for researchers to record images and videos of auroras with a digital camera and a professional optical instrument simultaneously and to evaluate the accuracy of the digital camera data. In addition, to take full advantage of the fine spatial resolution, it is highly demanded to automatically point the digital camera to the region of active aurora. In this study, we developed a system for simultaneous observation of an aurora by a commercial digital camera and the ALIS_4D, a large-scale optical observation project operating in Kiruna, Sweden. In order to perform automated data acquisition, the machine-learning-based aurora detection software Tromsoe AI (Nanjo et al., 2022) was tuned for observations in Kiruna, and a function to point the digital camera in the direction where the aurora appeared was implemented. A gimbal manufactured by DJI was used to control the orientation of the digital camera, and a small PC and SONY's official SDK were used to control the start and end of the recording. In the presentation, we plan to introduce the videos obtained by this system and evaluate the feasibility of this dynamic auroral observation system. We also discuss how we can employ the current automated and adaptive auroral observations system for the next generation of 3D observations of the auroral ionosphere with the EISCAT_3D.

磁気嵐が発生した際には、極域の広い領域で激しいオーロラが観測されるため、デジタルカメラ（デジカメ）やスマートフォン（スマホ）によるオーロラの動画像が SNS へ数多くアップロードされる。これらの動画像のほとんどでは、70 – 80 度の画角を持つ広角レンズが用いられているが、研究用途の光学観測では、画角が 180 度の魚眼レンズを用いることが多い。全天観測には、観測所から見られる全てのオーロラを記録できるという利点があるが、限られたセンササイズで全天を撮像するため、デジカメやスマホに比べ空間分解能が劣る。また、デジカメやスマホによる動画像では、RGB の 3 チャネルが同時に記録できるのに対し、研究用途の光学観測では単色の撮像となることが多い。RGB チャネルの波長帯域は広い（半値幅〜100 nm）ため、デジカメやスマホは厳密な多波長観測器とは言えないが、B チャネルと G チャネルの比から降下電子の平均エネルギーを定性的に推定する手法が提案されており（Nanjo et al., 2021）、単色の光学観測にはない利点がある。つまり、デジカメやスマホによる動画像をオーロラの観測的研究に有効活用するためには、記録される RGB 値が、オーロラの明るさをどの程度正確に反映するのかを明らかにすることが不可欠である。そのためには、研究者自身が本格的な光学観測装置と同時にデジカメでオーロラを撮影し、得られるデータの精度評価を行う必要がある。また、高い空間分解能を生かすために、カメラをオーロラが出現している領域に向けるような自律的観測を行うことも求められる。そこで、本研究ではスウェーデン・キルナにおいて運用されている光学観測プロジェクト ALIS_4D との同時観測を行うことを目的として、市販のデジカメを用いたアクティブなオーロラ観測システムを開発した。このシステムでは、無人でデータの取得を行うため、オーロラの自動検出ソフト Tromsø AI (Nanjo et al., 2022) をキルナでの観測用に調整し、オーロラが出現した方角にデジカメを自動的に向けた上で動画を撮影する機能を実装した。デジカメの向きの制御は DJI 社製のジンバルを用い、撮影開始・終了の制御は小型 PC と SONY の公式 SDK を用いた。発表では、本システムで得られた動画像の紹介を行いながらシステムのフィージビリティを評価した結果を報告する。さらに、今回開発したアクティブかつアダプティブなオーロラ観測が、EISCAT_3D を用いた次世代の極域電離圏観測にどのように活用できるのかについても議論を行う予定である。

R006-16
C 会場 ：11/5　PM2 （15:45-18:15）
18:00～18:15

オーロラ活動に伴う銀河強度の変動：南極昭和基地における掃天フォトメータ観測

#門倉　昭[1)]
([1]ROIS-DS/極地研

Intensity variation of the Milky Way associated with auroral activity observed by the scanning photometer at Syowa Station

#Akira Kadokura[1)]
([1]ROIS-DS/NIPR

Intensity variation of the Milky Way observed by the Scanning Photometer (SPM) at Syowa Station, Antarctica is analyzed. Following characteristics are recognized in the intensity variation:

1. Latitudinal location of the Milky Way in the SPM data shifts from lower to higher latitudes in the dusk side hours. Hence, there appears a “latitudinal gap” in the SPM data.
2. Sometimes, there appears a sinusoidal wavy variation in the latitudinal structure.
3. Intensity of the Milky Way is clearly enhanced when auroral activity expands from higher or lower latitude sides to the latitudes of the Milky Way.

In this presentation, those results will be shown, and possible cause of the intensity variation will be discussed.

南極昭和基地での掃天フォトメータ（SPM：Scanning Photometer）のデータには、特にプロトンオーロラの発光波長に、天の川（銀河）の星団からの光が顕著に現れている。2009 年から 2022 年までの SPM のデータを調べたところ、その天の川からの発光に下記のような特徴的な変動が認められた：

１．夕方側の時間帯で、低緯度側から高緯度側へ緯度的にシフトし、発光緯度のギャップが見られる。
２．緯度構造に周期５～10 分程度の正弦波状の周期的な変動が現れることがある。
３．高緯度側または低緯度側よりオーロラ発光領域が広がる時、天の川の発光強度が顕著に増大する。

講演では、上記１～３の解析結果を示し、その原因について考察する。

R006-17
A 会場 ：11/6　AM2 （10:45-12:30）
11:00〜11:15

#平原　聖文 [1)], 高須　敦也 [2)], 横田　勝一郎 [3)]
([1] 名大・宇地研,([2] 名大・宇地研,([3] 阪大・理

Triple-dome electrostatic sensor for simultaneous electron/ion measurements with hemispheric field-of-view by an angular deflector

#Masafumi Hirahara[1)], Atsuya Takasu[2)], Shoichiro Yokota[3)]
([1]ISEE, Nagoya Univ.,([2]ISEE, Nagoya Univ.,([3]Osaka Univ.

For these decades, numerous space exploration missions have been conducted or planned based on miniaturized satellite/spacecraft bus systems. Newly-developed satellite configurations symbolized by “micro-satellite” or “cubesat” are prevailingly applied also for innovative or state-of-the-art missions dedicated to in-situ space plasma measurements. As known well, the in-situ plasma measurements should involve several observational targets achieved by completely different measurement principles, which is apt to require substantial mission resources like dimension, weight, power, telemetry, and so on. In the case of the space plasma particle measurements, almost identical but independent electrostatic energy analyzers have been adopted as the most conventional plasma particle sensors, which means that the mission has to afford the fabrication and installation of at least two independent sensor heads separately for electrons and ions. While the common dimensions and weights of these space plasma particle sensors are not unrealistically large for the application to miniaturized satellites, it would get more plausible and fruitful to install a newly-designed plasma particle instrument on an exploration satellite if two sensor heads for electron and ion measurements could be unified into one sensor head. The characteristic energy range of the plasma particles in the terrestrial/planetary space environment is mainly from a few eV to several tens of keV, requiring several kV outputs at most from high-voltage power supply units in the sensor head. The unified sensor head for electrons and ions could share the high-voltage power supply units to reduce the instrumental resources. It is also crucial to obtain a wide field-of-view by the sensor unit to achieve accurate measurements for three-dimensional velocity distribution functions of the hot components in the space plasma. In addition to the current development for the first type of unified electron/ion sensors with a fully planar field-of-view, as reported in the past presentations by our group, we are also leading the development of the second type of unified sensor covering a hemispheric field-of-view by an “electrostatic angular deflector”. The most characterized feature of this sensor unit is the integrated angular defector commonly used for electrons and ions for expanding the conical field-of-view to a hemispheric range. After both electrons and ions pass through the angular deflector, an “electron/ion separator” divides the electron and ion trajectories into individual routes reaching the energy-discriminating section consisting “triple-dome” type of electrostatic analyzer. The triple-dome electrostatic analyzer could make the simultaneous energy analyses for the electrons and ions only by using a common high voltage applied to the middle dome. This high-voltage output is also applied to the electron/ion separator after a linear attenuation by a simple resistivity dividing circuit, contributing to the resource reduction. The engineering model of this sensor head has been fabricated and experimentally evaluated through the initial calibrations by using our electron/ion beamline facility. The design and calibration results are discussed in this presentation.

R006-18
A 会場 ：11/6　AM2 （10:45-12:30）
11:15〜11:30

#田中　誠志郎 [1)], 平原　聖文 [1)], 笠原　慧 [2)], 久保　信 [3)]
([1 名古屋大学 ISEE,([2 東京大学,([3 クリアパルス株式会社

Initial experiments of a particle sensor combining floating-mode APD and an electrostatic analyzer for low/medium-energy electrons

#Seishiro Tanaka[1)], Masafumi Hirahara[1)], Satoshi Kasahara[2)], Shin Kubo[3)]
([1Nagoya University ISEE,([2The University of Tokyo,([3Clear Pulse Co., Ltd.

Avalanche PhotoDiodes (APDs) are prevailing for medium-energy (10s-keV) electron detections with rough energy analyses in space observations. For instance, the electron detector system of the Medium-Energy Particle instrument for electrons (MEP-e) for ERG mission consists of an array of APDs [Kasahara et al., EPS 2018]. Kasahara et al. [NIM, 2012] reported that the minimum detectable energy with an APD is 5 keV at 20 ℃.

We aim to reduce the lowermost energy of electron energy analyses for medium-energy electron analyzers using floating-mode APD. In the future, we hope to apply APDs in low-energy electron analyzers.

To detect lower-energy electrons below 5 keV, we applied the floating voltage to APD so that the incident electrons could be accelerated up to energies enough large for APD detection.

In our previous research, we have already achieved the world-first detection of 10-eV electrons by applying +5 kV to APD. We found that the energy resolution for the floating mode did not decline compared to that for the non-floating mode. In this presentation, we report the results of experiments using floating-mode APD installed in an engineering model of MEP-e. After the electrons are filtered due to passing through the ElectroStatic Analyzer (ESA) of MEP-e, the electrons accelerated by the floating voltage are successfully detected by APD at the corresponding energy channels.

We could detect from a few tens of eV to 10-keV electrons by floating-mode APD while the energy range of MEP-e using normal APDs is from 7 to 87 keV. The energy resolution for the 5-keV electrons accelerated to 10 keV (the 5-kV floating mode) was 1.50 keV, which was comparable to our previous results. We have confidence that the floating-mode APDs applied to medium-energy electron analyzers for 10s-keV measurements allow us to lower the energy range of the analyzers. Our results also show that the floating-mode APDs could be applied as low-energy electron detectors with a high sensitivity and a rough energy analysis capability.

R006-19
A 会場 ：11/6　AM2 （10:45-12:30）
11:30〜11:45

MCP・APD を用いた宇宙プラズマ粒子検出器の基礎特性実験

#片岡　ひな子 [1)], 田中　誠志郎 [2)], 平原　聖文 [3)], 笠原　慧 [4)]
([1] 名古屋大学 ISEE,([2] 名古屋大学 ISEE,([3] 名大・宇地研,([4] 東京大学

Experiments on fundamental characteristics of space plasma particle detectors using MCP and APD

#Hinako Kataoka[1)], Seishiro Tanaka[2)], Masafumi Hirahara[3)], Satoshi Kasahara[4)]
([1]Nagoya University ISEE,([2]Nagoya University ISEE,([3]ISEE, Nagoya Univ.,([4]The University of Tokyo,

Avalanche photodiodes (APDs) are photodiodes with internal amplification gain due to an increase in the current inside the APD when a voltage of approximately 150 to 180 V is applied, and can detect electrons of several keV (≧ 5 keV) by enhancing the signal pulse heights. For the ERG mission, an electron sensor (MEP-e) composed of a cusp-type electrostatic analyzer (ESA) and APDs for the measurements of medium-energy (~7-87 keV) electrons in space. Since the signal pulse height of APD is almost proportional to the energy of incident particles in the medium energy range, the energy analysis of incident particles can be performed independently of the electrostatic energy analyzer. This also has the advantage of helping to reduce background in observations in harsh radiation environments.

Microchannel plates (MCPs) are charge amplifiers that multiply secondary electrons produced by incident particles and have high detection efficiency for low-energy particles. As the incident energy of electrons increases, detection efficiency decreases. The gain of the MCP depends on the number of MCP layers and the applied voltage, and a high voltage (2 to 3 kV or higher) is required to detect particles. Since MCP cannot analyze the energy of incident particles or identify particles, it is often used for particle detection in combination with an electrostatic energy analyzer or TOF mass spectrometer. Therefore, we are conducting fundamental experiments to develop a hybrid detector by combining MCPs and APDs. The hybrid detector is expected to reduce the number of MCP layers and the required voltage by using a low-noise charge amplifier and an APD. We are also carrying out experiments to obtain the basic characteristics of both MCP and APD.

We have conducted experiments using a hybrid detector consisting of a 1-layer MCP and an APD without and with 2 μ m aluminum-coating on the incident surface, irradiated with electron beams of 20 to 100 keV. The results are as follows:

A. 1-layer MCP and non-coated APD

1. The signal of the electron cloud amplified by the MCP and irradiated to the incident surface of the APD was confirmed.

2. The amplification of the electron cloud from the MCP inside the APD produces a signal pulse height about 3 to 10 times higher than that of A.1, and the pulse height is roughly proportional to the energy of the electron cloud.

3. The signal of electrons penetrating the MCP and entering the APD was confirmed at 20 to 100 keV.

B. 1-layer MCP and coated APD

1. The electron cloud from the MCP was identified.

2. When the electron cloud from the MCP was applied so that secondary electrons were emitted from the incident surface of the APD, the signal was almost as large as the signal from the electron cloud in B.1.

3. In the case of electrons penetrating the MCP and incident on the APD, the signal is roughly half that of A.3 because the aluminum-coated layer reduces the energy, and the minimum detected energy increases to about 30 keV.

The detection of electrons from 10 eV to 100 keV was also performed using a 3-layer MCP and a coated APD. From these experiments, it was found that the detection efficiency of the 3-layer MCP is highest between 600 eV and 1 keV, and that the pulse height signal is approximately twice as high as those at tens of eV and tens of keV.

We are currently planning to perform experiments to confirm how the results of pulse height analysis change depending on the ion species to a non-coated APD and a hybrid detector consisting of a 1-layer MCP and an APD.

Avalanche photodiode（APD）は約 150〜180 V の電圧をかけることで APD 内部の電流が増加することによって増幅利得を持つフォトダイオードであり、信号波形を高めることで数 keV（5 keV 以上）の電子を検出することができる。そのため、ジオスペース探査衛星「あらせ」に搭載された中エネルギー分析器 MEP-e に使用されている。APD は中エネルギー範囲において、信号の波高が入射粒子のエネルギーにほぼ比例するため、静電型エネルギー分析器とは独立して入射粒子のエネルギー分析を行うことができる。また、このことは厳しい放射線環境下の観測でのバックグラウンド低減に役立つという利点がある。

Microchannel plate（MCP）は入射した粒子の作る 2 次電子を増幅する電子増倍素子であり、低エネルギー粒子に高い検出効率を持つ。エネルギーが増加すると検出効率は低下する。また、MCP の利得は MCP の枚数と印加電圧に依存し、粒子の検出には高電圧（2〜3 kV 以上）が必要となる。MCP のみでは入射した粒子のエネルギー分析や粒子の識別はできないため、静電型エネルギー分析器や TOF 型質量分析器などと合わせて粒子の検出に使用されることが多い。そこで、我々は MCP と APD を組み合わせハイブリッド型検出器とすることで開発に向けた基礎実験を行っている。ハイブリッド型検出器では、低雑音チャージアンプと APD を用いることで MCP の枚数を減らし、必要な電圧を低く抑えることが期待される。また、MCP と APD それぞれの基礎特性を得るための実験も行っている。

我々は 1 枚式 MCP と入射面に 2 μ m のアルミ蒸着のない APD とある APD を組み合わせてハイブリッド型検出器とし、20〜100 keV の電子ビームを照射する実験を行った。その結果、

A. 1 枚式 MCP ＋アルミ蒸着なし APD

1. MCP によって増幅された電子雲が APD の入射面に照射された信号を確認した。

2. MCP からの電子雲が APD 内部で増幅されることにより、1.1 に比べ約 3〜10 倍の信号波高が得られ、その波高は電子雲のエネルギーとほぼ比例関係にある。

3. MCP を突き抜けて APD に入射する電子の信号を 20〜100 keV で確認した。

B. 1 枚式 MCP ＋アルミ蒸着あり APD

1. MCP からの電子雲を確認した。

2. MCP からの電子雲を当て、APD の入射面から 2 次電子が放出されるようにした場合、2.1 の電子雲の信号とほぼ同程度の大きさの信号が得られた。

3. MCP を突き抜けて APD に入射した電子の場合、アルミ蒸着層があることでエネルギーを減らすため、1.3 と比べて信号がおおよそ半分程度になり、最低検出エネルギーも約 30 keV 程度にまで上昇する。

また、3 枚式 MCP とアルミ蒸着のある APD を用いて 10 eV から 100 keV の電子の検出を行った。この実験から、3 枚式 MCP は 600 eV〜1 keV で最も検出効率が高くなり、効率の低くなる数十 eV や数十 keV の場合のおよそ 2 倍の波高信号が得られることが分かった。

現在、アルミ蒸着のない APD および 1 枚式 MCP と APD のハイブリッド型検出器にイオンを照射することで、イオンの種別によって波高分析の結果がどう変化するかを確認する実験を予定している。

R006-20
A 会場 ：11/6　AM2 （10:45-12:30）
11:45〜12:00

宇宙プラズマ測定用小型イオン・電子エネルギー分析器の開発

#和馬　正木 [1)], 齋藤　義文 [2)]
[(1] 東大,[(2] 宇宙研

The Development of the compact ion and electron energy spectrometer for space plasma

#Kazuma Masaki[1)], Yoshifumi Saito[2)]
[(1]UT,[(2]ISAS

In recent years, there has been a growing trend to use many small satellites for constellation observations in the magnetosphere and ionosphere.

CubeSat, for example, is a candidate for small satellites, but since these small satellites are only about 10cm x 10cm x 10cm in size, the onboard analyzers must necessarily be small enough to accommodate them. However, there are currently no suitable small instruments for observing charged particles in the low-energy range (several eV to several 10keV), and their development is desired.

We are developing a compact ion and electron energy spectrometer for space plasma measurement. In this study, we have evaluated the performance of a proto-model analyzer. The energy spectrometer is a concentrically stacked 90-degree cylindrical electrostatic analyzers, which can make ”in-situ” observation of low energy charged particles ranging from a few eV to several tens of keV. The analyzers are made of PEEK plastic which is partially metalized and have a radius of about 2cm, making it small and lightweight. By assembling multiple analyzers, we can detect charged particles from various directions. Ions and electrons are simultaneously energy analyzed by the stacked cylindrical electrostatic analyzers. The energy analyzed electrons and ions from different analyzer are detected using CEM or MCP. However, because of the small size of the analyzer, it is difficult to detect the position of charged particles that have passed through different analyzers and separate them. We are now investigating the angular characteristics of the analyzer. In parallel, we are developing a method to separate the signals obtained from the different analyzers without position detection. We are also trying to reduce the expected influence of solar ultraviolet light. By solving these problems, we will be able to use the analyzer in space in the future.

So far, we have evaluated the performance of the prototype analyzer through experiments and simulations. In the experiments, we placed the analyzer on a gimbal in a vacuum chamber and rotated the gimbal in various directions while being irradiated with nitrogen ion beam of about 2keV energy to investigate the angular dependence of the analyzer. The detectors were a CEM with a 1cm square inlet or an MCP with a 4cm diameter inlet. When solar ultraviolet light passes through the analyzer and reaches the detector, it brings noise. So, UV irradiation was also performed to investigate the response against UV light of the analyzer with carbon black painting. In the simulation, we investigated the angular dependence of the analyzer and compared the results with the actual experiment data.

As a result of the experiment, it was found that all the charged particles that passed through the analyzer were not fully detected in the test using the CEM because the size of the entrance to the CEM was too small. So, the results showed that the angular characteristics of the analyzer deviated significantly from the simulation results, but when the new test was conducted using an MCP with a large aperture, the deviation between the experimental and simulation results was smaller than before.

The results of the UV irradiation test with black painting showed that the UV-derived counts were suppressed to less than 100/sec for most of the angular range.

However, without the black painting, the UV-derived counts exceeded 10000/sec easily, indicating that the black painting is very useful in removing UV light. Due to the small size of the analyzer, there is concern that the reduction in the distance between electrodes due to the thickness of the black paint will have a significant impact on the analyzer characteristics. Therefore, it is necessary to investigate how the UV characteristics change when the thickness of the painting is reduced, and further development is needed, such as examining methods of blackening analyzers other than black painting.

It was found that there can be a method to separate the signals of ions and electrons passing through different analyzers without positional detection. This method takes advantage of the different energy-voltage characteristics of each analyzer. We think that further study is needed to keep the number of voltages sweeps to a realistic value and obtain necessary energy information on the charged particles.

近年地球磁気圏や電離圏等の領域で、多数の小型衛星によるコンステレーション観測を行おうとする機運が高まっている。小型衛星の候補としては CubeSat などを挙げることができるが、そういった小型衛星は 10cm x 10cm x 10cm 程度の大きさしかないため、搭載する分析器は必然的にそれに適した小型の物を採用しなければならない。しかし、現在低エネルギーレンジ (数 eV〜数 10keV) の荷電粒子を観測するための小型観測装置には適当なものが無く、開発が望まれているところである。

そこで、本研究では人工衛星や観測ロケットに搭載して低エネルギー荷電粒子を測定するための小型イオン・電子エネルギー分析器を開発し、そのプロトモデルの性能評価を行った。本機器は 90 度円筒型の静電分析器であり、数 eV〜

数 10keV 程度の低エネルギー荷電粒子を「その場」観測するためのものである。分析器本体の材質はピーク樹脂プラスチックを部分的にメタライズしたものであり、なおかつ半径 2cm ほどの大きさであるため、小型・軽量であることが大きな特徴である。そのため、CubeSat 等の超小型衛星に搭載することが可能であり、複数の分析器を組み合わせて搭載することで様々な方向からの荷電粒子を検出することも可能となる。本分析器は複数の円筒型静電分析器が同心円状に重なった形状をしている。イオンと電子を隣り合う円筒型静電分析器で交互に観測し、エネルギー分析されたイオン、電子を分析器ごとに個別に検出することを目標としている。ただし、分析器全体が小型であるがゆえに、それぞれ異なる分析器を通過した荷電粒子を位置検出し分離しようとしても検出器に到達するまでに混ざってしまうという問題がある。そこで、目下の課題は分析器の角度特性を調査し、予期される太陽紫外光の影響を軽減した上で、別々の分析器から得られた信号を位置検出することなく分離できる手法を開発することである。我々の開発している小型分析器を観測ロケットや衛星に搭載し、実際に利用するためにはこれらの課題を解決する必要があると考えている。

これまでの研究では実験とコンピュータによるシミュレーションを通し、分析器のプロトモデルの性能評価を行った。実験では分析器のプロトモデルを真空チャンバー中のジンバル上に設置し、2keV の窒素イオンビームを照射しながらジンバルを様々な方向に回転させることで、分析器の角度特性を調査した。検出器は 1cm 四方の入口を有する CEM と、口径 4cm の入口を有する MCP を用いた。また、分析器に炭素による黒色塗装を行った上で、太陽紫外光を模擬した紫外線照射実験も行い、紫外線に対する分析器の感度も調査した。シミュレーションでは実験と同様に分析器の角度特性を計算し、実際の実験データとの比較を行った。

実験の結果、これまで使用していた CEM を用いた試験では、CEM の入り口の大きさが小さ過ぎて、分析器を通過した荷電粒子を全て検出しきれていないことがわかった。また、その結果、分析器の角度特性がシミュレーションの結果と大きくずれた結果となってしまっていたことも判明した。今回新たに大きな口径を有する MCP を用いて実験を行ったところ、実験結果とシミュレーション結果の乖離を以前よりも小さくすることができた。

太陽紫外線が分析器を通過して検出器に到達すると、ノイズとなってしまう。そこで、紫外線の検出器への侵入を軽減するために、黒色塗装を行った分析器に紫外線を照射する試験を行った。その結果、ほとんどの角度範囲において紫外線由来のカウント数が 100/sec 以下に抑えられることがわかった。黒色塗装を施さない場合は紫外線由来のカウント数が容易に 10000/sec を超えてしまうので、黒色塗装は紫外線除去に大きく役立つことがわかった。しかし、分析器が小型であるがゆえに、使用した黒色塗装の厚みによる電極間距離の減少が、分析器の特性に大きな影響を及ぼすことが懸念されている。それゆえに、塗装の厚さを薄くした場合に、紫外線特性がどのように変化するかを調べる必要がある他、黒色塗装以外の分析器の黒色化の方法を検討するなど、さらなる開発が必要であることがわかった。

分析器を通過した荷電粒子を位置検出せずに、異なる分析器を通過した荷電粒子由来の信号を分離する手法に関しては、それぞれの分析器のエネルギー-電圧特性が異なることを利用することで実現できる可能性のあることがわかった。ただし、電圧の掃引回数を現実的な値に抑え、なおかつ必要な荷電粒子のエネルギー情報を十分に得るためには、今後のさらなる検討が必要になると考えている。

R006-21
A 会場 ：11/6　AM2 （10:45-12:30）
12:00〜12:15

#前田　大輝 [1)], 能勢　正仁 [1)], 野村　太志 [1)], 足立　匠 [1)], 市原　寛 [2)], 岩永　吉広 [3)], 河野　剛健 [3)], 浅利　晴紀 [4)], 平原　秀行 [4)], 海東　恵 [4)], 長町　信吾 [4)]
([1] 名大・宇地研,[2] 名古屋大学地震火山研究センター,[3] 愛知製鋼株式会社,[4] 気象庁地磁気観測所

Low-cost magnetometer using magneto-impedance (MI) sensors

#Taiki Maeda[1)], Masahito Nose[1)], Hiroshi Nomura[1)], Takumi Adachi[1)], Hiroshi Ichihara[2)], Yoshihiro Iwanaga[3)], Takeshi Kawano[3)], Seiki Asari[4)], Hideyuki Hirahara[4)], Megumi Kaitou[4)], Shingo Nagamachi[4)]
([1]ISEE, Nagoya Univ.,[2]Nagoya University,[3]Aichi Steel Corporation,[4]Kakioka Magnetic Observatory, JMA,

Magneto-impedance (MI) effect was discovered about 30 years ago and a micro-size magnetic sensor that utilizes this effect becomes commercially available. We made some modifications to the commercially available MI sensors as they can cover the range of the geomagnetic field. For the period of March 30 to April 27, 2018, we conducted experimental observations of geomagnetic field variations with the MI sensors at Mineyama observation site, which is located about 100 km north-west of Kyoto. Data obtained with the MI sensors were compared with those from the fluxgate magnetometer that has been working at the site. Results showed that the MI sensor recorded geomagnetic variations with amplitudes of ˜1 nT that were also detected with the fluxgate magnetometer. This suggests that MI sensors are useful for researches in geomagnetism or space physics, although they are much less expensive than fluxgate magnetometers.

Nomura [2021] developed a triaxial magnetometer which is composed of the MI sensors, Raspberry Pi, low-cost 24-bit A/D converters, and stable power supply circuits. This magnetometer is named MIM-Pi, and the cost of MIM-Pi is about one-tenth of that of fluxgate magnetometer. However, the result of the test at Inabu observation site in Japan (26.8º, − 152.5º in geomagnetic coordinates) showed that MIM-Pi had step noises with amplitudes of 2 − 3 nT which originated from an A/D converter. Therefore, we replaced the A/D converter with a new A/D conversion module (ADPi) and confirmed that the modified MIM-Pi did not have such step noises. We performed a long-term observation at Inabu with MIM-Pi for the period of Nov. 19, 2021 to Jan. 14, 2022. Results shows that MIM-Pi can record Sq variations and geomagnetic pulsations with amplitudes of 1 − 2 nT that were also detected with the fluxgate magnetometer. We also performed a long-term observation at Kakioka Magnetic Observatory and found that MIM-Pi succeeded in capturing Pc4. For the deployment of MIM-Pi to construct a dense magnetometer network in Kanto-Tohoku area, we made a jig for MI sensors and a case for the controller. In presentation, we will show the MIM-Pi data and discuss future plan.

R006-22
A 会場 ：11/6　AM2 （10:45-12:30）
12:15〜12:30

#中田　雅彦 [1)], 村田　直史 [2)], 松岡　彩子 [3)], 栗田　怜 [4)], 小嶋　浩嗣 [4)]
([1] 京大 工学研究科,[(2]JAXA,[(3] 京大 理学研究科,[(4] 京大 生存圏研究所

Design and Performance Evaluation of an ASIC Chip Dedicated to Fundamental Mode Orthogonal Fluxgate Magnetometers

#Masahiko Nakata[1)], Naofumi Murata[2)], Ayako Matsuoka[3)], Satoshi Kurita[4)], Hirotsugu Kojima[4)]
([1]Engineering, Kyoto U.,[(2]JAXA,[(3]Science, Kyoto U.,[(4]RISH, Kyoto U.,

We are working on the design of an analog circuit chip dedicated to Fundamental Mode Orthogonal Fluxgate Magnetometers (FM-OFG) for future scientific satellites. Fluxgate magnetometers are often used on space missions to measure variations in DC and low-frequency magnetic fields. Conventional parallel type fluxgate magnetometers use ring-core sensors, which have excellent noise characteristics and output offset voltage stability. On the other hand, a sufficiently large core is required to achieve low-noise detection, which is not suitable for miniaturization. However, recent development of micro and nano-satellites has increased the need for smaller onboard devices.

Therefore, we focused on a new type of fluxgate magnetometer. The sensor of the FM-OFG magnetometer consists of a pair of amorphous wire cores and a pickup/feedback coil. There is no need of excitation coils that are necessary for the ring-core sensor. While it is difficult to get below 10 gram per axis with a ring-core sensor, the FM-OFG sensor can be made much lighter at about 1 gram per axis.

In order to pursue smaller and lighter fluxgate magnetometers, it is also important to reduce the size of the electronic circuit. In this research, we focus on developing an analog chip called ASIC (Application Specific Integrated Circuit) to miniaturize the electronic circuit of the FM-OFG magnetometer. The electronic circuit of the FM-OFG consists of a drive circuit that excites the wire core, and a pickup circuit that picks up the signal from the sensor head and extracts the waveform of detected magnetic fields based on the feedback system. In this paper, we have designed the ASIC chip for the latter circuit by using the circuit simulator T-Spice and the layout tool Virtuoso. In addition, the designed ASIC chip was embedded in the evaluation board and performance test was conducted.

R006-23
A 会場 ：11/7　AM1 （9:00-10:30）
09:15〜09:30

あらせ衛星の観測による放射線帯、プラズマ圏の長期変動

#三好　由純[1)], 栗田　怜[2)], 片岡　龍峰[3)], 齊藤　慎司[4)], 今城　峻[5)], 堀　智昭[1)], 中村　紗都子[6)], 田　采祐[7)], 寺本　万里子[8)], 三谷　烈史[9)], 篠原　育[10)], 高島　健[11)], 東尾　奈々[12)], 笠原　慧[13)], 横田　勝一郎[14)], 桂華　邦裕[15)], 浅村　和史[9)], 松岡　彩子[16)], 土屋　史紀[17)], 熊本　篤志[17)], 北原　理弘[1)], 松田　昇也[18)], 笠原　禎也[19)], 風間　洋一[20)],Wang　S.-Y.[21)],Tam　Sunny W. Y.[22)]
([1 名大 ISEE,([2 京都大学 生存研,([3 極地研,([4 情報通信研究機構,([5 京大・地磁気センター,([6IAR&ISEE,([7 名大 ISEE 研,([8 九工大,([9 宇宙研,([10 宇宙研／宇宙機構,([11 宇宙研,([12JAXA,([13 東京大学,([14 大阪大,([15 東大・理,([16 京都大学,([17 東北大・理・惑星プラズマ大気,([18 金沢大学,([19 金沢大,([20ASIAA,([21 台湾・中央研究院,([22 国立成功大学宇宙・プラズマ科学研究所

Long-term variations of relativistic electrons of the outer radiation belt, plasma sheet electrons and plasmasphere

#Yoshizumi Miyoshi[1)], Satoshi Kurita[2)], Ryuho Kataoka[3)], Shinji Saito[4)], Shun Imajo[5)], Tomoaki Hori[1)], Satoko Nakamura[6)], ChaeWoo Jun[7)], Mariko Teramoto[8)], Takefumi Mitani[9)], Iku Shinohara[10)], Takeshi Takashima[11)], Nana Higashio[12)], Satoshi Kasahara[13)], Shoichiro Yokota[14)], Kunihiro Keika[15)], Kazushi Asamura[9)], Ayako Matsuoka[16)], Fuminori Tsuchiya[17)], Atsushi Kumamoto[17)], Masahiro Kitahara[1)], Shoya Matsuda[18)], Yoshiya Kasahara[19)], Yoichi Kazama[20)], S.-Y. Wang[21)], Sunny W. Y. Tam[22)]
([1ISEE, Nagoya Univ.,([2RISH, Kyoto Univ.,([3NIPR,([4NICT,([5WDC for Geomagnetism, Kyoto, Kyoto University,([6IAR&ISEE,([7ISEE, Nagoya Univ.,([8Kyutech,([9ISAS/JAXA,([10ISAS/JAXA,([11ISAS, JAXA,([12JAXA,([13The University of Tokyo,([14Osaka Univ.,([15University of Tokyo,([16Kyoto University,([17Planet. Plasma Atmos. Res. Cent., Tohoku Univ.,([18Kanazawa Univ.,([19Kanazawa Univ.,([20ASIAA,([21ASIAA, Taiwan,([22Institute of Space and Plasma Sciences, National Cheng Kung University, Taiwan

The Arase satellite has observed the inner magnetosphere since 2017 and provided long-term observation data about plasma/particles and field/waves, which covers the declining phase of the solar cycle 24 and the following early rising phase of the cycle 25. We investigate spatio-temporal variations in the phase space density that indicate evolution of the acceleration region for energetic electrons. For several magnetic storms, glowing peaks of the phase space density are found during the recovery phase and this fact indicates that the local acceleration processes work for the large flux enhancement of the outer belt electrons. In addition, we find that the location of the glowing peaks in the phase space density varies with the plasmapause location as well as the inner edge of the plasma sheet electrons. This result is consistent with the cross-energy coupling processes driven by wave-particle interactions in which the electron acceleration driven by whistler mode waves is regulated by the ratio of the plasma frequency (fp) and cyclotron frequency (fc) as well as the source electrons for the wave generation.

R006-24
A 会場 ：11/7　AM1 （9:00-10:30）
09:30〜09:45

#パンディヤ　メグハ マヘンドラ [1)],Ebihara Yusuke[1)],Tanaka Takashi[2)]
[(1] 京都大学,[(2] 京都大学

Generation of the Electron Zebra Stripes in the Earth's Inner Magnetosphere

#Megha Pandya[1)], Yusuke Ebihara[1)], Takashi Tanaka[2)]
[(1]Research Institute for Sustainable Humanosphere, Kyoto University, Uji, Japan,[(2]International Research Center for Space and Planetary Environmental Science, Kyoto University

Energy versus L-value spectra of the electrons with 10's-100's of keV energies exhibit a banded structure that resembles the zebra-like patterns. Hence, they have been named as "zebra stripes". Zebra stripes are the unique feature observed in the Earth's inner magnetosphere where the electron flux intensities exhibit sharp repeated peaks and valleys in energy. In the present studies, we analysed the spatio-temporal growth of the electron zebra stripes that appeared during the intense geomagnetic storm of September 8, 2017. We employed an advection simulation for electrons, under the time-dependent electric and magnetic fields provided by a global magnetohydrodynamics (MHD) simulation, and found that electron zebra stripes were generated. To understand the evolutionary characteristics of the electrons comprising of the peaks and the valleys, we back-traced the bounce-averaged electron trajectories. Significant influence of the ionospheric electric fields were identified on the electron motion in the radial direction. The enhancement of the westward electric field in the premidnight to postdawn region transports the electrons earthward, triggering the formation of the peaks. The electrons comprising of the valleys have not experienced such earthward transport. The generation of the westward electric field has its roots in the Region 1 field aligned current (FAC) in the polar ionosphere. The electric field penetrates deep into the lower latitudes, and propagates into the inner magnetosphere. In addition, the non-uniform ionospheric conductivity at the equatorward edge of the auroral oval distorts the electrical potential patterns, and extend the westward electric field region to the dawn. Our study highlights the coupling of the solar wind and the deep inner magnetosphere for the formation of electron zebra stripes.

R006-25
A 会場 ：11/7　AM1 （9:00-10:30）
09:45〜10:00

#Kumar　Sandeep[1)], 三好　由純 [1)], ジョルダノヴァ　ヴァニア [2)],Kistler　Lynn M.[1,3)],Porunakatu Radhakrishna Shreedevi[1)], 浅村　和史 [4)], 横田　勝一郎 [5)], 笠原　慧 [6)], 風間　洋一 [7)],Wang　S.-Y.[7)],Tam　Sunny W. Y.[8)], 三谷　烈史 [4)], 東尾　奈々 [4)], 桂華　邦裕 [6)],Park　Inchun[1)], 堀　智昭 [1)], 田　采祐 [1)], 松岡　彩子 [9)], 今城　峻 [9)], 篠原　育 [4)]
([1]ISEE,NU,[2]LANL,[3]University of New Hampshire,[4] 宇宙研／宇宙機構,[5]Osaka University,[6]University of Tokyo,[7]ASIAA,Taiwan,[8]In of Space and Plasma Science, National Cheng Kung University,[9] 京大・地磁気センター

Plasma pressure distribution of ions and electrons in the inner magnetosphere during CIR and CME storms observed by Arase

#Sandeep Kumar[1)], Yoshizumi Miyoshi[1)], Vania Jordanova[2)], Lynn M. Kistler[1,3)], Shreedevi Porunakatu Radhakrishna[1)], Kazushi Asamura[4)], Shoichiro Yokota[5)], Satoshi Kasahara[6)], Yoichi Kazama[7)], S.-Y. Wang[7)], Sunny W. Y. Tam[8)], Takefumi Mitani[4)], Nana Higashio[4)], Kunihiro Keika[6)], Inchun Park[1)], Tomoaki Hori[1)], ChaeWoo Jun[1)], Ayako Matsuoka[9)], Shun Imajo[9)], Iku Shinohara[4)]
([1]ISEE,Nagoya Univ.,[2]Space Science and Application, LANL,[3]ISEOS, University of New Hampshire,[4]ISAS/JAXA,[5]Osaka Univ.,[6]The University of Tokyo,[7]ASIAA,Taiwan,[8]Institute of Space and Plasma Sciences, National Cheng Kung University, Taiwan,[9]WDC for Geomagnetism, Kyoto, Kyoto University

Geomagnetic storms are the main component of space weather, and the main phase of the geomagnetic storms are driven by Coronal Mass Ejections (CMEs) or Corotating Interaction Regions (CIRs). It is well known that CME-driven storms and CIR-driven storms have different evolutions of the Sym-H and the ion distributions in the inner magnetosphere [Miyoshi and Kataoka, 2005]. Enhancement of the ring current is a typical feature of the geomagnetic storm and a global decrease in the H component of the geomagnetic field is observed during the main phase of the geomagnetic storm. The ring current represents a diamagnetic current driven by the plasma pressure in the inner magnetosphere. The plasma pressure is mainly contributed by protons in an energy range of a few to a few hundreds of keV. The O+ contribution is also important, and sometimes dominates H+ during the geomagnetically active period. Recently, we showed that the electron pressure also contributes to the depression of ground magnetic field during the November 2017 CIR-driven storm by comparing Ring current Atmosphere interactions Model with Self Consistent magnetic field (RAM-SCB) simulation, Arase in-situ plasma/particle data, and ground-based magnetometer data [Kumar et al., 2021]. It has been shown that ion and electron distributions of CME/CIR-driven storms are different, especially for recovery phase [Miyoshi and Kataoka, 2005]. In this study, we examine statistically the spatial and temporal distribution of electrons and ions pressure with different energies and their contribution to the depression of the magnetic field during main phase, early recovery and late recovery phase for selected CIR and CME storms using in situ plasma/particle data obtained by Arase.

R006-26
A 会場 ：11/7　AM1 （9:00-10:30）
10:00〜10:15

#永谷　朱佳理 [1)], 三好　由純 [2)], 浅村　和史 [3)], 中村　紗都子 [4)], 小路　真史 [2)],Kistler　Lynn M.[2,5)], 小川　泰信 [6)], 関　華奈子 [7)], 篠原　育 [8)]
([1] 名大 ISEE,[2] 名大 ISEE,[3] 宇宙研,[4]IAR&ISEE,[5] ニューハンプシャー大,[6] 極地研,[7] 東大理・地球惑星科学専攻,[8] 宇宙研／宇宙機構

Time variations of molecular ions in the inner magnetosphere observed by Arase

#Akari Nagatani[1)], Yoshizumi Miyoshi[2)], Kazushi Asamura[3)], Satoko Nakamura[4)], Masafumi Shoji[2)], Lynn M. Kistler[2,5)], Yasunobu Ogawa[6)], Kanako Seki[7)], Iku Shinohara[8)]
([1]ISEE, Nagoya Univ.,[2]ISEE, Nagoya Univ.,[3]ISAS/JAXA,[4]IAR&ISEE,[5]ISEOS, University of New Hampshire,[6]NIPR,[7]Dept. Earth & Planetary Sci., Science, Univ. Tokyo,[8]ISAS/JAXA

In the Earth's magnetosphere, there are several kinds of ions originated from both the solar wind and the ionosphere. Molecular ions in the magnetosphere are originated in the Earth's ionosphere. For example, statistical studies based on 20 years of Geotail/STICS data has indicated that the count rates of magnetospheric molecular ion are sensitive to geomagnetic activity [Christon+, 2020].The Arase satellite has observed various kinds of ions since 2017 and two ion analyzers LEPi and MEPi cover energy range from 10 eV/q to 180 keV/q. Using the data from the MEPi instrument, variations of molecular ions to magnetic storms and solar wind conditions have been investigated, and molecular ions are observed in the inner magnetosphere even during small magnetic storms [Seki+, 2019]. However, observations about molecular ions are still not enough compared with other ion observations, and the mechanism of the outflow from the ionosphere as well as the long-term variations are not well known. In this study, we analyzed the time-of-flight (TOF) data from LEPi [Asamura+, 2018] onboard Arase to investigate variations of molecular ions in the inner magnetosphere and their dependence about magnetic activities and solar wind conditions. LEPi covers the energy range from 10 eV/q to 25 keV/q and counts as function of energy and TOF are obtained every 16 seconds. The TOF measurements of LEPi have been operated in the outbound pass every four revolutions around the Earth. In the analysis, we estimated counts of molecular ions by fitting the empirical functions onthe TOF profile using the non-linear least squares method. The estimated counts were calibrated by the time variations of efficiency of the LEPi instrument. Using this data set, we investigated relationships between molecular ion count and geomagnetic index and solar wind parameters. The results suggest that counts of molecular ions increase with solar wind speed as well as density. Also, we found that molecular ions appear in the magnetosphere during not only magnetic storms but also non-magnetic storms.

R006-27
A 会場 ：11/7　AM1 （9:00-10:30）
10:15〜10:30

ひさき衛星極端紫外線観測データを用いた木星イオプラズマトーラス突発増光時における Dusk 側からの Hot electron 流入

#古川　研斗 [1)], 土屋　史紀 [1)], 鍵谷　将人 [1)], 吉岡　和夫 [2)], 吉川　一朗 [2)], 木村　智樹 [3)], 北　元 [4)], 村上　豪 [5)], 山崎敦 [5)], 三澤　浩昭 [1)], 笠羽　康正 [1)]
[1 東北大学,[2 東京大学,[3 東京理科大学,[4 東北工業大学,[5JAXA/宇宙研

Localized hot electron inflow on the dusk side during transient brightening in Io plasma torus observed by Hisaki/EXCEED.

#Kento Furukawa[1)], Fuminori Tsuchiya[1)], Masato Kagitani[1)], Kazuo Yoshioka[2)], Ichiro Yoshikawa[2)], Tomoki Kimura[3)], Hajime Kita[4)], Go Murakami[5)], Atsushi Yamazaki[5)], Hiroaki Misawa[1)], Yasumasa Kasaba[1)]
[1Tohoku University,[2The Univ. of Tokyo,[3Tokyo University of Science,[4Tohoku Institute of Technology,[5JAXA/ISAS

The Hisaki satellite has observed 10% transient increases in the intensity of the Io plasma torus (IPT) emission in the inner magnetosphere (r<8Rj) over a time scale of several to ten hours after a transient brightening of Jupiter's UV auroral emission. Since the plasma convection in the Jovian magnetosphere is dominated by the planetary rotation, it has been considered that the fast transport of energy in the radial direction is not significant. However, this transient phenomenon suggests that the effects of transient energy release in the middle or outer magnetospheres, which cause auroral brightening, extend to the IPT on a time scale of a few tens of hours. Considering that the relaxation time of hot electrons with energy of several hundred eV in the IPT due to Coulomb collisions is comparable to the time scale of the brightening, previous studies interpreted the cause of brightening as the influx of hot electrons into the IPT from outer part of the magnetosphere. In this study, we investigated the start local time (LT) of the IPT brightening from the extreme ultraviolet (EUV) spectra observed by the HISAKI satellite and clarified the inflow position of hot electrons in the IPT.

The field-of-view of the EUV spectrograph onboard the HISAKI satellite is 360 arcsec, which enables to observe the radial spatial structure of the IPT emission in both dawn and dusk sides. We obtained the intensity of sulfur ion emission by integrating the EUV spectrum from 65 to 77 nm in wavelength, and then determined the start LT of the IPT brightening by dividing the spatial distribution of the IPT into 10 parts in each dawn and dusk region (20 regions in total). The integration time was set to 10 minutes. In order to detect the IPT brightening with an amplitude of 10%, the trend of the intrinsic periodic variations in the torus (System III period: 9.93 h, System IV period: 10.14 h, and Io's orbital period: 42.46 h) were fitted by the least-squares method and eliminated from the data.

23 brightening events were identified in 2014-2016. 18 events started in the dusk side, and 13 of them were localized at LT14-16. Assuming that the cause of the brightening is the inflow of hot electrons, this result indicates that inflow of hot electrons in the IPT tend to localize on the dusk side. In the rotation-dominant magnetosphere, the transport of plasma in the radial direction is thought to be caused by interchange instability driven by centrifugal forces. Since the centrifugal force which acts on plasmas is independent of LT, it is expected that inflow of hot electron would occur in all LT region. The result presented here shows different picture of Jovian magnetosphere from that previously thought.

R006-28
A 会場 ：11/7　AM2 （10:45-12:30）
11:00〜11:15

#栗田　怜 [1)], 三好　由純 [2)], 齊藤　慎司 [3)], 加藤　雄人 [4)], 松田　昇也 [5)], 笠原　慧 [6)], 横田　勝一郎 [7)], 笠原　禎也 [8)], 松岡　彩子 [9)], 篠原　育 [10)]
([1] 京都大学 生存研,[2] 名大 ISEE,[3] 情報通信研究機構,[4] 東北大・理・地球物理,[5] 金沢大学,[6] 東京大学,[7] 大阪大,[8] 金沢大,[9] 京都大学,[10] 宇宙研／宇宙機構

High temporal variation in electron fluxes during flux burst events observed by the Arase satellite

#Satoshi Kurita[1)], Yoshizumi Miyoshi[2)], Shinji Saito[3)], Yuto Katoh[4)], Shoya Matsuda[5)], Satoshi Kasahara[6)], Shoichiro Yokota[7)], Yoshiya Kasahara[8)], Ayako Matsuoka[9)], Iku Shinohara[10)]
([1]RISH, Kyoto Univ.,[2]ISEE, Nagoya Univ.,[3]NICT,[4]Dept. Geophys., Grad. Sch. Sci., Tohoku Univ.,[5]Kanazawa Univ.,[6]The University of Tokyo,[7]Osaka Univ.,[8]Kanazawa Univ.,[9]Kyoto University,[10]ISAS/JAXA

We examine the high temporal variation in electron fluxes during flux burst events observed by Medium Energy Particle experiment-electron analyzer (MEP-e) onboard the Arase satellite. The flux burst event is characterized by a flux increase of 17-30 keV electrons within 30 seconds at an oblique (60-80 degrees) pitch angle range, which is accompanied by a decrease in electron fluxes at lower energy and pitch angle ranges [Kurita et al., 2018]. The rapid flux variation is observed in association with the appearance of intense upper-band chorus emissions. It is suggested that the nonlinear wave-particle interaction between electrons and the upper-band chorus is a plausible mechanism of the flux variation. The importance of the nonlinear wave-particle interaction is examined by a test-particle simulation, and it is found that the acceleration through nonlinear phase-trapping is essential to cause the rapid flux increase [Saito et al., 2021]. It is of interest to further examine whether signatures of nonlinear electron acceleration are captured by MEP-e during the flux burst event. The flux burst event was analyzed using the MEP-e data with a time resolution of ˜8 seconds (1 spin period). On the other hand, MEP-e has the capability to derive pitch angle distributions every 250ms because of its 2-pi radian disk-like field-of-view and measurement scheme. Using the pitch angle distribution with the high temporal resolution, we investigate sub-second flux variations during the flux burst event in detail. We find that the flux increase consists of two components: one is the almost same increase as the 1-spin average increase, and the other is a much larger flux increase than the 1-spin average. The larger increase is less frequently observed compared to the smaller one. Thus the larger flux increase does not significantly contribute to the 1-spin averaged flux variation. It is possible that the large flux increase seen in the 250-ms MEP-e data is a signature of electron acceleration through nonlinear wave-particle interactions. It is suggested that this possibility can be investigated by performing a virtual observation in a test-particle simulation.

R006-29
A 会場 ：11/7　AM2 （10:45-12:30）
11:15〜11:30

#齊藤　慎司 [1)], 栗田　怜 [2)], 三好　由純 [3)], 加藤　雄人 [4)], 松田　昇也 [5)]
([1] 情報通信研究機構,[2] 京都大学 生存研,[3] 名大 ISEE,[4] 東北大・理・地球物理,[5] 金沢大学

High temporal variation in electron fluxes during the flux burst event: Test-particle simulation

#Shinji Saito[1)], Satoshi Kurita[2)], Yoshizumi Miyoshi[3)], Yuto Katoh[4)], Shoya Matsuda[5)]
([1]NICT,[2]RISH, Kyoto Univ.,[3]ISEE, Nagoya Univ.,[4]Dept. Geophys., Grad. Sch. Sci., Tohoku Univ.,[5]Kanazawa Univ.

Whistler-mode chorus wave is a plausible cause to scatter radiation belt electrons. The cyclotron resonance process has a crucial role to accelerate (decelerate) electrons through not only quasilinear diffusion process but also nonlinear scattering process. Kurita et al. (2018) found the flux enhancement of tens keV electrons accompanied with the enhancement of upper band whistler-mode chorus (UBC) waves within 30 seconds. Furthermore, Saito et al. (2021) demonstrated that the nonlinear scattering process causes the electron flux enhancement observed by Kurita et al. (2018) using a test-particle simulation. It is of interest to further investigate whether other observable signatures for nonlinear scattering processes can be seen during the flux burst event. By analyzing test-particle data obtained from the simulation by Saito et al. (2021), we found that the temporal variation of electron count during the flux enhancement in pitch angle of 60 -80 degree at the equator and energy of 24 keV - 25 keV showed the rapid electron count enhancement within the time scale well shorter than 1 spin period (about 8 seconds) of Medium Energy Particle experiment-electron analyzer (MEP-e) onboard the Arase satellite. The variance in the count distribution increases with increasing the temporal-averaged count during the flux burst event, which becomes significantly larger than the variance in Poisson distribution. The count distribution broader than the Poisson distribution suggests that the temporal variation in the counts includes factors caused by the wave-particle interactions other than statistical noise. The similar trend seen in the count distribution has been found by the MEP-e on board the Arase [Kurita et al., SGEPSS 2022]. We study a cause of the broadening of the count distribution using the test-particle simulation. The simulation results suggest that nonlinear scattering processes by UBC waves contribute to the rapid enhancement of the electron count in the time scale of well less than 1 spin period. In this talk we will report the role of nonlinear scattering of electrons by UBC for the broad count distribution.

R006-30
A 会場 ：11/7　AM2 （10:45-12:30）
11:30〜11:45

沿磁力線電流とリングカレントの観測に基づく ULF 波動励起のドリフト運動論シミュレーション

#山本　和弘 [1)]
(1 東大・理・地惑

Drift-kinetic simulation study of ULF wave excitation based on the field-aligned current and ring current observations

#Kazuhiro Yamamoto[1)]
(1UTokyo

Ring current ions can excite poloidal (radial oscillation of a field line) ULF waves through drift-bounce instability (Southwood et al., 1969). The wave-particle interaction between poloidal waves and ring current ions has been focused on since the excited waves can also interact with radiation belt electrons (Ukhorskiy et al., 2009). One of the motivations of ULF wave modeling is assessment of its influence on space plasma environment because numerical simulation can provide spatial distributions of ULF waves, which is an important parameter for the total amount of the wave-particle interaction on the drift path of resonance particles. However, recent modeling of ULF waves excited by local plasma instability (Yamakawa et al., 2019, 2020, 2022[Revised]) assumed steady field-aligned currents in the ionosphere and symmetric distributions of injected ions with respect to the midnight in the magnetosphere. Therefore, the aim of this study is to clarify the ULF wave excitation with realistic simulation setting of the field-aligned current and injected ions for a specific date.

We used a coupling model of an ionospheric potential solver (GEMSIS-POT, Nakamizo et al,, 2012) and a drift-kinetic ring current model which solves Vlasov equation with 5D-phase space density f(x, v_{jj}, mu) (GEMSIS-RC, Amano et al., 2011). Field aligned current is an important input of this coupling model because it changes the ionospheric potential, convection E field in the magnetosphere, and hence the ExB drift of ions at <~10 keV. The inputs of the Region 1 field aligned current (j_{R1FAC}) and injected ions are based on satellite observations in this study: the Iridium and LANL satellites, respectively. Van Allen Probes detected poloidal waves with a proton injection at 5.3-5.7 Re on the dusk side on 29th October 2013, thus we consider this event as a reference.

The energy spectra of ion dispersionless injection detected by three LANL satellites on the night side (19.6 MLT to 3.9 MLT) were used to determine the boundary condition of ion distribution at the geosynchronous orbit. We obtained three fitting parameters of the Kappa distribution (J = CW(1+W/(KW_0))-(K+1)), where J is the ion differential flux, W is energy, C is a scale factor, W_0 is the characteristic energy, and K is the kappa index. We set the phase space density of injected ions within 19.6 MLT to 3.9 MLT. K has a MLT dependence, thus we linearly interpolated $\log_{10}$K from K= 20 to 200 to obtain phase space density at each MLT of a simulation grid. As for C and W_0, we used their averaged values because they did not show a clear MLT dependence.

Current density of the Region 1 field-aligned current was fitted with Gaussian function in a latitude and longitude plane. The criteria of R1FAC detection are as follows: 1) current direction should be downward/upward at 00-12/12-24 MLT at its maximum (MLT_{max}), 2) the maximal current density j_{max} is >0.5 uA/m^2, and 3) the latitude of the maximal current density $MLAT_{max}$ is within 60-80 deg. We obtained five fitting parameters of R1FAC-like current: j_{max}, MLT_{max}, $MLAT_{max}$, Sg_{MLT}, and Sg_{MLAT}, where Sg is the standard deviation in the Gaussian function fitting. Using the fitted current density and auroral conductivity of Hardy et al. (1987), we set the auroral conductivity which is proportional to the current density. This is because the calculation of the ionospheric potential does not converge if the conductivity has a large gradient in the R1FAC.

Finally, we have successfully combined the fitting data with the GEMSIS-POT and GEMSIS-RC coupling model and made it possible to simulate the ring current development under realistic conditions based on the satellite observations. In this presentation, we will discuss the influence of a time-varying convectional field on the excitation of poloidal ULF waves.

R006-31
A 会場 ：11/7　AM2 （10:45-12:30）
11:45〜12:00

#山川　智嗣 [1)], 関　華奈子 [1)], 天野　孝伸 [1)], 三好　由純 [3)], 高橋　直子 [2)], 中溝　葵 [2)], 山本　和弘 [1)]
([1] 東大・理,[2]NICT,[3] 名大 ISEE

Control of the dynamics of cold particles on the excitation of ULF waves based on the magnetosphere-ionosphere coupled model

#Tomotsugu Yamakawa[1)], Kanako Seki[1)], Takanobu Amano[1)], Yoshizumi Miyoshi[3)], Naoko Takahashi[2)], Aoi Nakamizo[2)], Kazuhiro Yamamoto[1)]
([1]School of Science, The University of Tokyo,[2]NICT,[3]ISEE, Nagoya Univ.

Storm-time Pc5 ULF waves are electromagnetic pulsations (1.67-6.67 mHz), which can be generated by ring current ions associated with the injection from the magnetotail during substorms. The excitation mechanism and global distribution of ULF waves are keys to understand the dynamic variation of the outer radiation belt, since they can drive radial transport of radiation belt electrons [e.g. Elkington et al., 2003]. Theoretically, drift-bounce resonance has been considered to be a candidate excitation mechanism [Southwood, 1976]. Previous spacecraft observations suggest both drift resonance and drift-bounce resonance excitation of ULF waves [e.g. Dai et al., 2013; Oimatsu et al., 2018]. Recently, Yamakawa et al. [2022, submitted] could reproduce both the drift resonance and drift-bounce resonance excitation of storm-time Pc5 ULF waves based on the magnetosphere-ionosphere coupled model. The coupled model could enhance the amplitude of ULF waves. However, this simulation was performed under the condition of constant density and how the dynamics of cold particles affects the excitation of storm-time Pc5 waves is not well understood.

We used magnetosphere-ionosphere coupled model between GEMSIS-RC [Amano et al., 2011] and GEMSIS-POT model [Nakamizo et al., 2012]. GEMSIS-RC model solves 5-D drift-kinetic equation for the PSD of ions and Maxwell equations self-consistently. GEMSIS-POT is a 2-D potential solver in the ionosphere. We developed the simulation code for updating the density of cold particles in GEMSIS-RC model in order to include the dynamics of cold particles. We compared simulation results between two cases; Case a (constant density, Yamakawa et al. [2022, submitted]) and Case b (including the dynamics of cold particles).

Simulation results have shown the excitation of two types of Pc5 ULF waves for both cases. First, we find the drift resonance excitation of Pc5 waves in the dayside. They are driven by the positive energy gradient of the PSD of ions with the energy of 50-120 keV. Second, Pc5 waves excited associated with the drift-bounce resonance are seen in the duskside. They are driven by inward gradient of ion PSD. We find that if we include the dynamics of cold particles, the region where second harmonic mode waves are generated extend to the region of lower L shell. The excitation region of fundamental mode is similar between two cases. We will also report on the time evolution of density and its effect on the excitation of ULF waves.

R006-32
A 会場 ：11/7　AM2 （10:45-12:30）
12:00〜12:15

SuperDARN レーダーで観測された Pc5 帯 ULF 波動のモードおよび m-number 解析

#森田　洸生 [1)], 西谷　望 [1)], 堀　智昭 [1)]
([1] 名大 ISEE

Mode and m-number analysis of ULF waves in the Pc5 frequency range with SuperDARN radars

#Koki Morita[1)], Nozomu Nishitani[1)], Tomoaki Hori[1)]
([1]ISEE, Nagoya Univ.

Ultralow frequency (ULF) waves can be observed by satellites, Super Dual Auroral Radar Network (SuperDARN) and ground-based magnetometers. ULF waves observed in the ionosphere with SuperDARN contain poloidal and toroidal modes with respect to their oscillation direction. Previous studies on ULF waves with SuperDARN analyzed ULF waves with single-beam line-of-sight plasma velocity data, and no study identified the primary mode of ULF waves with SuperDARN. In this study, we have identified the modes and m-number (azimuthal wave number) by comparing the amplitude and phase of ULF waves in the Pc5 frequency range (1.7-6.7 mHz) on the basis of multiple-beam line-of-sight ionospheric plasma velocity data obtained by the Hokkaido East/West and other SuperDARN radars. Next, we conducted a statistical analysis of the resultant wave properties to reveal the magnetic latitude (MLAT) and magnetic local time (MLT) dependence of the primary modes and m-number. The statistical results show that in the mid-latitude region, the occurrence rate of both poloidal and toroidal Pc5 waves was high at premidnight and postmidnight, and toroidal mode Pc5 waves occurred more frequently than poloidal ones. Furthermore, we checked the geomagnetic and solar activity dependence of the occurrence rates of both modes. We discussed possible driving mechanisms for generating these Pc5 waves other than the field line resonance (FLR) as the FLR at these latitudes should yield much higher eigenfrequencies than the frequencies observed in this study.

R006-33
A 会場 ：11/7　AM2 （10:45-12:30）
12:15〜12:30

#田中　健太郎 [1)], 大矢　浩代 [1)], 土屋　史紀 [2)], 塩川　和夫 [3)], 三好　由純 [3)], 寺本　万里子 [4)], 野崎　憲朗 [5)],Connors Martin[6)], 中田　裕之 [1)]
([1] 千葉大・工・電気,[2] 東北大・理・惑星プラズマ大気,[3] 名大宇地研,[4] 九工大,[5] 電通大,[6]Centre for Science, Athabasca Univ.

ULF-modulated energetic electron precipitation in magnetically quiet time using OCTAVE VLF/LF observations

#Kentaro Tanaka[1)], Hiroyo Ohya[1)], Fuminori Tsuchiya[2)], Kazuo Shiokawa[3)], Yoshizumi Miyoshi[3)], Mariko Teramoto[4)], Kenro Nozaki[5)], Martin Connors[6)], Hiroyuki Nakata[1)]
([1]Engineering, Chiba Univ.,[2]Planet. Plasma Atmos. Res. Cent., Tohoku Univ.,[3]ISEE, Nagoya Univ.,[4]Kyutech,[5]UEC,[6]Centre for Science, Athabasca Univ.

Energetic electron precipitation (EEPs, >100 keV) from radiation belts to the D-region ionosphere during substorms has been studied since the 1960's using very-low frequency (VLF, 3-30 kHz)/low frequency (LF, 30-300 kHz) transmitter signals and riometers (Thorne and Larsen, 1976). Modulation of D-region due to EEP by ultra-low frequency (ULF) waves during a substorm was reported (Miyashita et al., 2020). However, there was only one report for the EEP associated with ULF modulation using VLF/LF transmitter signals. In this study, we investigate the EEP event associated with the ULF modulation that occurred on 11:15-11:40 UT on October 9, 2017 (magnetically quiet time), using VLF/LF transmitter signals of "Observation of CondiTion of ionized Atmosphere by VLF Experiment (OCTAVE)" network. The VLF/LF transmitter signals from four transmitters (NLK, NDK, WWVB and NAA, USA) were received at Athabasca (ATH), Canada. We found oscillations in intensities on the NDK-ATH and NLK-ATH paths with a period of 200-300 s during magnetically quiet time in 11:00-12:00 UT on 9 October, 2017. However, the VLF/LF oscillations were not seen on the WWVB-ATH path. The calculation results based on wave-hop method showed that even if the height decreases due to the EEPs, the electric field strength of WWVB-ATH path would oscillate. Because of the characteristics of the WWVB-ATH path, we considered that there were no variations in the WWVB-ATH amplitude during the EEPs. H-component of magnetic field variations (Δ B_H) at ATH and the low latitudes in the wide longitudes also oscillated with the same periods of 200-300 s. The VLF waves and magnetic data were almost in-phase. It is reported that when the solar wind speed is less than 300 km/s, Pi2 pulsations with a long period (>200 s) is generated by the cavity mode of the magnetosphere (Kwon et al., 2013). We concluded that the VLF oscillations showed EEPs modulated by Pi2 ULF magnetic pulsation. In this presentation, we will discuss the cause of the VLF/LF oscillations in detail.

R006-34
A 会場 ：11/7　PM1 （13:45-15:30）
13:45〜14:00

#Porunakatu Radhakrishna Shreedevi[1,2)],Yu Yiqun[1)],Miyoshi Yoshizumi[2)],Tian Xingbin[1)],Kumar Sandeep[2)],Nakamura Satoko[2)],Jun Chae-Woo[2)],Shiokawa Kazuo[2)],Jordanova Vania[3)],Hori Tomo[2)],Asamura K[4)],Shinohara I[4)],Yokota S[5)],Kasahara S[6)],Keika K[6)],Matsuoka A[7)]
[(1]BUAA,[(2]ISEE,[(3]LANL,[(4]ISAS/JAXA,[(5]Osaka University,[(6]University of Tokyo,[(7]Kyoto University

EMIC wave induced proton precipitation during the 27-28 May 2017 storm: Modelling and Observations

#Shreedevi Porunakatu Radhakrishna[1,2)], Yiqun Yu[1)], Yoshizumi Miyoshi[2)], Xingbin Tian[1)], Sandeep Kumar[2)], Satoko Nakamura[2)], Chae-Woo Jun[2)], Kazuo Shiokawa[2)], Vania Jordanova[3)], Tomo Hori[2)], K Asamura[4)], I Shinohara[4)], S Yokota[5)], S Kasahara[6)], K Keika[6)], A Matsuoka[7)]
[(1]BUAA,[(2]ISEE,[(3]LANL,[(4]ISAS/JAXA,[(5]Osaka University,[(6]University of Tokyo,[(7]Kyoto University

Electro Magnetic Ion Cyclotron (EMIC) waves are known to cause the ion precipitation into the mid-latitude ionosphere during geomagnetic storms. Recent studies have shown that the ion precipitation induced by EMIC waves can contribute significantly to the total energy flux deposited into the ionosphere and severely affect the magnetosphere-ionosphere coupling. In this study, the temporal and spatial evolution of the proton precipitation into the ionosphere and its correspondence to the EMIC wave activity in the inner magnetosphere is examined using simulations of the BATSRUS+RAM-SCBE model. During the geomagnetic storm of 27-28 May 2017, the Van Allen Probes observed typical signatures of EMIC waves in the inner magnetosphere i.e., at 4 to 6 Re in the evening sector. Ground magnetometers at high latitude stations also showed the presence of PC1/EMIC waves after 1600 UT on 27 May 2017. During the main phase of the storm, the DMSP satellites observed enhanced proton precipitation at locations where the ground/space-based magnetic field measurements detected enhanced EMIC wave activity. The source and distribution of proton temperature anisotropy in the equatorial plane associated with EMIC waves are investigated to understand the excitation of the waves. A comparison of the precipitating proton fluxes obtained from the simulations with the particle measurements from the DMSP satellites show that EMIC wave scattering can account for the 30 keV proton precipitation at subauroral latitudes. The results are also compared with the proton fluxes/EMIC wave activity measured by the Arase satellite.

R006-35
A 会場 ：11/7　PM1 （13:45-15:30）
14:00〜14:15

３年間の地上多点観測データを用いたサブオーロラ帯の銀河電波吸収の増強の統計解析

#加藤　悠斗[1)], 塩川　和夫[1)], 田中　良昌[2,3,5)], 尾崎　光紀[4)], 門倉　昭[2,3,5)], 大山　伸一郎[1,5,9)], 西谷　望[1)],Oinats Alexey[6)],Baishev　Dmitry[8)],Connors　Martin[7)]
([1] 名大 ISEE,[2] 情報システム研究機構 / 極域環境データサイエンスセンター,[3] 総研大,[4] 金沢大,[5] 極地研,[6] ロシア太陽地球系物理学研究所,[7] アサバサカ大学,[8] ロシア宇宙物理学・航空学研究所,[9] オウル大学

Study of steep increases of cosmic noise absorption at subauroral latitudes using 3-year multipoint ground-based observations

#Yuto Kato[1)], Kazuo Shiokawa[1)], Yoshimasa Tanaka[2,3,5)], Mitsunori Ozaki[4)], Akira Kadokura[2,3,5)], Shin ichiro Oyama[1,5,9)], Nozomu Nishitani[1)], Alexey Oinats[6)], Dmitry Baishev[8)], Martin Connors[7)]
([1]ISEE, Nagoya Univ.,[2]Joint Support-Center for Data Science Research / Polar Environment Data Science Center,[3]The Graduate University for Advanced Studies,[4]Kanazawa Univ.,[5]National Institute of Polar Research,[6]Institute of Solar-Terrestrial Physics, Irkutsk, Russia,[7]Athabasca University, Canada,[8]Yu.G.Shafer Institute of Cosmophysical Research and Aeronomy, Yakutsk, Russia,[9]University of Oulu, Oulu, Finland

Electron density enhancements in the ionospheric D-region due to the precipitation of high-energy electrons (>30 keV), have been measured as increasing in cosmic radio noise absorption (CNA) using ground-based riometers. However, there have been few studies of CNA observations at multi-point stations distributed in longitudes at subauroral latitudes. Thus, the spatio-temporal development of the global distribution of CNA at subauroral latitudes is not well understood. In this study, we analyzed the longitudinal development of CNA using simultaneous riometer observations at six stations at subauroral latitudes in Canada, Alaska, Russia, and Iceland over 3 years from 2017 to 2020. These stations are located encircling the earth at ˜60 degree magnetic latitudes. In order to study CNA produced by the substorm particle injection, we focused on the steep enhancements of CNA that is defined as dCNA/dt larger than 0.04 dB/min at the CNA onset with maximum amplitudes larger than 0.4 dB within 30 min. The occurrence rate of these CNA enhancements tends to be larger at nightside to the morning (˜0.02-0.05 events per hour), suggesting that the CNA enhancements are associated with substorm electron injections and eastward electron drift. In the presentation we will also discuss the expansion velocity of CNA, associated electron energy ranges, based on the timing difference of the CNA onsets between two neighboring stations, their dependence on solar wind and substorm indices, and magnetospheric ELF/VLF waves through superposed epoch analysis.

R006-36
A 会場 ：11/7　PM1 （13:45-15:30）
14:15〜14:30

ベイズ推定を活用したプラズマ波動の伝搬方向推定手法の詳細評価

#田中　裕士[1)], 太田　守[2)], 松田　昇也[1)], 笠原　禎也[1)]
[(1] 金沢大,[(2] 富山高専

Detailed Evaluation with Bayesian k-vector Estimation Method for Plasma Waves

#Yuji Tanaka[1)], Mamoru Ota[2)], Shoya Matsuda[1)], Yoshiya Kasahara[1)]
[(1]Kanazawa Univ.,[(2]National Institute of Technology, Toyama College

The analysis of plasma waves obtained from in-situ observation by scientific satellites is effective for understanding the physics of near-Earth space and space plasmas in general. k-vector direction of plasma waves, using plasma wave characteristics and remote sensing technology, provides information for understanding the global features of space plasma.

k-vector direction is generally estimated from a spectral matrix, which is the electromagnetic field's correlation matrix. Ideally, determining the k-vector direction including the absolute direction requires the observation results of at least 5-electromagnetic field components. However, there is often a need for k-vector direction estimation in situations where some sensors are missing due to sensor damage or some constraints of the scientific satellites. Further, k-vector should be estimated with different sensor noise levels.

In this study, we introduce a k-vector estimation method based on the wave distribution function method [Storey+, 1979, Storey+, 1980]. The method is based on the Bayesian inference, so the extent of estimation accuracy can easliy visualized. Using this method, we evaluated the extent of estimation accuracy considering the number of sensors and the noise integration kernel [Tanaka+, 2021].

References

[Storey+, 1979] L. R. O. Storey and F. Lefeuvre, The analysis of 6-component measurements of a random electromagnetic wave field in a magnetoplasma - I. The direct problem, Geophysical Journal of the Royal Astronomical Society, vol. 56, no. 2, 1979.

[Storey+, 1980] L. R. O. Storey and F. Lefeuvre, The analysis of 6-component measurements of a random electromagnetic wave field in a magnetoplasma - II. The integration kernels, Geophysical Journal of the Royal Astronomical Society, vol. 62, no. 1, 1980.

[Tanaka+, 2021] Y. Tanaka, M.Ota and Y. Kasahara, Noise integration kernel design for the wave distribution function method: robust direction finding with different sensor noise levels, Radio Science, vol. 56, no. 9, 2021.

R006-37
A 会場 ：11/7　PM1 （13:45-15:30）
14:30〜14:45

あらせ衛星で観測されるコーラスに関連した静電波の出現特性

#江田　大輝[1)], 栗田　怜[2)], 吉田　永遠[3)], 小嶋　浩嗣[4)], 笠原　禎也[5)], 松田　昇也[6)], 松岡　彩子[7)], 中村　紗都子[8)], 三好　由純[9)], 篠原　育[10)]
([1] 京大院工,[2] 京都大学 生存研,[3] 京大,[4] 京大・生存圏,[5] 金沢大,[6] 金沢大学,[7] 京都大学,[8]IAR&ISEE,[9] 名大 ISEE,[10] 宇宙研／宇宙機構

Occurrence characteristics of electrostatic waves associated with whistler mode chorus observed by the Arase satellite

#Eda Daiki[1)], Satoshi Kurita[2)], Towa Yoshida[3)], Hirotsugu Kojima[4)], Yoshiya Kasahara[5)], Shoya Matsuda[6)], Ayako Matsuoka[7)], Satoko Nakamura[8)], Yoshizumi Miyoshi[9)], Iku Shinohara[10)]
([1]Engineering, Kyoto U.,[2]RISH, Kyoto Univ.,[3]Engineering, Kyoto U.,[4]RISH, Kyoto Univ.,[5]Kanazawa Univ.,[6]Kanazawa Univ.,[7]Kyoto University,[8]IAR&ISEE,[9]ISEE, Nagoya Univ.,[10]ISAS/JAXA

Electrostatic waves associated with whistler mode chorus waves have been observed in the magnetosphere. Reinleitner et al. (1983) reported the electrostatic waves associated with chorus waves. The electrostatic waves have dominant wave power in the direction parallel to the ambient magnetic field. The similar phenomenon is reported in Li et al. (2017) based on the Van Allen Probes observation. These studies suggest that the electrostatic waves are excited by electron beams, which are generated by the landau resonance between electrons and chorus waves. However, since these studies discuss only a few events, further data analysis is necessary to reveal the mechanism of the event that chorus waves cause the electrostatic waves. Therefore, in this study, we aimed to examine this chorus-induced electrostatic waves by analyzing the relationship of these waves using the data obtained by the Arase satellite in statistical sense.

We used OFA-MATRIX data to determine the electric field components perpendicular and parallel to the background magnetic field projected onto the satellite spin plane. These electric field components were used to identify the electrostatic waves reported by the previous studies. We successfully identified a large number of the narrowband and broadband electrostatic waves associated with chorus waves. To investigate the relationship between the spectral shape of chorus and the occurrence of the electrostatic waves, we calculated the power of lower-band (0.1-0.45 fce), inter-band (0.45-0.5 fce), and upper-band (0.5-0.8 fce) chorus to automatically determine the spectral shape of chorus associated with the electrostatic waves. We found that the electrostatic waves are associated with banded chorus that has a wave power gap at 0.5 fce. The electrostatic waves are also accompanied by the chorus without a wave power gap at 0.5fce. The electrostatic waves are observed near the magnetic equator on the night side. In addition, the electrostatic waves associated with lower-band chorus were observed not only near the magnetic equator but also at the mid-latitudes.

We also analyzed the bandwidth of the electrostatic waves. The electrostatic waves with the bandwidth wider than 2kHz were mostly observed near the magnetic equator on the nightside, while the electrostatic waves with the bandwidth narrower than 2kHz were also observed at the mid-latitude on the dayside. We analyzed the relationship between the bandwidth of the electrostatic waves and the spectral structure of chorus. We found that the broadband electrostatic waves are associated with banded chorus that has no gap. In the presentation, we show the analysis results mentioned above, and discuss the physical mechanism based on the theory of the landau resonance between electrons and chorus emissions [Omura et al., 2009; Yagitani et al., 2014].

地球磁気圏では、コーラスに関連した静電波が観測されており、Reinleitner et al.(1983) ではコーラスに伴って磁力線平行方向に電界が卓越した静電波が報告されている。Li et al.(2017) でも類似の現象が報告されており、コーラスが静電波を励起する現象について議論している。これらの研究によれば、コーラス波動と電子のランダウ共鳴により電子が磁力線平行方向に加速され、この電子により静電波が励起されると考えられている。しかし、これらの論文で議論されている事例は数例にとどまっているため、コーラスが静電波を励起する現象の全容解明には更なるデータ解析が必要であると考えられる。そこで本研究では、あらせ衛星に搭載されているプラズマ波動観測器 PWE の受信器の一つである OFA で取得されたデータを用いて、コーラスと静電波の関係を統計的に解析し、この現象の物理過程を理解することを目的とする。

OFA によって取得されるデータのうち、電界 2 成分から得られたスペクトルマトリックス (OFA-MATRIX) のデータを用いて、スピン面内における背景磁場に垂直および平行な電界成分とその比を求めることにより、静電波の自動抽出を試みた。その結果、コーラスに関連した静電波には、狭帯域および広帯域にわたるものが多数確認された。次に、コーラスを lower-band(0.1-0.45 fce), inter-band(0.45-0.5 fce), upper-band(0.5-0.8 fce) の 3 つの帯域に分け、各帯域のパワーを計算し、静電波と関係性の強いコーラスのスペクトル構造の同定と、その空間分布を求めた。その結果、0.5fce に強度のギャップをもつバンド状のコーラスと、lower-band から upper-band まで繋がったコーラスに関連する静電波が、夜側磁気赤道付近で多く観測されることが分かった。また、lower-band のみに関連する静電波は中緯度でも見られた。

次に、静電波の周波数幅について解析を行った。周波数幅と磁気緯度及び磁気地方時の関係について解析したところ、周波数幅が 2kHz 以上の静電波はほとんど夜側磁気赤道付近で観測された一方、2kHz 以下の静電波は中緯度及び昼側でも観測された。また、コーラスの各帯域と静電波の周波数幅の関係について解析を行った結果、広帯域の静電波は gap の

無いバンド状のコーラスに関連していることが分かった。

発表では、上記の解析結果を示すとともに、これらの解析結果についてコーラス波動のランダウ共鳴に関する理論 [Omura et al.(2009); Yagitani, et al.(2014)] に基づいて考察した結果を報告する予定である。

R006-38
A 会場 ：11/7　PM1 （13:45-15:30）
14:45〜15:00

Arase 衛星を用いた高緯度・プラズマポーズ近傍におけるホイッスラーモードコーラスのダクト伝搬の事例解析

#安福　友梨 [1)], 土屋　史紀 [1)], 栗田　怜 [2)], 笠羽　康正 [1)], 加藤　雄人 [3)], 吹澤　瑞貴 [4)], 三好　由純 [5)], 篠原　育 [6)], 笠原　禎也 [6)], 松田　昇也 [7)], 熊本　篤志 [3)], 松岡　彩子 [8)], 中村　紗都子 [5)], 北原　理弘 [3)]
([1] 東北大学 惑星プラズマ大気研究センター,[2] 京都大学 生存圏研究所,[3] 東北大学 理学研究科,[4] 国立極地研究所,[5] 名古屋大学 宇宙地球環境研究所,[6] 宇宙科学研究所,[7] 金沢大学 自然科学研究科,[8] 京都大学 理学研究科

Ducted propagation of whistler mode chorus waves observed by the Arase satellite near the plasmapause at high latitudes

#Yuri Ampuku[1)], Fuminori Tsuchiya[1)], Satoshi Kurita[2)], Yasumasa Kasaba[1)], Yuto Katoh[3)], Mizuki Fukizawa[4)], Yoshizumi Miyoshi[5)], Iku Shinohara[6)], Yoshiya Kasahara[6)], Shoya Matsuda[7)], Atsushi Kumamoto[3)], Ayako Matsuoka[8)], Satoko Nakamura[5)], Masahiro Kitahara[3)]
([1]Planetary Plasma and Atmospheric Research Center, Tohoku University,[2]Research Institute for Sustainable Humanosphere, Kyoto University,[3]Graduate School of Science, Tohoku University,[4]National Institute of Polar Research,[5]Institute for Space-Earth Environmental Research, Nagoya University,[6]Japan Aerospace Exploration Agency, Institute of Space and Astronautical Science,[7]Graduate School of Natural Science and Technology, Kanazawa University,[8]Graduate School of Science, Kyoto University

Whistler mode chorus is a type of plasma waves generated near the geomagnetic equator by wave-particle interactions. Chorus scatters pitch angle of energetic electrons and causes the electrons to precipitate into the atmosphere. The resonance energy of electrons becomes higher as the wave propagates at higher latitudes, resulting in the scattering of relativistic electrons into the loss cone. Thus, the propagation of chorus is of great importance for the generation of microbursts and resultant loss of radiation belt electrons. The loss of radiation belt electrons results in significant ionization of the upper atmosphere as well as an impact on the middle atmosphere. The mechanism of the chorus propagation from the equator to higher latitudes has not been clarified. One of the most promising theories is the propagation along a field-aligned density duct. However, only a few observations of chorus propagating in duct structures have been reported [Chan et al. 2021, Haque et al. 2011, Moullard et al. 2002]. In this study, we report on chorus propagating in duct structures observed by the Arase satellite near the plasmapause at the geomagnetic latitude of $>10^o$.

During the period from April to July in 2017 and 2018, we identified 23 cases of chorus propagating in the duct-like structure near the plasmapause with Plasma Wave Experiment (PWE) / Onboard Frequency Analyzer (OFA). We examined properties of the chorus for three cases: (1) a duct-like structure characterized by density enhancement at geomagnetic latitude of -14^o and McIlwain L of 4.2 at 11:30 UT, June 6, 2018, (2) density depression, geomagnetic latitude of -14.2^o and McIlwain L of 4.3 at 11:32 UT, June 6, 2018, (3) density depression, geomagnetic latitude of 32.2^o and McIlwain L of 4.6 at 02:52 UT, July 14, 2017.

We estimated the wave normal angles (WNAs) using the Singular Value Decomposition (SVD) method [Santolik et al., 2003] with the assumption on the presence of a single plane wave. We used the background magnetic vector observed by Magnetic Field Experiment (MGF), the spectral matrix of the magnetic field component of chorus observed by OFA for the estimation using the SVD method. We obtained a theoretical relation between the wave frequency and the electron density which satisfies the Snell's law and the dispersion relation with the quasi-longitudinal approximation using the WNAs. We compared the theoretical relation with the observed electron density and the chorus frequency range.

The observational results for each case are as follows. (1) The WNAs were concentrated around 0 deg. The observed chorus was LBC that was consistent with the dispersion relation with WNA=0 deg. (2) The WNAs were scattered around 0 deg – Gendrin angle(θ_G). The observed chorus was LBC that was consistent with the dispersion relation with WNA=0 deg – θ_G. (3) The WNAs were concentrated around θ_G. The observed chorus was LBC that was consistent with the dispersion relation between WNA=0 deg and WNA= θ_G. We examined other events in the same way and identified 10, 11, and 2 events in total which were categorized as cases (1), (2), and (3), respectively.

We interpreted each result based on ducting theory. Case (1) was consistent with the ducting theory for the LBC propagating along the density enhancement with WNA of around 0 deg, Case (2) the ducting theory along the density depression with WNAs distributed between 0 deg and θ_G, and Case (3) the ducting theory along the density depression with WNAs of around θ_G. We discuss the planarity of the observed chorus waves derived from the SVD method. The planarity close to 1 means that the wave can be regarded as a single plane wave. For Case (1), the planarity of the observed chorus was about 0.8. For Cases (2) and (3), the planarity of the observed chorus was about 0.3 – 0.6, similar value to the background noise floor. Therefore, the WNAs are not reliable. There are two possibilities for the low planarity. Based on

the ducting theory, LBC ducting along the density depression could have wide WNA. If chorus waves with various WNAs coexist, the planarity is evaluated to low. The planarity is evaluated to be a lower value if the amplitude of the observed chorus is not large enough compared to the noise floor.

To investigate characteristics of the low planarity in the density depression duct, we plan to perform detailed analysis for ducted chorus events for which waveform data observed by PWE/Waveform Capture (WFC) is available.

ホイッスラーモードコーラス波 (以下、コーラス) は、波動粒子相互作用により磁気赤道面付近で発生する。コーラスによりピッチ角散乱を受けた高エネルギー電子は極域に降下し、diffuse aurora を発生させる。特に、高緯度に伝搬したコーラスは電子との共鳴エネルギーが高くなり、相対論的電子を大気に降下させうるため、マイクロバーストの発生、放射線帯電子の消失、中層大気への影響といった観点で注目されている。コーラスを高緯度まで減衰することなく伝搬させるメカニズムとして、磁力線に沿って電子密度が増加/減少した「ダクト構造」内の伝搬が有力とされてきた。しかし、ダクト構造内を伝搬するコーラスの観測例は数例にとどまり [Chan et al. 2021, Haque et al. 2011, Moullard et al. 2002]、コーラスの伝搬特性は明らかとなっていない。本研究では、磁気緯度 10 度以上の領域で Arase 衛星がとらえた、ダクト構造内を伝搬するとみられるコーラスの観測を複数例示す。

Arase 衛星の遠地点が朝側に位置していた 2017 年 4 – 7 月及び 2018 年 4 – 7 月の観測データから、電子密度の増加/減少によるダクト構造とダクト内を伝搬するとみられるコーラスをプラズマポーズ近傍で 23 例同定した。そのうち、電子密度変化とそれに対応するコーラスの強度変化が明瞭な 3 例について詳細な解析を行った。

Arase 衛星に搭載された Plasma Wave Experiment (PWE) の High Frequency Analyzer (HFA) は (1) 2018 年 6 月 6 日 11:30 UT、磁気緯度-14 度、L 値 4.2 にて、電子密度の増加によるダクト構造を、(2) 2018 年 6 月 6 日 11:32 UT、磁気緯度-14.2 度、L 値 4.3 と (3) 2017 年 7 月 14 日 02:52 UT、磁気緯度 32.2 度、L 値 4.6 にて、電子密度の減少によるダクト構造を観測した。Onboard Frequency Analyzer (OFA) はこれらのダクト内を伝搬するとみられるコーラスを観測した。単一平面波近似の下、Singular Value Decomposition(SVD) 法 [Santolik et al., 2003] によりコーラスの wave normal angle (WNA) を導出した。この際、OFA が計算した磁界スペクトルマトリクス、Magnetic Field Experiment (MGF) が観測した背景磁場ベクトルを使用した。さらに、背景磁場強度と WNA をスネルの法則と準縦方向近似した分散関係式に当てはめ、コーラスの周波数とコーラスが伝搬可能な電子密度の関係を得た。この周波数と電子密度の関係を、OFA が観測したコーラスの周波数帯及び HFA が観測した電子密度と比較した。その結果、(1) のコーラスの WNA は 0 deg 付近に集中していた。周波数は、WNA=0 deg の分散関係に対応した lower-band chorus(LBC) の帯域であった。 (2) のコーラスの WNA は 0 deg – Gendrin angle(θ_G) 付近に広がっていた。周波数は WNA=0 deg から θ_G にまたがる分散関係に対応した LBC の帯域であった。 (3) のコーラスの WNA は θ_G 付近に集中していた。周波数は WNA=0 deg と WNA= θ_G の中間となる分散関係に対応した LBC の帯域であった。23 例のコーラスについて同様の解析を行い、(1)、(2)、及び (3) の特徴を示すコーラスをそれぞれ 10 例、11 例、2 例確認した。

ダクト伝搬理論より、減少ダクトにトラップされる LBC には WNA が 0 deg から θ_G 付近に跨るモードと WNA が θ_G 付近で伝搬するモード、増加ダクトにトラップされる LBC には WNA=0 deg 付近で伝搬するモードが存在できると予測されている。3 つに分類されたコーラスの観測結果をダクト伝搬理論に基づいて解釈すると、(1) は増加ダクトに沿った WNA が 0 deg 付近となる LBC のダクト伝搬、(2) は減少ダクトに沿った WNA が 0 deg – θ_G 付近となる LBC のダクト伝搬、(3) は減少ダクトに沿った WNA が θ_G 付近となる LBC のダクト伝搬と捉えて矛盾がないことが明らかになった。また、SVD 法で計算した観測したコーラスの planarity について議論する。planarity が 1 に近いほど SVD 法における単一平面波近似の妥当性が高い。(1) のタイプではいずれのイベントも planarity は 0.8 程度であった。よってコーラスは単一の平面波と仮定でき、伝搬角解析の結果の信頼性は高いと判断できる。一方、(2)、(3) のタイプのイベントでは、いずれのイベントも planarity が 0.3 – 0.6 前後で背景ノイズの planarity と同程度の値であった。よって伝搬角解析結果の信頼度は低いと言える。(2)、(3) のイベントで planarity が低くなる理由は 2 点考えられる。1 点目は、ダクト伝搬理論に基づくと減少ダクト内での LBC の伝搬モードは 2 通り存在することから、波面の異なる複数の LBC が重なっている可能性である。2 点目は、観測装置のノイズレベルに対して解析したコーラスの磁場成分の強度が十分でないため planarity がより低く計算されている可能性である。

本講演では、信頼性の高い伝搬角解析結果を得るため、PWE の Waveform Capture (WFC) による波形データが存在するイベントの解析事例を併せて報告予定である。

R006-39
A 会場 ：11/7　PM1 （13:45-15:30）
15:00〜15:15

#風間　洋一[1)], 栗田　怜[2)], 三好　由純[3)], 加藤　雄人[4)], 小嶋　浩嗣[5)], 笠原　禎也[6)], 田　采祐[7)], 堀　智昭[3)],Wang B.-J.[8)],Wang　S.-Y.[9)],Tam　Sunny W. Y.[10)],Chang　T. F.[11)], 浅村　和史[12)], 松田　昇也[13)], 土屋　史紀[14)], 熊本　篤志[14)], 中村　紗都子[15)], 松岡　彩子[16)], 寺本　万里子[17)], 高島　健[18)], 篠原　育[19)]
([1ASIAA,([2 京都大学 生存研,([3 名大 ISEE,([4 東北大・理・地球物理,([5 京大・生存圏,([6 金沢大,([7 名大 ISEE 研,([8ASIAA, Taiwan,([9 台湾・中央研究院,([10 国立成功大学宇宙・プラズマ科学研究所,([11 台湾・國立成功大学,([12 宇宙研,([13 金沢大学,([14 東北大・理・惑星プラズマ大気,([15IAR&ISEE,([16 京都大学,([17 九工大,([18 宇宙研,([19 宇宙研／宇宙機構

Banded chorus and no-gap chorus: What makes the difference?

#Yoichi Kazama[1)], Satoshi Kurita[2)], Yoshizumi Miyoshi[3)], Yuto Katoh[4)], Hirotsugu Kojima[5)], Yoshiya Kasahara[6)], Chae-Woo Jun[7)], Tomoaki Hori[3)], B.-J. Wang[8)], S.-Y. Wang[9)], Sunny W. Y. Tam[10)], T. F. Chang[11)], Kazushi Asamura[12)], Shoya Matsuda[13)], Fuminori Tsuchiya[14)], Atsushi Kumamoto[14)], Satoko Nakamura[15)], Ayako Matsuoka[16)], Mariko Teramoto[17)], Takeshi Takashima[18)], Iku Shinohara[19)]
([1ASIAA,([2RISH, Kyoto Univ.,([3ISEE, Nagoya Univ.,([4Dept. Geophys., Grad. Sch. Sci., Tohoku Univ.,([5RISH, Kyoto Univ.,([6Kanazawa Univ.,([7ISEE, Nagoya Univ.,([8ASIAA, Taiwan,([9ASIAA, Taiwan,([10Institute of Space and Plasma Sciences, National Cheng Kung University, Taiwan,([11PSSC, NCKU, Taiwan,([12ISAS/JAXA,([13Kanazawa Univ.,([14Planet. Plasma Atmos. Res. Cent., Tohoku Univ.,([15IAR&ISEE,([16Kyoto University,([17Kyutech,([18ISAS, JAXA,([19ISAS/JAXA

Whistler-mode chorus wave is a high-intensity plasma wave frequently observed in the inner magnetosphere. Chorus wave is sometimes characterized by its distinct emission gap near the electron half-gyrofrequency. The mechanism of forming an emission gap has been intensively studied, but a consensus has not yet been reached. One of the candidates is the Landau damping. If the Landau damping causes the emission gap of chorus wave, a correlation between chorus emissions and resonant electrons can be expected. In this presentation, we discuss the results of an analysis of the relation between fluxes of resonant electrons and interband emissions of chorus by using Arase satellite observations.

R006-40
A 会場 ：11/7　PM1 （13:45-15:30）
15:15〜15:30

#謝　怡凱 [1)], 大村　善治 [2)]
([1 京大生存研,([2 京大・生存圏

Energetic electron precipitation induced by very oblique chorus waves in the Earth's inner magnetosphere

#Yikai Hsieh[1)], Yoshiharu Omura[2)]
([1RISH, Kyoto Univ.,([2RISH, Kyoto Univ.

Electrons trapped in the Earth's magnetic field can be scattered by whistler-mode chorus emissions and precipitate into the Earth's upper atmosphere. Whistler mode chorus waves propagating in the Earth's inner magnetic field are not always parallel or quasi-parallel to the magnetic field line. Sometimes the waves are observed with very large wave normal angles. We aim to figure out the relation between the large wave normal angles and electron precipitation. In this study, our target chorus emissions contain large wave normal angles, which are 90 percent of the resonance cone angle. We use test-particle simulation to trace the behaviors of electrons interacting with the waves and create a Green's function set for electrons initially at kinetic energies 10-6000 keV and equatorial pitch angles 5-89 degrees. We also calculate the Green's function sets for parallel and slightly oblique chorus waves for comparison. The simulation results show that the very oblique chorus waves contribute to more electron precipitation than the other two chorus wave models, especially at 50-100keV. At this range, the electron precipitation rates of the very oblique case are about 1.5 and 1.2 times those of the parallel and slight oblique cases, respectively. Checking the highest initial equatorial pitch angles of the precipitated electrons, we find that the very oblique chorus waves can precipitate electrons from greater than 45 degrees. In contrast, the other chorus waves can only precipitate electrons from less than 30 degrees. Furthermore, we theoretically derive the precipitation rate and verify that nonlinear trapping via the n=-1 anomalous cyclotron resonance contributes to effective electron precipitation in the very oblique chorus wave-particle interactions.

R006-P01
ポスター 1 ：11/4　PM1/PM2 （13:45-18:15）

Echo state network によるサブストーム活動の確率モデル

#中野　慎也 [1,2)], 片岡　龍峰 [3)]
[(1] 統計数理研究所,[(2] データサイエンス共同利用基盤施設データ同化研究支援センター,[(3] 国立極地研究所

Probabilistic model of substorm activity based on an echo state network

#Shin'ya Nakano[1,2)], Ryuho Kataoka[3)]
[(1]The Institute of Statistical Mathematics,[(2]Center for Data Assimilation Research and Applicatios,[(3]National Institute of Polar Research

A substorm is one of fundamental physical phenomenon in the magnetosphere-ionosphere system. Since a substorm is a main cause of geomagnetic disturbances in the polar ionosphere which may affect electric infrastructure, many studies have attempted to predict the substorm onsets. However, those studies showed that the prediction of each individual substorm occurrence is highly difficult.

In this study, we hypothesize the difficulty in the prediction of a substorm onset is due to the stochastic nature of a substorm. In order to consider the stochastic occurrences of substorms, we represent the sequence of substorm onsets with a nonstationary Poisson process, which is a probabilistic model describing event time series. The occurrence rate of substorms is then modelled with an echo state network model. The echo state network is a kind of recurrent neural networks where the connections and weights between hidden state variables are fixed. We use solar wind data as inputs of the echo state network model.

After training the model with the solar wind data and a substorm event list for 11 years, we calculated the occurrence rate of substorms for artificial solar-wind conditions. The results show that the following well-known characteristics are reproduced with our model.

1. Substorm occurrences are mainly controlled by IMF Bz and solar-wind velocity.
2. Short-term variations of IMF Bz and solar-wind velocity are not likely to be effective for substorm occurrences. The occurrence rate is highly enhanced after a few hours of duration of high-speed solar wind with southward IMF.

In addition, the result suggests the followings.

3. The expected substorm occurrence rate is also highly controlled by solar wind density.
4. Substorm occurrences appear to be stochastic during a long duration of southward IMF.

These results show that the probabilistic model is effective for describing
substorm activity.

R006-P02
ポスター 1 ：11/4　PM1/PM2 （13:45-18:15）

定常状態における磁気圏 dynamics による Null-separator 構造が作る磁場構造の変形について

#藤田　茂 [1)], 渡辺　正和 [2)], 蔡　東生 [3)], 田中　高史 [4)]
([1] データサイエンスセンター/統数研,[2] 九大・理・地惑,[3] 筑波大・シス情,[4] 九大・国際宇宙天気科学教育センター

Deformation of he null-separator structure by the plasma dynamics in the stationary magnetosphere

#Shigeru Fujita[1)], Masakazu Watanabe[2)], DongSheng Cai[3)], Takashi Tanaka[4)]
([1]ROIS-DS/IMS,[2]Earth & planetary Sci., Kyushu Univ.,[3]ISIS, U Tsukuba,[4]REPPU code Institute,

The open magnetosphere model advocated by Dungey (1962) is accepted widely as the model of explaining the magnetosphere-ionosphere convection system. Later, the open model evolves into a 3D magnetic field topology formed by the solar wind-magnetosphere interaction [Cowley, 1973; Stern, 1973]. The null points and the separator lines characterize the 3D magnetic topology [Lau and Finn, 1990; Siscoe et al., 2000]. Identification of the null points and separator lines is useful to classify the topology mathematically, but it seems a symbolized one. For example, only information about the null points and the separator lines is not useful to understand the interaction between the magnetic field associated with the null-separator magnetic field topology and the plasma dynamics because only that information does not show the real configuration of the magnetic field. We newly developed a simple method of drawing the boundary surfaces between different magnetic field regimes. In the talk, we will present the preliminary results of the interaction between the magnetic field derived from the null-separator structure and the plasma dynamics in the stationary condition.

The main findings of this research are as follows;

1) The dipole magnetic field superposed by a uniform field forms a torus by closed field lines and, at the same time, two cylinders extending parallel and anti-parallel to the IMF direction [Lau and Finn, 1990]. In the solar wind environment, the two cylinders are extended anti-sunward direction by the solar wind and form the lobes in the northern and southern hemispheres. Furthermore, the cylinder in the vacuum condition is deformed to a narrow slot extending anti-sunward. The torus of the closed field lines is also extended anti-sunward direction by the solar wind. The plasma sheet is formed as a sandwiched region between the two cylinders. In the tail region behind the torus of the closed field lines (that is to say, the plasma sheet), the two cylinders are separated and the distance between the cylinders becomes gradually large. The magnetic field of the solar wind intrudes the wedge-type region between the two cylinders in the equatorial region beyond the plasma sheet.

2) The slot of the open field lines in the magnetotail plays an interesting role in the magnetospheric dynamics as the window across which plasma electromagnetic energy enters into the magnetosphere. When IMF is northward, the slot is located in the magnetopause near the plasma sheet. The magnetic field intensity is weaker there. Thus, this configuration promotes the plasma plume in the lobe. This mechanism of the plume will work with that explained by Ebihara and Tanaka [2016]. On the other hand, in the southward IMF condition, the slot appears apart from the plasma sheet in the magnetopause where the magnetic field intensity is rather stronger. Then, the plasma plume seems to be suppressed. The east-west width of the slot is wider in the southward IMF condition than in the northward one. Thus, the voltage difference across the slot (this voltage will be related to the cross-polar cap potential) becomes larger in the southward IMF condition.

3) Energy entry to the dayside magnetosphere in the separator reconnection depends on the north-south component of the IMF. In the northward IMF condition, the Poynting flux passing the morning side of the separator line in the northern hemisphere and the flux passing the afternoon side of the separator line in the southern hemisphere enter the magnetosphere. The Poynting flux passing the other regions does not enter the magnetosphere. This result seems to be related to interchange reconnection in the northward IMF condition [Watanabe et al., 2004]. In the southward IMF condition, all the solar-wind Poynting fluxes passing all regions around the separator line enter the magnetosphere. This result is consistent with the fact that magnetic field lines in a wide range are reconnected along the separator line in the southward IMF condition [Tanaka, 2007]. The Poynting flux entry in the northward IMF condition is almost confined to the polar cap region. On the other hand, the flux in the southward IMF condition arrives at not only the polar cap but also at the lower latitude region of the ionosphere.

Cowley, S. W. H. (1973), Radio Sci., 8(11), 903-913, doi:10.1029/RS008i011p00903.

Dungey, J. W., AFCRL-62-423, 1962.

Ebihara, Y., and T. Tanaka (2016), J. Geophys. Res. Space Physics, 121, 1201-1218, DOI: 10.1002/2015JA021831.

Lau, Y.-T. and Finn, J. M. (1990), Astrophysical Journal, 350, 672-691.

Siscoe, G. L., N. U. Crooker, G. M. Erickson, B. U. Sonnerup, K. D. Siebert, D. R. Weimer, W. W. White, and N. C. Maynard (2000), Magnetospheric Current Systems, Geophys. Monogr. Ser., vol. 118, edited by S. Ohtani et al., pp. 41-52,

AGU, Washington, D. C., doi:10.1029/GM118p0041.

Stern, D. P. (1973), J. Geophys. Res., 78(31), 7292-7305, doi:10.1029/JA078i031p07292.

Tanaka, T. (2007), Space Sci Rev, 133, 1-72, DOI 10.1007/s11214-007-9168-4.

Watanabe, M., G. J. Sofko, D. A. Andre, T. Tanaka, and M. R. Hairston (2004), J. Geophys. Res., 109, A01215, doi:10.1029/2003JA009944.

R006-P03
ポスター 1 ：11/4　PM1/PM2 （13:45-18:15）

極冠分岐の磁場トポロジー

#渡辺　正和 [1)], 蔡　東生 [2)], 熊　沛坤 [2)], 藤田　茂 [3)], 田中　高史 [4)]
([1] 九大・理・地惑,[2] 筑波大・シス情,[3] データサイエンスセンター/統数研,[4] 九大・国際宇宙惑星環境研究センター

Magnetic topology of polar cap bifurcation

#Masakazu Watanabe[1)], DongSheng Cai[2)], Peikun Xiong[2)], Shigeru Fujita[3)], Takashi Tanaka[4)]
([1]Earth & planetary Sci., Kyushu Univ.,[2]ISIS, U Tsukuba,[3]ROIS-DS/IMS,[4]International Research Center for Space and Planetary Environmental Science,

The global magnetic topology of the magnetosphere consists of two magnetic nulls and two separators connecting them (the so-called 2-null, 2-separator structure). This basic structure is stable and is seen persistently, in particular, during periods of northward interplanetary magnetic field (IMF). In this topology, the polar cap is a circle at ionospheric altitudes. On the other hand, in numerical simulations, an ”island” of closed magnetic flux appears inside the polar cap occasionally; or conversely, an ”island” of open magnetic flux emerges in the closed field line region equatorward of the polar cap boundary. We call this phenomenon ”polar cap bifurcation.” Although polar cap bifurcation can occur even for periods of steady solar wind and IMF conditions, we have learned from numerical simulations under various solar wind and IMF conditions that it occurs almost certainly, and that extensively, with a timelag of 60-80 min after a solar wind or IMF jolt. Evidently, polar cap bifurcation indicates the breakdown of the basic 2-null, 2-separator structure, but its underlying magnetic topology is far from understood. From our topological analysis so far, we know that (1) there are no magnetic nulls in the magnetotail up to 80 Re from the Earth, and (2) the two nulls on the dayside become clustered with multiple nulls (mostly the same type of null). In order to elucidate the magnetic topology of the bifurcated polar cap, we extend the search region of nulls beyond 80Re. We also consider the possibility for nulls to be located outside the simulation region. At the same time, since numerical analysis seems hopeless in determining the internal null cluster structure, we try theoretical approach, for example, asymptotic expansion of the magnetic field in the vicinity of the magnetic nulls. We will report the results of these attempts in the presentation.

磁気圏の大域的磁場トポロジーの基本は，零点 2 個とそれらを結ぶ 2 本のセパレータで構成される構造である（2-零点，2-セパレータ構造）。特に惑星間空間磁場（IMF）北向き時には，この構造は安定して普遍的にみられる。この場合，電離圏高度で極冠は円となる。しかし数値シミュレーションでは，極冠内に時折閉磁力線の”島”が発生したり，あるいは逆に極冠境界より低緯度側の閉磁力線領域に開磁力線の”島”が現れたりする。この現象を”極冠分岐”と呼ぶ。極冠分岐は定常太陽風・定常 IMF の下でも起こるが，太陽風または IMF に擾乱を与えると，60 分− 80 分の時間差でほぼ確実に，しかも大々的に起こることが，様々な太陽風・IMF パラメータでのシミュレーションでわかってきた。極冠分岐は明らかに 2-零点，2-セパレータ構造が壊れているが，実際どのようなトポロジーが背景にあるのか皆目わからない。我々がこれまで行ってきたトポロジー解析では以下のことがわかっている：(1）地球から 80Re までの磁気圏尾部には新たな零点は見つかっていない；(2）昼間側の 2 つの零点はクラスター化して零点群になる（主に同種の零点で構成される）。極冠分岐の磁場トポロジーを解明するため，今後零点探索の領域を 80Re より広げるとともに，シミュレーションの領域外に零点が存在する可能性も検討する。また，零点クラスター内の構造は数値的に追跡することが困難なので，磁場の漸近展開などの理論的考察も試みる。講演ではそれらの結果について報告する。

R006-P04
ポスター 1 ：11/4　PM1/PM2 （13:45-18:15）

#今城　峻 [1)], 三好　由純 [2)], 風間　洋一 [3)], 浅村　和史 [4)], 篠原　育 [4)], 塩川　和夫 [2)], 笠原　禎也 [4)], 笠羽　康正 [5)], 松岡　彩子 [1)],Wang　Shiang-Yu[3)],W. Y. Tam　Sunny[3)], 田　采祐 [2)], 中村　紗都子 [2)], 小路　真史 [2)], 北原　理弘 [6)], 寺本　万里子 [7)], 栗田　怜 [1)], 堀　智昭 [2)]
([1] 京都大学,[2] 名大 ISEE,[3] 中央研究院天文・宇宙物理学研究所,[4] 宇宙研,[5] 金沢大学,[6] 東北大学,[7] 九州工業大学

Precipitation of auroral electrons accelerated at very high altitudes: Arase satellite observations

#Shun Imajo[1)], Yoshizumi Miyoshi[2)], Yoichi Kazama[3)], Kazushi Asamura[4)], Iku Shinohara[4)], Kazuo Shiokawa[2)], Yoshiya Kasahara[4)], Yasumasa Kasaba[5)], Ayako Matsuoka[1)], Shiang-Yu Wang[3)], Sunny W. Y. Tam[3)], ChaeWoo Jun[2)], Satoko Nakamura[2)], Masafumi Shoji[2)], Masahiro Kitahara[6)], Mariko Teramoto[7)], Satoshi Kurita[1)], Tomoaki Hori[2)]
([1]Kyoto University,[2]ISEE, Nagoya Univ.,[3]Institute of Astronomy and Astrophysics, Academia Sinica, Taiwan,[4]ISAS/JAXA,[5]Kanazawa University,[6]Tohoku University,[7]Kyushu Institute of Technology

The Arase satellite observed precipitation and loss of auroral electrons accelerated from the high altitude above ~6 Re geocentric distance (32000 km altitude) during 5:50-6:00 UT on September 16, 2017. Downgoing electrons had a clear peak in phase space density at an energy of ~1 keV, i.e., a monoenergetic distribution, implying an acceleration caused by a parallel potential difference. During the event, the fine channels of the low-energy particle experiments – electron analyzer (LEPe) onboard Arase looked at pitch angles within ~5 degrees from the ambient magnetic field direction, and thereby have observed the detailed distribution of electron flux near the energy-dependent loss cone hyperbola. Upgoing electrons along the field line show an energy-dependent empty loss cone, which is wider in angular width for lower energy electrons. The observed width of the loss cone is consistent with that estimated from the energy of observed upgoing ion beams, corresponding to the potential drop below the satellite. By contrast, the downward loss cone was filled with downgoing electrons. These distributions near the loss cones of both downward and upward sides indicate that downgoing electrons that have been accelerated above the satellite precipitated and then lost into the atmosphere. The field-aligned current (FAC) density carried by net downgoing electrons inside the loss cone was estimated to be ~5 nA/m2, corresponding to ~1.2 microA/m as mapped at 100 km altitude, which is a typical value of FAC above auroral arcs. Upgoing electrons just outside the empty loss cone had energies higher than that of accelerated downgoing electrons, which fact indicates that accelerated downgoing electrons were further heated at lower altitudes and then came back to the satellite position. In addition to an electric field reversal and magnetic field deflection on a time scale of the event period (~10 minutes), the satellite also observed solitary-wave-like electric field variations and associated magnetic field deflections of sub-second time scale in association with beams. We discuss the acceleration mechanism and the structure of the acceleration region on the basis of the observational results, including physical processes at higher altitudes.

R006-P05
ポスター 1 ：11/4　PM1/PM2 （13:45-18:15）

磁気圏プラズマの沿磁力線分布モデルの開発と分散性 Alfvén 波の波動特性の研究

#齋藤　幸碩 [1)], 加藤　雄人 [1)], 木村　智樹 [2)], 川面　洋平 [1,3)], 北原　理弘 [1)], 熊本　篤志 [1)]
([1] 東北大・理・地球物理,[2] 東京理科大・理・物理,[3] 東北大・学際科学フロンティア研究所

Development of the magnetospheric plasma distribution model for the study of the characteristics of dispersive Alfven waves

#Koseki Saito[1)], Yuto Katoh[1)], Tomoki Kimura[2)], Yohei Kawazura[1,3)], Masahiro Kitahara[1)], Atsushi Kumamoto[1)]
([1]Dept. Geophys., Grad. Sch. Sci., Tohoku Univ.,[2]Dept. Phys., Grad. Sch. Sci., Tokyo Univ. Sci.,[3]FRIS, Tohoku Univ.

We develop the ”Plasma Distribution Solver (PDS),” a theoretical model that determines magnetospheric plasma profiles along a magnetic field line, and investigate the characteristics of dispersive Alfven waves (DAWs) by using PDS. Results observed by NASA’s spacecraft Juno have attracted attention to the role of DAWs in the electron acceleration process in planetary magnetospheres. The characteristics of DAWs are determined by the Alfven speed, and the ratio of plasma pressure to magnetic pressure, i.e., the plasma beta. We need a model that precisely obtains the field-aligned number density and pressure profiles to understand the electron acceleration process by DAWs.

Previous studies proposed theoretical/empirical models to calculate magnetospheric plasma profiles along a field line [e.g., Angerami and Thomas, 1964]. However, the number density distribution is determined under the assumed plasma temperature profile. There is no theoretical model to obtain the number density and pressure profiles that are mutually consistent with each other, which is realized by the developed PDS.

We develop PDS based on the Static Vlasov Code (SVC) [Ergun et al., 2000; Su et al., 2003; Matsuda et al., 2010]. SVC is a theoretical model to calculate the plasma number density profiles by integrating the velocity distribution function over the velocity space. In this calculation, SVC considers the accessibility over the velocity space and the spatial variation of the volume element in the velocity space [e.g., Persson, 1966], while the value of the velocity distribution function is assumed to be conserved along the particle’s path [Chiu and Schultz, 1978]. We revised SVC and reconstructed it to PDS by considering the appropriate spatial variation of the velocity distribution function and that of the volume element in real space along a field line. We obtain the plasma profiles in the Jupiter-Io system using PDS and compare those calculated by SVC. The results show that the characteristics are different between the PDS and SVC results. In particular, the minimum number density is located at lower latitudes in the PDS result than in the SVC result, which can influence the consideration of the dominant regions of kinetic/inertial Alfven waves regarding the characteristics of DAWs. The difference obtained indicates a typical example caused by the different treatment of the velocity distribution function in PDS and SVC. Besides, we introduce the details of the method and results of PDS and discuss the comparison with SVC and discuss the spatial change of characteristics of DAWs clarified from the PDS results.

本研究では、磁気圏プラズマの沿磁力線分布を求める理論モデル「Plasma Distribution Solver (PDS)」を開発して、その結果を用いて分散性 Alfvén 波 (Dispersive Alfvén wave: DAW) の波動特性について考察する。木星探査機 Juno による観測結果を契機として、惑星磁気圏における DAW の電子加速過程に及ぼす役割が注目されている。DAW の特性は Alfvén 速度や、プラズマの圧力と磁気圧の比、すなわちプラズマベータ値により決定される。DAW による電子加速過程を理解する上で、背景プラズマの数密度と圧力の沿磁力線分布を与えるモデルが必要不可欠である。

過去の研究により、惑星磁気圏におけるプラズマ分布に関する様々な理論・経験モデルが提案されてきた [e.g., Angerami and Thomas, 1964]。しかしながら、従来のモデルでは、仮定されたプラズマの温度分布の下で数密度が決定されており、数密度と圧力の双方を変数として相互に矛盾のない解を求める理論モデルは、これまで提案されてこなかった。DAW による電子加速過程を理解するためには、惑星磁気圏におけるプラズマの数密度と圧力を互いに consistent に求める理論モデルが必要であり、本研究で開発する PDS はそれを実現するものである。

PDS は沿磁力線数密度分布を求める理論モデルである Static Vlasov Code (SVC)[Ergun et al., 2000; Su et al., 2003; Matsuda et al., 2010] を基に開発した。磁力線上の各位置における数密度は、速度分布関数を速度空間で積分することにより求める。SVC ではこの速度空間での積分において、プラズマの速度空間上の accessibility と、速度空間における体積要素の沿磁力線方向の空間変化を考慮する [e.g., Persson, 1966] 一方で、速度分布関数の値は粒子の経路に沿って保存されるとした [Chiu and Schultz, 1978]。この点について、我々は実空間の体積要素と速度分布関数の空間変化の取り扱いについて再検討し、より現実的なプラズマ数密度を得られるように改良を施した。さらに、磁力線上の各位置における速度分布関数に基づいてプラズマ圧が計算できるようにモデルを拡張した。本講演では、本研究により開発された PDS を木星-イオ系に適用し、SVC で得られるプラズマ分布との違いを調べた結果について報告する。モデル計算の結果から、PDS の解と SVC の解では数密度の分布の傾向が異なることが示された。特に、数密度が最小となる地点は PDS の方が SVC よりも低緯度に位置する解が得られ、DAW の特性に関して、kinetic Alfvén 波と inertial Alfvén 波がそれぞれ卓越する領域の考察に影響し得ることが示された。この違いは、PDS と SVC における速度分布関数の取り扱いの違いによる影響を顕著に示すものである。本講演ではさらに、PDS と SVC の理論の差異と得られた結果の詳細を報告するとともに、プラズマ分布から得られる DAW の特性の空間変化について議論する。

R006-P06
ポスター１：11/4　PM1/PM2（13:45-18:15）

#小野澤　秀治[1)], 加藤　雄人[2)], 熊本　篤志[3)], 笠原　禎也[4)], 北村　成寿[5)]
([1 東北大・理・地球物理,([2 東北大・理・地球物理,([3 東北大・理・地球物理,([4 金沢大,([5 名大・宇地研

Study of the wave mode contributing to the ion heating events in the Earth's polar region based on the Akebono observation

#Shuji Onosawa[1)], Yuto Katoh[2)], Atsushi Kumamoto[3)], Yoshiya Kasahara[4)], Naritoshi Kitamura[5)]
([1Dept. Geophys., Grad. Sch. Sci., Tohoku Univ.,([2Dept. Geophys., Grad. Sch. Sci., Tohoku Univ.,([3Dept. Geophys., Grad. Sch. Sci., Tohoku Univ.,([4Kanazawa Univ.,([5ISEE, Nagoya University

We investigate the characteristics of broadband plasma waves related to ion heating in the polar regions based on the Akebono satellite observations and dispersion relation of waves in cold plasma. Heavy ions such as oxygen ions flow out from the Earth's polar region during geospace storms. Previous studies suggested that wave-particle interactions with broadband ELF (BBELF) waves, whose intensity decreases power-law from DC to several kilohertz, play important roles in the acceleration process of heavy ions. BBELF waves appear in the spectra electromagnetic in the frequency range below fcO, where fcO represents the cyclotron frequency of oxygen ion, and electrostatic in the frequency range over fcO. Ishigaya (2017) performed an event analysis of two strong ion heating events and four weak ion heating events observed by the Akebono satellite. They found that the ratio of the electric field amplitude to the magnetic field amplitude (E_w/B_w) exceeded 10^8 m/s, larger than the Alfven speed (~2 x 10^6 m/s), in the frequency range between fcH and fLH in the strong ion heating events, where fcH and fLH indicate the cyclotron frequency of proton and the lower hybrid resonance frequency, respectively. Their results suggested the importance of the enhancement of electrostatic waves in the frequency range from fcH to fLH in addition to the enhancement of waves below fcO in the strong ion acceleration process.

Based on the dispersion relation of plasma waves in cold plasma, R-mode waves can exist as well as electrostatic waves in the frequency range from fcH to fLH. Since the phase velocity of R-mode waves propagating purely along a field line exceeds the Alfven speed, electrostatic components categorized by Ishigaya (2017) may consist of R-mode waves. To identify the wave modes of plasma waves in the frequency range higher than fcH, we reanalyzed 6 events studied by Ishigaya (2017) and compared E_w/B_w with the phase velocity of R-mode waves in the frequency range from fcH to fLH. We used electric and magnetic field amplitude data from the VLF/MCA onboard the Akebono satellite. We analyzed the spectra from 100 Hz to 1 kHz, corresponding to the frequency range from fcH to fLH during the 6 events. We calculated the dispersion relation using plasma parameters and the background magnetic field intensity used in Ishigaya (2017). We compared the observed E_w/B_w with the phase velocity of R-mode waves propagating purely along a field line, which is the condition corresponding to the largest E_w/B_w of R-mode waves. In strong ion heating events, E_w/B_w was about ten times higher than the phase velocity of R-mode waves. In contrast, in weak ion heating events, the ratio was comparable with the phase velocity of R-mode waves. These results clarify that electrostatic waves were dominant in the frequency range from fcO to fLH during the strong ion heating events and suggest that R-mode waves were dominant in weak ion heating events. Since the wave electric field vector of R-mode waves rotates around the background magnetic field in the opposite direction to the ion cyclotron motion, the cyclotron resonance condition is not satisfied between R-mode and oxygen ions in the polar region. Thus the presence of the R-mode waves does not contribute to the ion heating. The result of the present study confirmed the presence of electrostatic waves and their importance in the strong ion heating events of Ishigaya (2017).

R006-P07
ポスター 1 ：11/4　PM1/PM2 （13:45-18:15）

#西野　真木 [1)], 齋藤　義文 [2)],Lavraud　Benoit[3)], 宮下　幸長 [4,5)], 長谷川　洋 [2)], 野和田　基晴 [6)], 長井　嗣信 [7)]
([1] 東大・理,[2] 宇宙研,[3]Universite de Bordeaux, CNRS,[4]KASI,[5]KUST,[6] 山東大学威海校,[7]Retired

An observation of the dawnward-expanded magnetosphere during low Alfven Mach number solar wind

#N Nishino Masaki[1)], Yoshifumi Saito[2)], Benoit Lavraud[3)], Yukinaga Miyashita[4,5)], Hiroshi Hasegawa[2)], Motoharu Nowada[6)], Tsugunobu Nagai[7)]
([1]University of Tokyo,[2]ISAS,[3]Universite de Bordeaux, CNRS,[4]KASI,[5]KUST,[6]Shandong University at Weihai,[7]Retired

The density of the solar wind plasma near the Earth's magnetosphere sometimes decreases to only several per cent of the usual value, and such density extrema result in a significant reduction of the dynamic pressure and Alfven Mach number (M_A) of the solar wind flow. While a symmetric expansion of the Earth's magnetosphere by the low dynamic pressure was assumed in previous studies, a global magnetohydrodynamic (MHD) simulation study predicted a remarkable dawn-dusk asymmetry in the shape of the magnetosphere under low-density solar wind and Parker-spiral interplanetary magnetic field (IMF) configuration. Here, we present observational evidence of the asymmetric deformation of the magnetosphere under low-M_A solar wind and Parker-spiral IMF conditions, focusing on the significant expansion of the dawn-flank magnetosphere detected by the Geotail spacecraft. The solar wind flow had a non-negligible dusk-to-dawn component and partly affected the dawnward expansion of the magnetosphere. Antisunward ion beams detected at the dawn-flank magnetopause suggest that magnetic reconnection frequently occurred due to the very low beta in the magnetosheath. The Walen analysis for the magnetopause boundary data with the ion jets showed high correlations between the ion velocity in the de Hoffmann-Teller frame and the local Alfven velocity, which is consistent with the assumption that the observed ion beams were generated by magnetic reconnection. These observations suggest that altered and enhanced plasma acceleration by magnetic reconnection at the dawnside magnetopause operates under the low-M_A solar wind and Parker spiral IMF conditions and that an altered plasma transport across the dawnside magnetopause is at work under such a low-M_A condition.

R006-P08
ポスター１：11/4　PM1/PM2（13:45-18:15）

#桂華　邦裕[1)], 浅見　隆太[1)], 星野　真弘[1)],Fuselier　Stephen A.[2,3)]
[(1] 東京大学大学院理学系研究科,[(2] サウスウェスト研究所,[(3] テキサス大学サンアントニオ校

Global Characteristics of Cold Protons Around Midnight in the Magnetotail: MMS/HPCA observations

#Kunihiro Keika[1)], Ryuta Asami[1)], Masahiro Hoshino[1)], Stephen, A. Fuselier[2,3)]
[(1]Graduate School of Science, University of Tokyo,[(2]Southwest Research Institute,[(3]University of Texas at San Antonio

We investigate plasma transport to and plasma heating in the plasma sheet in the noon-midnight meridian, characterizing protons with temperature colder than the core plasma sheet protons (<700 eV). We extract the density and temperature of the cold protons from velocity distribution functions measured by the HPCA (Hot Plasma Composition Analyzer) instrument on board the MMS (Magnetospheric Multiscale) spacecraft in the radial distance (r) of 6 – 25 Re, performing two-component Maxwellian fits. We selected time intervals with no fast flow (>70 km/s) observed, to examine the characteristics of magnetotail plasma not directly affected by magnetic reconnection and associated phenomena. In the region of r >~ 10 Re, the two-component populations are identified more frequently near the plasma sheet boundary than the central plasma sheet. The cold component density peaks near the boundary, in contrast to the hot components which display high density near the central plasma sheet. These characteristics suggest that cold protons are convected from the lobe and then efficiently heated and mixed with the plasma sheet hot plasma near the lobe-plasma sheet boundary. The statistical features of the extracted cold components indicate that, in the tailward regions (r >~ 20 Re), temperature increases with decreasing vertical distance from the plasma sheet (represented by plasma β) in a similar trend to the hot components. In the near-Earth plasma sheet (r <~ 15 Re), cold proton temperature is lower at higher-β regions; the density decreases as increasing r. These features suggest that cold protons in the near-Earth plasma sheet are of ionospheric origin, transported to the plasma sheet in the closed magnetic field configuration.

Reference:
Keika, K., Asami, R., Hoshino, M., & Fuselier, S. A. (2022). Global characteristics of cold protons around midnight in the magnetotail: Implication for efficient heating and origin. Journal of Geophysical Research: Space Physics, 127, e2021JA029576. https://doi. org/10.1029/2021JA029576

R006-P09
ポスター 1 ：11/4　PM1/PM2 （13:45-18:15）

#能勢　正仁 [1)], 野村　麗子 [2)], 寺本　万里子 [3)], 浅村　和史 [2)], 細川　敬祐 [4)], 三好　由純 [1)], 三谷　烈史 [2)], 坂野井　健 [5)], 滑川　拓 [6)], 河野　剛健 [7)], 岩永　吉広 [7)], 平原　聖文 [1)]
([1] 名大・宇地研,[2] 宇宙研,[3] 九工大,[4] 電通大,[5] 東北大・理・PPARC,[6] 東大・理・地惑,[7] 愛知製鋼株式会社,[8] 愛知製鋼株式会社

Field-aligned currents associated with pulsating auroral patches: Observation with Magneto-Impedance Magnetometer on board LAMP

#Masahito Nose[1)], Reiko Nomura[2)], Mariko Teramoto[3)], Kazushi Asamura[2)], Keisuke Hosokawa[4)], Yoshizumi Miyoshi[1)], Takefumi Mitani[2)], Takeshi Sakanoi[5)], Taku Namekawa[6)], Takeshi Kawano[7)], Yoshihiro Iwanaga[7)], Masafumi Hirahara[1)]
([1]ISEE, Nagoya Univ.,[2]ISAS/JAXA,[3]Kyutech,[4]UEC,[5]PPARC, Grad. School of Science, Tohoku Univ.,[6]Earth and Planetary Science, Tokyo Univ.,[7]Aichi Steel Corporation,[8]Aichi Steel Corporation

Magneto-impedance (MI) effect is described that the impedance of an amorphous wire sensitively changes as a function of an external magnetic field when a high-frequency current is applied through the wire as a carrier. A micro-size magnetic sensor that utilizes this effect becomes commercially available. We made some modifications to the commercially available MI sensors as they can cover the range of the geomagnetic field. Ground observations with the MI sensors revealed that they can record geomagnetic field variations with amplitudes of ~1 nT which were also observed with a fluxgate magnetometer. This suggests that MI sensors are useful for researches in geomagnetism or space physics, although they are much less expensive than fluxgate magnetometers.

For an experimental performance test of MI sensors on sounding rockets, we have been developing a triaxial magnetometer using the modified MI sensors (Magneto-Impedance Magnetometer, MIM) since autumn 2018. MIM is composed of the sensor component (MIM-S) and the data processing electronics component (MIM-E). MIM-S measures the geomagnetic field in the range of +-80,000 nT with a sampling frequency of 200 Hz and has the noise level of approximately 50 pT/sqrt(Hz). The dimensions, mass, and power consumption of MIM-S are as small as 70 mm by 70 mm by 50 mm, <0.5 kg, and ~3 W, respectively. MIM-E digitizes the output from MIM-S with a 24-bit A/D converter, resulting in a nominal resolution is ~10 pT, and processes the data with a Raspberry Pi3. Its dimensions, mass, and power consumption are 150 mm by 150 mm by 44 mm, ~1.3 kg, and ~6 W, respectively. We have conducted a thermal vacuum test, a vibration test, and an orthogonality and sensitivity calibration of MIM, and provided it with the Loss through Auroral Microburst Pulsations (LAMP) sounding rocket.

The LAMP sounding rocket was launched at 11:27:30 UT on March 5, 2022 from Poker Flat Research Range, Alaska at altitude of ~430 km. MIM successfully made an observation of the geomagnetic field in the ionosphere during pulsating aurora. This is the first mission that delivers MI sensors at the ionospheric altitude by a sounding rocket. From a detailed analysis of the MIM data, we found magnetic field variations at approximately 220 km altitude which are likely caused by small-scale field-aligned currents associated with pulsating auroral patches. In presentation, we will display data from LAMP/MIM and propose a possible model of the field-aligned currents to explain the observation. We will also discuss future possibility of MI sensors as magnetometers for sounding rockets or microsatellites.

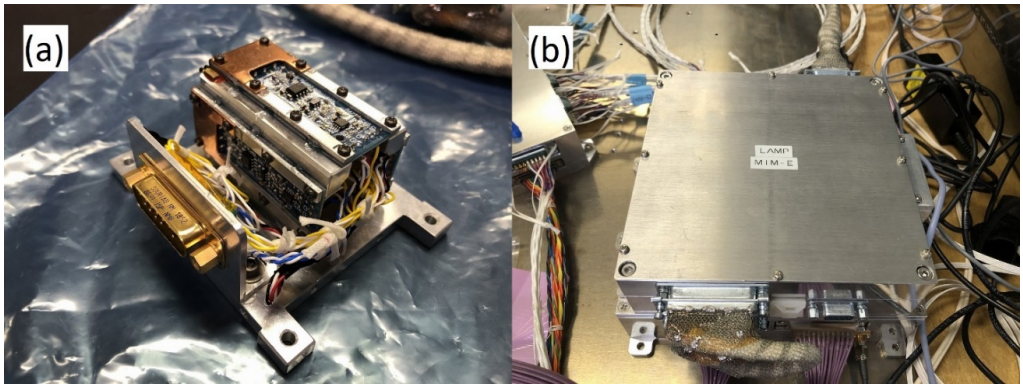

R006-P10
ポスター 1 ：11/4　PM1/PM2 （13:45-18:15）

観測パッケージ PARM-HEP による脈動オーロラに伴うマイクロバースト現象の観測

#滑川　拓 [1,2], 三谷　烈史 [2], 浅村　和史 [2], 三好　由純 [3], 細川　敬祐 [4], 坂野井　健 [5], 川村　美季 [6], 能勢　正仁 [7], 野村　麗子 [8], 寺本　万里子 [9], 小川　泰信 [10]
([1] 東大・理・地惑,([2] 宇宙研,([3] 名大 ISEE,([4] 電通大,([5] 東北大・理・PPARC,([6] 東北大学,([7] 名大・宇地研,([8]JAXA,([9] 九工大,([10] 極地研

PARM-HEP Observation of Microburst Precipitation associated with Pulsating Aurora

#Taku Namekawa[1,2], Takefumi Mitani[2], Kazushi Asamura[2], Yoshizumi Miyoshi[3], Keisuke Hosokawa[4], Takeshi Sakanoi[5], Miki Kawamura[6], Masahito Nose[7], Reiko Nomura[8], Mariko Teramoto[9], Yasunobu Ogawa[10]
([1]Earth and Planetary Science, Tokyo Univ.,([2]ISAS/JAXA,([3]ISEE, Nagoya Univ.,([4]UEC,([5]PPARC, Grad. School of Science, Tohoku Univ.,([6]TU,([7]ISEE, Nagoya Univ.,([8]JAXA,([9]Kyutech,([10]NIPR

Microbursts are that a large number of radiation belt electrons of several hundred keV to several MeV precipitate to the Earth's auroral atmosphere on a time scale of less than one second. It is suggested that microbursts are a loss mechanism of the outer radiation belt electrons [e.g., Thorne et al. 2005; Clilverd et al, 2006; Dietrich et al. 2010; Lorentzen et al. 2001]. Although microbursts are suggested to be caused by pitch angle scattering due to magnetospheric whistler-mode chorus waves propagating from the magnetic equatorial plane to higher magnetic latitudes, observational verification has not been made yet [Miyoshi et al., 2020]. The mechanism of microbursts under consideration is similar to that of pulsating aurora observed in the Earth's polar region. Thus, the origin of microburst can be clarified by simultaneous observation of microbursts and pulsating auroras.

We have developed a high-energy electron detector (HEP) to observe of sub-relativistic - relativistic electrons. HEP is one of core instruments of the Pulsating AuRora and Microburst (PARM) instrument package developed for the simultaneous observation of the pulsating aurora and microburst. The international student sounding rocket experiment RockSat-XN, that installed the first model of HEP, launched on the dayside (MLT = 12.4h) under quiet condition at 09:13:00 UT on January 13, 2019. HEP onboard RockSat-XN observed the energy spectrum of quasi-relativistic energy electrons that were likely to be caused by the wave-particle interactions between whistler-mode waves and sub-relativistic electrons in the quiet dayside magnetosphere [Namekawa et al. 2021]. Loss through Auroral Microburst Pulsation (LAMP) sounding rocket experiment, that installed an improved version of HEP, launched at 11:27:30 UT (MLT = 0.1h) on March 5, 2022. LAMP simultaneously observed pulsating auroras and quasi-relativistic electron microbursts with inverse energy dispersion where the high energy electrons appear after the low energy electrons. The observed inverse energy dispersion is consistent with the theoretical expectation [Miyoshi et al., 2020]. In this presentation, we will show the outline of HEP and the observation results of RockSat-XN and LAMP experiments.

マイクロバーストと呼ばれる放射線帯の数 100keV〜数 MeV の電子が 1 秒以下の時間スケールで大量に降り込む現象は、放射線帯の高エネルギー電子の散逸に大きく関連していると考えられている [e.g. Thorne et al., 2005; Clilverd et al., 2006; Dietrich et al., 2010; Lorentzen et al., 2001]。マイクロバーストを引き起こす原因として、磁気赤道面からより高磁気緯度に向けて伝播するホイッスラーモードコーラス波による放射線帯粒子のピッチ角散乱によって発生することが示唆されているが、いまだ観測的な実証はされていない [Miyoshi et al., 2020]。検討されているマイクロバーストの発生メカニズムは、地球極域で観測される脈動オーロラの発生メカニズムと類似のものであり、マイクロバーストと脈動オーロラの同時発生の観測的実証を行うことで、マイクロバーストの起源に迫ることができる。

私たちはマイクロバーストと脈動オーロラの同時観測を目的とする観測パッケージ PARM の中心的機器となる高エネルギー電子観測器（HEP）を開発した。本機器の最初のモデルが搭載された国際学生観測ロケット実験 RockSat-XN は 2019 年 1 月 13 日 9 時 13 分 UT に打ち上げられ、静穏時昼側磁気圏（MLT = 12.4h）におけるホイッスラー波に由来する可能性がある準相対論的エネルギー電子のエネルギースペクトルを観測した [Namekawa et al., 2021]。さらに本機器の 2 番目のモデルが搭載された観測ロケット実験 LAMP（Loss through Auroral Microburst Pulsation）は 2022 年 3 月 5 日 11 時 27 分 30 秒 UT（MLT = 0.1h）に打ち上げられ、脈動オーロラに同期した準相対論的電子によるマイクロバーストとそのエネルギー分散を観測した。特にエネルギー分散については、低エネルギー電子が高エネルギー電子の後に出現するという逆エネルギー分散が観測され、コーラス波動がマイクロバーストを起こすというモデルの予想と整合的な結果が得られた。本発表では、HEP の概要と RockSat-XN および LAMP の観測結果について説明する。

R006-P11
ポスター１：11/4　PM1/PM2（13:45-18:15）

#細川　敬祐[1)], 三好　由純[2)], 浅村　和史[3)], 坂野井　健[4)], 三谷　烈史[3)], 滑川　拓[5)], 能勢　正仁[6)], 小川　泰信[7)]
([1]電通大,[2]名大 ISEE,[3]宇宙研,[4]東北大・理・PPARC,[5]東大・理・地惑,[6]名大・宇地研,[7]極地研

Overview of the ground-based optical observations during the LAMP rocket experiment in Alaska

#Keisuke Hosokawa[1)], Yoshizumi Miyoshi[2)], Kazushi Asamura[3)], Takeshi Sakanoi[4)], Takefumi Mitani[3)], Taku Namekawa[5)], Masahito Nose[6)], Yasunobu Ogawa[7)]
([1]UEC,[2]ISEE, Nagoya Univ.,[3]ISAS/JAXA,[4]PPARC, Grad. School of Science, Tohoku Univ.,[5]Earth and Planetary Science, Tokyo Univ.,[6]ISEE, Nagoya Univ.,[7]NIPR

It is widely known that the energy of precipitating electrons causing pulsating aurorae (PsA) is higher than that of typical discrete aurorae. The tail of the energy spectra of PsA sometimes extends to a few tens/hundreds of keV. Such sub-relativistic electron precipitations can be explained by the propagation of chorus waves, which is the agent causing the electron precipitation through the wave-particle interaction, towards higher latitudes (e.g., Miyoshi et al., 2020). To understand the simultaneous precipitation of higher energy electrons during PsA, the LAMP sounding rocket was launched from the Poker Flat Research Range in Alaska on March 5, 2022. During the launch window of the rocket, three high-speed all-sky cameras were operative at three stations immediately below the trajectory of the rocket: Poker Flat, Venetie, and Fort Yukon. The all-sky cameras captured all-sky images with a temporal resolution of 100 Hz (80 Hz for the Fort Yukon case). By using these images, we are able to visualize the spatio-temporal variation of PsA during the entire flight of the rocket. In the presentation, we first introduce the ground-based observation during the entire period of the rocket launch. It is possible to estimate the altitude of aurora in regions where the fields-of-view of multiple cameras overlap. For example, the separation between Poker Flat and Venetie is only ˜100 km; thus, the central altitude of the PsA emission can be estimated in a large area between these two observation sites. When deriving the altitude of PsA emission, we simply applied a cross-correlation analysis to the data obtained from two observations sites. In the presentation, we discuss the temporal variation and spatial distribution of the altitude of PsA emission in comparison with data from particle sensors onboard the rocket.

R006-P12
ポスター 1 ：11/4　PM1/PM2 （13:45-18:15）

地磁気共役点における降り込みプロトンエネルギー及びフラックスの比較

#土谷　真希 [1)], 田口　真 [1)], 門倉　昭 [2)]
([1] 立教大・理・物理,[2]ROIS-DS/極地研

Comparison of precipitation energy and flux of proton aurora at geomagnetic conjugate points

#Maki Tsuchiya[1)], Makoto Taguchi[1)], Akira Kadokura[2)]
([1]Rikkyo. Univ,[2]ROIS-DS/NIPR

At geomagnetic conjugate points, which are two points in the northern and southern hemispheres connected by a single magnetic field line, auroras may have conjugacy such as similar shape and dynamics, because auroral particles in both hemispheres originate from the plasma sheet and enters the upper atmosphere along the magnetic field line. However, asymmetric auroras often appear actually because of differences in the Earth's magnetic field strength and ionospheric electric conductivity between the northern and southern hemispheres. Therefore, comparison of the brightness and shape of auroras at geomagnetic conjugate points is useful for probing the state of the magnetosphere and ionosphere. However, because most of the southern auroral zone is above the sea, there are only a few geomagnetic conjugate points located on land in both regions. The pair of Tjornes in Iceland and Syowa Station in Antarctica is one of them, and data obtained at these geomagnetic conjugate points are used in this study.

Proton auroras are not as bright as electron auroras, and, therefore, there have been few observations of them. In particular, there have been no observations of proton auroras at the geomagnetic conjugate points, except for those by Sato et al. [1986]. For this reason, an emission intensity ratio of proton auroras in both hemispheres, and spatial and temporal relationship of proton aurora with electron aurora have not yet been studied.

In this study, we observed proton auroras simultaneously between geomagnetic conjugate points in Iceland and Antarctica using Proton Aurora Spectrograph (PAS), which was designed to acquire an emission spectrum of auroras along a geomagnetic meridian. The main purpose is to compare the precipitation energy and flux of protons from a hydrogen Balmer beta line (486.1 nm) which is the brightest line among the proton auroras. The precipitation energy is estimated from a Doppler shift of the line. PAS is based on an all-sky optical system with a transmission grating and a slit, which enables spectroscopy of auroral emissions in one spatial dimension along the geomagnetic meridian. The observation wavelength range is from 417 nm to 579 nm, where emission lines of nitrogen molecular ion at 427.8 nm and 470.9 nm and an emission line of oxygen atom at 557.7 nm can be simultaneously observed as well as the hydrogen Balmer beta line. The data used for the analysis were mainly taken at the time of the spring equinox and autumn equinox when spectra obtained during dark nights are available in both hemispheres in 2018, 2020, and 2021. An image was acquired every minute with an exposure time of 55 seconds.

Sensitivity calibration of the Antarctic PAS was performed using a standard light source with an integrating sphere at the National Institute of Polar Research before it was transported to Antarctica, but the Iceland PAS was not due to time constraints. Therefore, sensitivity calibrations were performed on both instruments using stars in observed images for both Iceland and Antarctic PASs. This enabled us to compare the emission intensity of proton auroras in both hemispheres. Time series data of the simultaneously observed emission intensity of the hydrogen Balmer beta and oxygen atom emission lines as well as a comparison of the hydrogen Balmer beta line precipitation energies are presented. Relationship between the precipitation energy and flux of proton aurora and the geomagnetic activity level will be investigated.

一本の磁力線でつながった南北半球の二地点 (地磁気共役点) では、オーロラ粒子が両半球ともにプラズマシートに由来し、磁力線に沿って超高層大気に入射するため、オーロラが同じ形状や動態といった共役性を持つことがある。しかし、地球磁場や電離圏の電気伝導度の南北半球での違いにより実際に観測されたオーロラでは非対称性が生じることも多い。そのため地磁気共役点でのオーロラの明るさや形状の比較は、磁気圏や電離圏の状態の探査に有効である。しかし、南極域のオーロラ帯の大部分は海であるため、地磁気共役点の関係になっている南北両半球の地点は少なく、この研究で観測を行うアイスランド (チョルネス) と南極 (昭和基地) は地上に位置する数少ない地磁気共役点である。

プロトンオーロラはエレクトロンオーロラと比較して発光強度が小さく、観測例が少ない。特に地磁気共役点でのプロトンオーロラ観測は、Sato et al. [1986] による観測以後例がなく、両半球の発光強度比や電子オーロラとの空間的・時間的な関係といった点はまだわかっていない。

本研究は、地磁気子午線に沿ったプロトンオーロラ発光の抽出を目指して製作された Proton Aurora Spectrograph(PAS) を用いて、地磁気共役点 (アイスランド (チョルネス) と南極 (昭和基地)) 間で同時観測を行い、プロトンオーロラで最も明るい水素バルマーベータ線 (486.1nm) のドップラーシフトを用いた振り込みエネルギーやフラックスの比較を目的とする。PAS は、全天観測用の光学系に透過型回折格子とスリットを組み込まれ、地磁気子午線に沿った空間一次元のオーロラ発光を分光することを可能とする装置である。観測波長範囲は 417nm から 579nm で、窒素分子イオン 427.8nm, 470.9nm と酸素原子 557.7nm の発光が同時に取得できるようになっている。解析に使用するデータは主に 2018 年、2020 年、2021 年の両地点に暗夜のある春分秋分の時期のもので、露光時間は 55 秒で 1 分毎に撮像された。

南極 PAS では装置の現地輸送前に国立極地研究所で積分球校正光源を用いた感度校正が行われたが、アイスランド PAS では時間の都合で行っていない。そこで、画像に映りこむ恒星を用いた感度校正を両装置で行い、アイスランド PAS の感度を求めた。それにより、両半球の発光強度比較が可能となった。水素バルマーベータ線や酸素原子 557.7 nm の同時観測された発光強度時系列データや、水素バルマーベータ線の降り込みエネルギー比較について紹介する。今後は、地磁気活動度との関連を調査していく予定である。

R006-P13
ポスター１：11/4　PM1/PM2（13:45-18:15）

南極点アムンゼン・スコット基地ならびに南極冠域無人観測網における多波長同時オーロラ撮像計画にむけた新オーロライメージャー開発の現状

#近藤　大泰[1)], 坂野井　健[2)], 海老原　祐輔[3)], 片岡　龍峰[4)], 山科　佐紀[5)], 穂積　裕太[6)]
([1] 東北大・理・惑星プラズマ・大気研究センター,[2] 東北大・理・惑星プラズマ・大気研究センター,[3] 京都大学・生存圏研究所,[4] 国立極地研究所,[5] 京都大・理,[6] 国立研究開発法人情報通信研究機構

Development of new auroral imaging system for simultaneous multi-wavelength observations at the Amundsen-Scott South Pole station.

#Hiroyasu Kondo[1)], Takeshi Sakanoi[2)], Yusuke Ebihara[3)], Ryuho Kataoka[4)], Saki Yamashina[5)], Yuta Hozumi[6)]
([1]PPARC, Tohoku Univ.,[2]PPARC, Tohoku Univ.,[3]RISH, Kyoto Univ.,[4]NIPR,[5]Kyoto Univ.,[6]NICT

We are developing camera system to observe the aurora in the polar cap region because the number of auroral events will increase during the solar maximum period, which will provide the best opportunity for observation. In this presentation, we will report the latest status of the development of the all-sky monochromatic imager system to be installed at the South Pole. The polar cap region is the area where the Earth's magnetic field lines are directly connected to the solar wind and Interplanetary Magnetic Field and is open to space. Particularly during solar proton events(SEPs), the high energy particles directly precipitate along the magnetic field lines in the polar cap region and enter deep regions of the Earth's atmosphere. The precipitated particles cause changes in molecules such as SOx and HOx that make up the mesosphere. The phase X Priority Research Program of the National Institute of Polar Research, which began in FY2022, the purpose is to understand how the Earth's environment is an open system to space. So far, there have been few observations in the polar cap region because of limited observational places, and only a limited number of large space weather events such as solar proton events have been reported. During this Priority Research Program period, it comes the solar maximum, and we will require sufficient instruments not to miss this opportunity. Our group has continued auroral imaging since 2008 at the Amundsen-Scott Station at the South Pole. The current imaging system uses filters of five wavelengths(427.8nm, 557.7nm, 630.0nm, 486.1nm, and 589.0nm)alternately. However, the motor for rotating the filters has broken down, making it impossible to exchange wavelengths. Additionally, the CCD camera and its peripheral equipment are aging, so we needed a drastic update of the observation system. For this reason, we are planning to install several all-sky monochromatic imagers, combining an ASI183MM Pro CMOS camera(ZWO)and a FUJINON LENS FE185C086HA-1(Fujifilm, focal length 2.7 mm, F value 1.8for simultaneous multi-wavelength imaging. This all-sky imager observation system is based on the one used on the Antarctic research vessel Shirase until last year. We will develop 5 camera, each of which will use 391.4nm, 557.7nm, 630.0nm, 670.0nm: N2 First Positive Band, 844.6nm filters(Andover)to simultaneously image the entire sky with five wavelengths.

The cameras will be controlled by a small PCs(ESC LIVA-Q2, OS: Linux Ubuntu); one LIVA-Q2 is designed to control one camera, and five cameras will be operated in parallel. The imaging schedule is based on a program whose start and end times are automatically generated each day. This program determines the nighttime based on the time series of solar zenith angles and automatically determines the schedule. The imaging program uses a part of ZWO's "ASIStudio" library as a module, and automatic operation is performed based on the imaging schedule. This automatic operation uses "cron". The exposure time is set to 18 seconds and the interval to 20 seconds, but you can freely change this parameters according to the scientific purpose.

The imaged data is stored on a NAS(Synology DS918+)via network. The storage mode is RAID 1, and data is constantly mirrored and backed up to prevent data loss in the event of HDD failure. The NAS can be equipped with four HDDs. Therefore, if one 12TB HDD is used, the total capacity is 48TB, which means that NAS can store the observational data of 24TB.

The LIVA-Q2 and NAS are powered by an Internet switch(Watchboot by Meikyo Denki); Watchboot is capable of ping monitoring via the Internet, and when there is no response from the PC, it determines that the device has frozen and turns the power off and on. Continuous observation in the Shirase has proven that this method can recover the equipment and achieve stable automatic operation over a long period of time.

As for handling the data, the HDDs can be picked up only about once a year. Therefore, as with the Shirase observations, a Quick Look(QL)of the acquired data will be automatically generated and sent to Japan via e-mail every day to check whether the observation system is available.

The observation system is originally planned to be installed at the South Pole Station in November 2022, but due to COVID-19, the plan has not yet been decided officially. Therefore, in order to confirm the continuous operation of the observation system, we will have the 63rd Antarctic Research Expedition, which will depart this year, transport the equipment and install it at Showa Station in parallel with the plan.

我々は、これから迎える太陽活動の極大期ではオーロラのイベント数が増え、絶好の観測の機会を迎えるため、極冠域のオーロラを観測するためにカメラの開発を行っている。本発表では、南極点に設置予定の全天単色イメージャーのシステム開発について最新の状況を報告する。極冠域は、地球の磁力線が太陽風や惑星空間磁場と直接つながる領域で

あり、宇宙空間に開かれている。特に、太陽プロトンイベント（SEP）発生時には、高いエネルギーをもった粒子が磁力線に沿って極冠域に直接降り込み、地球大気の深い領域まで入り込む。降り込んだ粒子は中間圏を構成している SOx や HOx といった分子の変動を引き起こす。2022 年度より開始された国立極地研究所の第Ⅹ期重点研究計画では、地球環境がどう宇宙にオープンなシステムかを理解することを目的としている。これまで極冠域における観測は、拠点が少なかった上に、太陽プロトンイベントのような大きな宇宙天気のイベントは限られた数しか報告されていない。この重点研究計画期間に太陽活動の極大期を迎え、この機会を最大限に生かすために十分な観測装置が求められる。我々グループは、南極点のアムンゼン・スコット基地において 2008 年よりオーロラ撮像を継続してきた。現在設置されている撮像装置は、5 波長 （427.8nm, 557.7nm, 630.0nm, 486.1nm, 589.0nm) のフィルターを交互に使用し、撮像していた。しかし、現在フィルターの回転用のモーターが故障しており、波長交換できない上に、CCD カメラやその周辺機器の老朽化も見られるため、抜本的な観測システムの更新が必要である。このため我々は、CMOS カメラ ASI183MM Pro（ZWO 社製）と FUJINON LENS FE185C086HA-1（富士フィルム製、焦点距離 2.7mm、F 値 1.8 ）を組み合わせた全天単色イメージャーを複数台設置し、同時多波長撮像を実施する計画を進めている。この全天イメージャー観測システムは、昨年まで南極観測船しらせで実績があるものを採用した。これを 5 台開発し、それぞれに波長 391.4nm, 557.7nm, 630.0nm, 670.0nm:N☒ First Positive Band, 844.6nm のフィルター（Andover 社製）を用いることで、全天を 5 波長同時撮像する。

カメラの制御は、小型 PC（ESC 社製 LIVA-Q2、OS：Linux Ubuntu）を使用する。1 台の LIVA-Q2 は 1 台のカメラを制御する設計であり、5 台を並列に動作させる。撮像のスケジュールは、開始時刻と終了時刻が毎日自動生成されるプログラムをもとに決められる。このプログラムは、太陽天頂角の時系列から夜間を判定し、スケジュールを自動決定する。自作の撮像プログラムは、ZWO 社ライブラリ「ASIStudio」の一部をモジュールとして利用し、撮像スケジュールをもとに自動運用が行われる。この自動運用は、cron を用いる。撮像の露光時間は 18 秒、間隔は 20 秒としているが、これは科学目的に応じて自由に変更可能である。

撮像されたデータは、NAS（Synology 社製 DS918+）にネットワーク経由で保存する。保存には RAID1 を使用し、常にミラーリングしてバックアップをとるため、HDD 故障が生じてもデータの損失を防ぐことが可能である。なお、この NAS には 4 つの HDD を搭載可能である。したがって、1 つ 12TB の HDD を使用した場合、合計容量は 48TB になるため、24TB 分の観測データを保存可能である。

LIVA-Q2 や NAS の電源は、インターネットスイッチ（明京電気製 Watchboot）を用いる。Watchboot はインターネット経由で ping 監視が可能であり、PC からの応答がない場合はフリーズしたと判定して電源の OFF/ON を行う。これにより機器を復旧させて長期的に安定した自動運用を達成できることが、しらせにおける連続観測で実証されている。

HDD に記録された全データ回収は、1 年間に 1 回程度の機会しかない。このため、しらせ観測と同様に、取得データの Quick Look(QL) を自動作成し、毎日 E-mail により日本に送信して機器の健全性を確認する。

当初本観測システムは 2022 年 11 月に南極点基地に設置する計画であったが、COVID-19 の影響のため現状で未確定である。このため、観測システムの連続動作確認のために、本年出発する 63 次南極観測隊で機器を輸送し、昭和基地に設置計画を並行して進めている。

R006-P14
ポスター１：11/4　PM1/PM2（13:45-18:15）

#西山　尚典[1,5], 鍵谷　将人[2], 小川　泰信[1,5], 津田　卓雄[3], 古舘　千力[3], 岩佐　祐希[4], 土屋　史紀[2]
([1]極地研,[2]東北大・理・惑星プラズマ大気研究センター,[3]電通大,[4]産総研・計量標準総合センター,[5]総研大

A new spectroscopic and imaging observation of SWIR aurora and airglow (1.1-1.3 μm) at Longyearbyen with EISCAT Svalbard radar

#Takanori Nishiyama[1,5], Masato Kagitani[2], Yasunobu Ogawa[1,5], Takuo Tsuda[3], Senri Furutachi[3], Yuki Iwasa[4], Fuminori Tsuchiya[2]
([1]NIPR,[2]PPARC, Tohoku Univ.,[3]UEC,[4]NMIJ, AIST,[5]The Graduate University for Advanced Studies, SOKENDAI

A new ground-based optical observation of aurora and airglow in short-wavelength infrared (SWIR) of 1.1-1.3 μm is being planned in Longyearbyen (78.2^{o}N, 15.6^{o}E) in conjunction with EISCAT Svalbard Radar (ESR). Two state-of-the-art instruments, a SWIR imaging spectrograph and a monochromatic camera, have been developed to focus on study on dayside magnetosphere-ionosphere-atmosphere coupling processes in the high polar regions.

The 2-D imaging spectrograph, NIRAS-2, has fast optics and high spectral resolution for the challenge of twilight/daytime auroral observations from the ground. It has a field of view of 55 degrees and an angular resolution of 0.11 degrees/pixel. It covers the SWIR wavelength range of 1.1-1.3 μm, where the sky background intensity is weaker than in visible light; it covers the strong auroral emission of N_2^+, the Meinel band (0-0) and the N_2 1st Positive band (1-2,0 -1). When a 30-μm slit is used, the spectral bandpasses around 1.1 μm are 0.53 nm and 0.21 nm for two gratings of 950 lpmm and 1500 lpmm, respectively. Test observations successfully measured airglow emission in the OH (5,2), (6,3), (7,4), and (8,5) bands at 1.07-1.33 μm and in the O_2 IR band at 1.27 μm. The 1500-lpmm grating and a 60-μm slit allowed us to resolve the OH (5,2) band well with a signal-to-noise ratio of 5-6. The peak intensity of the N_2^+(0,0) band is about 10 times that of the OH (5,2) $P_1(3)$ line. It was concluded that the spectrograph can detect auroras with a time resolution shorter than 30 sec and can investigate spatial and temporal variations due to solar wind-magnetospheric-ionospheric coupling and particle precipitations. For the upper mesosphere, the OH (8,5) band was sufficiently measured using a 950-lpmm grating and a 60-m slit. The rotational temperature can be estimated with a resolution of 10 minutes and an error of less than 3 K.

In addition to the spectrograph, we have developed a completely new SWIR camera, NIRAC, which focuses on auroral emission in the N_2^+ (0-0) band. The camera consists of several commercial SWIR lenses for security/defense applications, a plano-convex lens, a custom optical filter (center: 1112.76 nm, FWHM: 13.8 nm) and an InGaAs FPA (640 x 512 pixels). The entire optical system is fast (f-number 1.5), and the point spread function is less than 5 pixels at full width at half maximum, even near the edge of the FPA. The FOV is 92 x 73 degrees, slightly wider than the spectrograph.

Both instruments will be installed at The Kjell Henriksen Observatory/The University Centre in Svalbard (KHO/UNIS) by the end of FY2022. Taking advantage of the geographical location of this observatory, continuous 24-hour observation around the winter solstice is expected. Observational studies in conjunction with active and passive radio remote sensing such as ESR and VLF/LF radio receivers are also planned to accurately estimate the energy flux of precipitation particles associated with auroras and the associated changes in electron density and neutral and ion temperature. Scientific targets include dayside reconnection and wave-particle interactions monitored by auroral emissions, ion upflows seen as resonant scattering of N_2^+ ions, effects of high-energy particle precipitation on OH chemistry in the upper mesosphere, atmospheric wave activities, and disturbances of ionosphere in the E-F region. Observational strategies and future collaborations will also be discussed.

R006-P15
ポスター 1 ：11/4　PM1/PM2 （13:45-18:15）

惑星探査に向けた 10-100 keV 電子観測用アナログ-デジタル混載 ASIC 開発

#菅生　真 [1)], 笠原　慧 [2)], 池田　博一 [3)], 小嶋　浩嗣 [4)], 頭師　孝拓 [5)], 菊川　素如 [4)]
([1] 東大・理・地惑,([2] 東京大学,([3]JAXA,([4] 京大・生存圏,([5] 奈良高専

Development of mixed analog-digital ASIC for 10-100 keV electron sensor for planetary exploration

#Shin Sugo[1)], Satoshi Kasahara[2)], Hirokazu Ikeda[3)], Hirotsugu Kojima[4)], Takahiro Zushi[5)], Motoyuki Kikukawa[4)]
([1]Earth and Planetary Science, Univ. Tokyo,([2]The University of Tokyo,([3]JAXA,([4]RISH, Kyoto Univ.,([5]National Institute of Technology , Nara Col

We developed an ASIC (Application Specific Integrated Circuit) for signal processing circuits of APD (Avalanche PhotoDiodes) detectors to miniaturize a high energy electron sensor for future planetary explorations. Our sensor's objects are electrons with 10-100 keV energy, which is key energy range for the acceleration of electrons because that is transitional energy range from thermal to non-thermal distributions of energy spectrum. Recently, APDs, which are detectors with high detection efficiency for 10-100 keV electrons, have been applied to an energetic electron sensor onboard the Earth-orbiting satellite and have shown their effectiveness. On the other hand, the energy range of APD is narrow, and combined use with other detectors is indispensable to cover the wide energy range of electrons near the planet and leads to increasing weight. It is not suitable for planetary explorations, which place stringent limitation on payload mass. Therefore, we aim to miniaturize the sensor by applying the ASIC technology to signal processing circuits, which occupies a significant volume of the sensor. So far, we have designed an ASIC considering the characteristics of APDs with a built-in amplification and large detector capacitance, verified its operation through simulation, produced ASIC chips, about 100 times smaller than the previous circuit, and evaluated performance of the analog circuit of our ASIC chips. In this presentation, we will show the normality of operation of the digital circuit in addition to the analog circuit in our chip and that sufficient input/output linearity is obtained for the signal from the APD.

本研究では将来の惑星探査機搭載に向けて高エネルギー電子観測器の小型化を目指し、電子検出器 APD (Avalanche PhotoDiodes) 用信号処理回路の ASIC (Application Specific Integrated Circuit) 化開発を行っている。我々の電子観測器の観測エネルギーレンジは 10-100 keV であり、熱的な分布から非熱的な分布に遷移する、惑星周辺の電子加速機構の研究に重要なエネルギー領域である。近年この 10-100 keV 電子に感度の良い検出器として APD が地球周回衛星に搭載され、その有効性が示されている。一方で検出器 APD はエネルギーレンジが狭く、惑星近傍の電子の広いエネルギーレンジをカバーするためには他の検出器との併用が必要不可欠である。そのため重量が増加しペイロード重量制限の厳しい惑星探査機搭載や小型探査には向かない。そこで本研究では従来の電子観測器では信号処理回路が大きな体積を占めていることに着目し、検出器 APD の信号処理回路を ASIC 技術によって 100 分の 1 サイズに小型化した。これまでに我々は APD が増幅機構を内蔵し、大きな検出器容量を持つという特性を考慮した設計を行い、シミュレーションでその動作を確認した後、製作した ASIC チップのアナログ部の性能を評価してきた。本発表ではアナログ部に加えてデジタル部の動作の正常性と APD からの信号に対して十分な入出力の線形性が得られたことを示す。

R006-P16
ポスター 1 ：11/4　PM1/PM2 （13:45-18:15）

粒子センサ用高速検出回路の小型集積化に関する研究

#菊川　素如 [1)], 浅村　和史 [2)], 横田　勝一郎 [3)], 栗田　怜 [4)], 頭師　孝拓 [5)], 小嶋　浩嗣 [1)]
([1] 京大・生存圏,[2] 宇宙研,[3] 大阪大,[4] 京都大学 生存研,[5] 奈良高専

Study on Development and Integration of the High-Speed Current Detection Circuits in Particle Sensors

#Motoyuki Kikukawa[1)], Kazushi Asamura[2)], Shoichiro Yokota[3)], Satoshi Kurita[4)], Takahiro Zushi[5)], Hirotsugu Kojima[1)]
([1]RISH, Kyoto Univ.,[2]ISAS/JAXA,[3]Osaka Univ.,[4]RISH, Kyoto Univ.,[5]National Institute of Technology , Nara Col

Since space plasmas show a collision less feature, wave-particle interaction dominate electromagnetic environment. Observation of both particles and waves are essential to understand energy and momentum transfer mechanisms. For observations of spatially non-uniform space plasmas, it is critical to perform the formation flight consisting of multiple satellites. Recent trends of spacecraft fleet missions in the terrestrial magnetosphere such as Cluster II [Escoubet et al., 2001], THEMIS [Angelopoulos, 2008] and MMS missions [Burch et al., 2015] consist of at most five satellites. More satellites are necessary to observe spatial structures and temporal variations of the space plasmas in more detail. However, it is difficult to realize simultaneous multi-point observations of tens to hundreds satellites due to huge resource demands including weight, size and power consumption. The use of small satellites such as CubeSat is effective in realizing large-scale multi-point observations.

Minimization of weight, size and power consumption is essentially important for building an instrument onboard satellite. The present study focuses on the miniaturization of particle instruments. A time-of-flight (TOF) technique is commonly used for mass discrimination of incoming particles. Typical TOF measures speed of incoming particles using a timing difference between their passages at two points inside a sensor. Required resolution of the elapsed time measurement is 1 ns or more since particle path length of a TOF sensor is a few to tens of centimeters, and incoming particles have energies in keV range. Thus a high-speed particle detector that operates at 1 ns or faster is necessary to perform TOF measurements. A conventional particle detector consists of 15 substrates that are the size of 60 mm x 57 mm each, and consumes a volume of more than 1400 cm^3. Here we are developing an ASIC (Application Specific Integration Circuit) based fast particle detector for satellite-borne plasma particle sensors. By using ASIC technology, required size for the circuit can be drastically reduced. The new detector is a size of less than 5 mm x 5 mm (implemented on a chip) that can handle more than 1 million signals per second. Laboratory experiment shows that the developed ASIC can detect output signals of MCP (Micro Channel Plate) within timing fluctuation of 1 ns, which can be applied for typical TOF-based ion energy-mass spectrometers. We will report the performances of the developed ASIC and results of laboratory experiment using a TOF-based ion mass analyzer.

R006-P17
ポスター 1 ：11/4　PM1/PM2 （13:45-18:15）

#篠原　育 [1)], 三谷　烈史 [1)], 寺本　万里子 [2)], 浅村　和史 [1)], 川越　弓恵 [1)], 大野木　瞭太 [1)], 高島　健 [1)]
([1] 宇宙研／宇宙機構,([2] 九工大,([3] 九工大,([4] 宇宙研

The latest status of a high-energy electron analyzer (PINO) onboard a CubeSat (BIRDS-5)

#Iku Shinohara[1)], Takefumi Mitani[1)], Mariko Teramoto[2)], Kazushi Asamura[1)], Yumie Kawagoe[1)], Ryota Onogi[1)], Takeshi Takashima[1)]
([1]ISAS/JAXA,([2]Kyutech,([3]Kyutech,([4]ISAS, JAXA,

We have developed a compact high-energy electron analyzer, nicknamed PINO (Particle Instrument for NanO-satellite), supported by the JSPS KAKENHI and the collaboration with the Kyushu Institute of Technology. The development of the PINO Flight Model finished this spring, and it has been installed on a 2-U CubeSat, BIRDS-5J (Taka). All the function tests have been successfully completed, and the BIRDS-5 satellites have been delivered to JAXA. The BIRDS-5 fleet will be released from the international space station (ISS) in autumn 2022. Although the schedule of the operations in the commissioning phase is not fixed yet, in this presentation, we will report the initial status of PINO in space.

R006-P18
ポスター 1 ：11/4　PM1/PM2 （13:45-18:15）

内部磁気圏における ULF 波動の伝搬過程を解く MHD シミュレーションコードの開発

#礒野　航 [1)], 加藤　雄人 [1)], 川面　洋平 [1,2)], 熊本　篤志 [1)]
([1] 東北大・理・地球物理,[2] 東北大学学際科学フロンティア研究所,[3] 東北大・理・地球物理

Development of the MHD simulation code for the propagation of ULF waves in the inner magnetosphere

#Isono Ko[1)], Yuto Katoh[1)]Atsushi Kumamoto[1)]
([1]Dept. Geophys., Grad. Sch. Sci., Tohoku Univ.,[2]Frontier Research Institute for Interdis-ciplinary Sciences Tohoku University,[3]Dept. Geophys, Tohoku Univ.

The excitation and propagation of ultra-low frequency (ULF) waves are ubiquitously observed in the Earth's inner magnetosphere during geomagnetically disturbed periods. ULF waves are characterized by long wave periods of tens to hundreds of seconds and wavelengths of thousands of kilometers, globally distributed in the magnetosphere. The driving source of ULF waves is known to be an excitation process from outside the magnetosphere and a generation process inside the magnetosphere. The former is mainly due to solar wind pressure fluctuations and Kelvin-Helmholtz instability at the magnetopause, while the latter is mainly due to energetic ions injected into the inner magnetosphere during substorms (e.g., Takahashi, 2015). It has also been pointed out that ULF waves modulate the flux and pitch angle distributions of energetic electrons (Zhou et al., 2016). On the other hand, the feedback process from energetic electrons to ULF waves has not been discussed. However, in recent years, numerical simulations and observations revealed the effect of energetic electrons on ULF waves. Hori et al. (2018) clarified the simultaneous occurrence of the flux enhancement of energetic electrons drifting eastward and ULF waves propagating eastward from the simultaneous observations by the Arase satellite and the radar Super Dual Auroral Radar Network (SuperDARN). Ono et al. (2020) revealed in the Arase satellite observation that the flux and pitch angle distribution of energetic electrons are modulated by ULF waves, and suggested that the observed relationship can be explained by considering ULF waves with m-number larger than the typical value of toroidal mode ULF waves. These new observational findings suggest the need for a comprehensive study of the relationship between ULF waves and energetic electrons, including the energy exchange between them.

In this study, to discuss the interaction between energetic electrons and ULF waves in the magnetosphere, we develop an MHD simulation code to quantitatively compute the propagation of ULF waves in the inner magnetosphere. Since the amplitude of the ULF wave is sufficiently small with respect to the background magnetic field strength, the contribution of the nonlinear term is assumed to be small and only the linear term of the set of MHD equations is considered. To solve the propagation of ULF waves in the radial and longitudinal directions, we set a spatially three-dimensional simulation system using cylindrical coordinates [e.g., Southwood and Kivelson, 1984] with the Z axis in the magnetic field line direction, r axis in the radial direction, and theta axis in the meridional direction. The spectral method is used for both the Z and theta axes to reduce the computational cost. We assume a few wavenumber components in the Z axis for fundamental and lowest order harmonics of standing Alfven waves. We set tens of wavenumber components in the theta axis to treat high m-number ULF waves. Using the developed model, we calculate the propagation of fundamental ULF waves initially assumed in a specific longitude range, the equipartition of electromagnetic energy among toroidal and poloidal modes, and the mode conversion between fast and shear Alfven waves in the inner magnetosphere.

地球内部磁気圏では磁気嵐などに伴い、ULF 波動と呼ばれるプラズマ波動が観測されている。ULF 波動は周期が数十秒から数百秒と長く、波長が数千キロメートルと内部磁気圏全体にわたる現象である。ULF 波動の駆動源としては磁気圏外部からの励振過程ならびに磁気圏内部での発生過程の存在が明らかにされており、前者は太陽風動圧の変動や磁気圏界面におけるケルビン-ヘルムホルツ不安定、後者は磁気擾乱時にサブストーム等により注入される高エネルギーイオンが主な要因とされている (e.g., Takahashi, 2015)。また、内部磁気圏で発生した ULF 波動により、高エネルギー電子のフラックスやピッチ角分布に変化が生じることが指摘されている (Zhou te al., 2016)。一方で、高エネルギー電子が ULF 波動に与える影響については論じられてこなかった。

しかしながら近年、数値計算や観測から高エネルギー電子と ULF 波動との様々な関係性が指摘されている。Hori et al. (2018) はあらせ衛星と短波レーダー SuperDARN の同時観測から、朝側にドリフトする高エネルギー電子と朝側に伝搬する ULF 波動が同時に生じている様相を明らかにした。また、Ono et al. (2020) は、あらせ衛星による観測結果から、ULF 波動によって高エネルギー電子のフラックスおよびピッチ角分布が変調を受けている現象を見出し、典型的な値よりも大きな方位角方向モード数 (m-number) を示す ULF 波動を考えることで説明できることを明らかにした。これらの新たな観測事実は、ULF 波動と高エネルギー電子の関係性について相互作用も含めた包括的な研究の必要性を示唆している。

本研究では、磁気圏内での高エネルギー電子と ULF 波動の相互作用を議論するために内部磁気圏における ULF 波動

の伝搬と波動特性を定量的に明らかにすることを目的として、MHD 方程式系を基礎方程式とするシミュレーションコードを開発している。ULF 波動の振幅は背景磁場強度に対して十分に小さいことから、非線形項の寄与は小さいとして、線形化した MHD 方程式系を取り扱う。磁気圏内における ULF 波動の動径方向、経度方向への伝搬を解こうために、磁力線方向に z 軸、動径方向に r 軸、経度方向に θ 軸を取る円筒座標系 [e.g., Southwood and Kivelson, 1984] を用いた空間 3 次元方向のシミュレーション空間を設定する。ここで磁力線方向、経度方向についてスペクトル法を用いることにより、計算コストの削減を図る。波数空間としては磁力線方向については一桁、経度方向については二桁程度の波数を対象とする。このモデルを用いて、特定の経度範囲において存在する fundamental mode のＵＬＦ波動がどのように伝搬し、toroidal mode と poloidal mode の分配ならびに fast mode と shear Alfven wave 間でのモード変換がどのように生じるかについて考察する。

R006-P19
ポスター 1 ：11/4　PM1/PM2 （13:45-18:15）

#河野　英昭 [1)], 行松　彰 [2)], 西谷　望 [3)], 田中　良昌 [4)], 才田　聡子 [5)], 堀　智昭 [3)]
([1] 九大・理・地球惑星/九大・i-SPES,[2] 国立極地研究所/総研大,[3] 名大 ISEE,[4] 国立極地研究所/ROIS-DS/総研大,[5] 北九州高専

Effects of increasing the frequency resolution of FFT on the density estimation from the SuperDARN data

#Hideaki Kawano[1)], Akira Sessai Yukimatu[2)], Nozomu Nishitani[3)], Yoshimasa Tanaka[4)], Satoko Saita[5)], Tomoaki Hori[3)]
([1]Dept. Earth Planet. Sci., and i-SPES, Kyushu Univ.,[2]NIPR/SOKENDAI,[3]ISEE, Nagoya Univ.,[4]NIPR/ROIS-DS/SOKENDAI,[5]NITkit

There are several kinds of waves driven by the solar wind, including those associated with sudden impulses (SI). The upstream impulses and/or waves can propagate into the magnetosphere, and can excite eigen-oscillations of the field line with frozen-in plasma, that is, field-line resonance (FLR), where the wave frequency matches the eigen-frequency of a geomagnetic field line. It is known that the gradient methods (collective name for the amplitude-ratio method and the cross-phase method) enable us to effectively extract FLR signals from observed data including non-FLR signals as well. From thus identified FLR frequency one can estimate the mass density of plasma along the magnetic field line, because, in a simplified expression, 'heavier' field line oscillates more slowly.

We have been applying the gradient methods to the VLOS (Velocity along the Line of Sight) data of the SuperDARN radars. The radars emit azimuthally-collimated beams of radio waves in the HF range, and some of them are backscattered by the ionosphere (mainly through 1/2-hop paths), while some others are backscattered by the ground and the sea (mainly through one-hop paths). From the Doppler shift of backscattered signals, one can calculate VLOS. Ionosphere-backscattered signals yield VLOS of the horizontally-moving ionospheric plasma (at mid- to low latitudes, VLOS also has vertical component, because the ambient magnetic field is tilted), while ground/sea-backscattered signals yield VLOS corresponding to the vertical motion of the ionospheric plasma, because the length of the ray path of a beam can only be changed by the vertical motion of the ionosphere.

For a 30-min-interval event after an SI, we applied the gradient methods to VLOS data obtained from different beams and range gates, and successfully identified the FLR in both the ionosphere-backscattered signals and sea-backscattered signals. The mass density was thereby estimated using both scatters. As a result, the latter was significantly smaller than the former.

We infer that this large difference could come from a fairly large frequency spacing of the FFT analysis due to the fairly small duration (30min) of the event. Thus, in this paper we have increased the frequency resolution by zero-padding; it is worth noting here that the gradient methods use timeseries data obtained at two locations and takes the ratio of the FFT results of the two data, and thus that the decrease in the amplitude due to zero-padding is cancelled out.

As a first test, we zero-padded certain periods just after the observed period so that the time length was elongated to 90 min. As a result, the frequency resolution became three times higher, and thus the FLR frequency became more precise. From these higher-precision FLR frequencies we estimated plasma densities, and the above-stated density difference between the ionosphere-backscattered signals and the sea-backscattered signals became smaller. In this presentation we report the results of further testing and examination of the zero-padding, bearing in mind that it will be meaningful to compare the result of zero-padding with the result of applying the Lomb-Scargle method to the original data.

R006-P20
ポスター１：11/4　PM1/PM2（13:45-18:15）

#寺本　万里子[1)], 能勢　正仁[2)], 松岡　彩子[3)], 笠原　禎也[4)], 浅村　和史[5)], 熊本　篤志[6)], 土屋　史紀[6)], 新堀　淳樹[2)], 三好　由純[2)], 小路　真史[2)], 中村　紗都子[2)], 北原　理弘[6)], 今城　峻[3)], 篠原　育[5)]
([1] 九工大,[2] 名大・宇地研,[3] 京都大学,[4] 金沢大,[5] 宇宙研,[6] 東北大・理・惑星プラズマ大気

Temporal evolution of nightside plasma mass in the inner magnetosphere during a geomagnetic storm using the Arase measurement

#Mariko Teramoto[1)], Masahito Nose[2)], Ayako Matsuoka[3)], Yoshiya Kasahara[4)], Kazushi Asamura[5)], Atsushi Kumamoto[6)], Fuminori Tsuchiya[6)], Atsuki Shinbori[2)], Yoshizumi Miyoshi[2)], Masafumi Shoji[2)], Satoko Nakamura[2)], Masahiro Kitahara[6)], Shun Imajo[3)], Iku Shinohara[5)]
([1]Kyutech,[2]ISEE, Nagoya Univ.,[3]Kyoto University,[4]Kanazawa Univ.,[5]ISAS/JAXA,[6]Planet. Plasma Atmos. Res. Cent., Tohoku Univ.

We investigate the spatial and temporal evolution of the ion mass density and average ion mass on the nightside in the inner magnetosphere during a geomagnetic storm that stated on 25 August 2018. To evaluate the ion mass density and average ion mass on the nightside, we applied the magnetoseismic technique for the 29 transient toroidal waves (TTWs) observed at substorm onsets by the Arase satellite. These TTWs are excited on the nightside (22-03 magnetic local time) and in the southern hemisphere from -30 to -15 magnetic latitudes. We determined the fundamental eigen frequency of TTWs from the spectra of the azimuthal component of the magnetic field and derived the mass density from the eigen frequency. We also determined the electron number density from the plasma wave experiment (PWE) from Arase. We found that the average ion mass enhancement exists around the plasmapause in the early and late recovery phases of the geomagnetic storm and the ion mass enhancement around the plasmapause disappears during the end of the early recovery phase. These results may suggest that the oxygen torus are formed on the nightside during the recovery phase and they do not stay steady locations on the nightside.

R006-P21
ポスター 1 ：11/4　PM1/PM2 （13:45-18:15）

#田　采祐[1)], 三好　由純[1)], 堀　智昭[1)], 中村　紗都子[1)], 小路　真史[1)],Kistler　Lynn[1,2)],Yue Chao[3)],Bortnik　Jacob[4)], 浅村　和史[5)], 横田　勝一郎[6)], 笠原　慧[7)], 桂華　邦裕[7)], 篠原　育[5)], 松岡　彩子[8)],Lyons　Larry[4)]
([1] 名大 ISEE 研,[2]University of New Hampshire,[3]Institute of Space Physics and Applied Technology, Peking University, Beijing, China,[4]UCLA,[5] 宇宙研,[6] 大阪大,[7] 東京大学,[8] 京都大学

A statistical study of energetic ions (H+, He+, and O+) in the inner magnetosphere using the Arase satellite observations

#ChaeWoo Jun[1)], Yoshizumi Miyoshi[1)], Tomoaki Hori[1)], Satoko Nakamura[1)], Masafumi Shoji[1)], Lynn Kistler[1,2)], Chao Yue[3)], Jacob Bortnik[4)], Kazushi Asamura[5)], Shoichiro Yokota[6)], Satoshi Kasahara[7)], Kunihiro Keika[7)], Iku Shinohara[5)], Ayako Matsuoka[8)], Larry Lyons[4)]
([1]ISEE, Nagoya Univ.,[2]University of New Hampshire,[3]Institute of Space Physics and Applied Technology, Peking University, Beijing, China,[4]UCLA,[5]ISAS/JAXA,[6]Osaka Univ.,[7]The University of Tokyo,[8]Kyoto University

We perform a statistical study of energetic ions (H+, He+, and O+) in the inner magnetosphere depending on geomagnetic conditions using the Arase satellite observations from March 2017 to December 2021. We used a combined dataset for ions (LEPi and MEPi) onboard the Arase satellite with a combined energy range of 0.01-187 keV. In order to examine the spatial distributions of energetic ions depending on geomagnetic conditions, the energy fluxes for all species were sorted by the magnetic local time (MLT), L∗shell, energy, and three Kp steps (quiet: Kp<1, intermediate: Kp=1-3, disturbed: Kp>3). Overall, all ion species showed similar spatial distributions. Taking a close look at the resultant L∗-energy and L∗-MLT spectra, we can find four distinct H+ populations within different energy ranges: (1) plasmaspheric H+ (E <30 eV) at L <5, (2) warm plasma cloak at energies of several tens eV - several keV, (3) the ring current population (E = 1 keV − several tens of keV) with nose structures, (4) high-energy ring current particles (E >30 keV) with symmetric distributions in MLT, and these populations exhibited different behaviors as Kp increases. At E=0.05-1 keV, other heavy ions (He+ and O+) show higher energy fluxes near the earth region (L∗˜2) and the energy flux has the tendency that keeps decreasing as L∗increases. On the other hand, H+ exhibits significant energy flux variations inside and outside the plasmasphere, and a higher energy flux of H+ appears outside the plasmasphere. Ion nose structures appeared at energies of ˜several keV in the noon and dusk sectors. These structures showed inner boundaries at different L∗locations for different ion species (L∗˜4 for H+, L∗˜2 for He+ and O+). The difference in L∗is due to a longer charge exchange lifetime for heavy ions as compared to that for H+. We discuss the underlying physical dynamics and the possible origins of the different populations and compare the observational results with a model calculation using simple electric and magnetic fields.

R006-P22
ポスター 1 ：11/4　PM1/PM2 （13:45-18:15）

#堀　智昭 [1)], 三好　由純 [1)], 中村　紗都子 [2)], 笠羽　康正 [3)], 中川　朋子 [4)], 北原　理弘 [5)], 松田　昇也 [6)], 西谷　望 [1)],Shepherd　Simon G.[7)],Ruohoniemi　John M.[8)], 熊本　篤志 [9)], 土屋　史紀 [9)], 笠原　禎也 [10)], 浅村　和史 [11)], 田　采祐 [12)], 風間　洋一 [13)],Wang　Shiang-Yu[14)],Tam　Sunny W. Y.[15)], 桂華　邦裕 [16)], 笠原　慧 [17)], 横田　勝一郎 [18)], 松岡　彩子 [19)], 篠原　育 [20)]
([1] 名大 ISEE,[2]IAR&ISEE,[3] 東北大・理,[4] 東北工大・工・情報通信,[5] 東北大・理・地球物理,[6] 金沢大学,[7]Dartmouth College,[8] バージニア工科大,[9] 東北大・理・惑星プラズマ大気,[10] 金沢大,[11] 宇宙研,[12] 名大 ISEE 研,[13]ASIAA,[14] 中央研究院天文及天文物理研究所,[15] 国立成功大学宇宙・プラズマ科学研究所,[16] 東大・理,[17] 東京大学,[18] 大阪大,[19] 京都大学,[20] 宇宙研／宇宙機構

SAPS electric field and particle boundaries in the equatorial magnetosphere as observed by Arase

#Tomoaki Hori[1)], Yoshizumi Miyoshi[1)], Satoko Nakamura[2)], Yasumasa Kasaba[3)], Tomoko Nakagawa[4)], Masahiro Kitahara[5)], Shoya Matsuda[6)], Nozomu Nishitani[1)], Simon G. Shepherd[7)], John M. Ruohoniemi[8)], Atsushi Kumamoto[9)], Fuminori Tsuchiya[9)], Yoshiya Kasahara[10)], Kazushi Asamura[11)], ChaeWoo Jun[12)], Yoichi Kazama[13)], Shiang-Yu Wang[14)], Sunny W. Y. Tam[15)], Kunihiro Keika[16)], Satoshi Kasahara[17)], Shoichiro Yokota[18)], Ayako Matsuoka[19)], Iku Shinohara[20)]
([1]ISEE, Nagoya Univ.,[2]IAR&ISEE,[3]Tohoku Univ.,[4]Tohoku Inst. Tech.,[5]Dept. Geophys., Grad. Sch. Sci., Tohoku Univ.,[6]Kanazawa Univ.,[7]Dartmouth College,[8]ECE, Virginia Tech,[9]Planet. Plasma Atmos. Res. Cent., Tohoku Univ.,[10]Kanazawa Univ.,[11]ISAS/JAXA,[12]ISEE, Nagoya Univ.,[13]ASIAA,[14]Institute of Astronomy and Astrophysics, Academia Sinica, Taiwan,[15]Institute of Space and Plasma Sciences, National Cheng Kung University, Taiwan,[16]University of Tokyo,[17]The University of Tokyo,[18]Osaka Univ.,[19]Kyoto University,[20]ISAS/JAXA

Electric field (E-field) enhancement of subauroral polarization streams (SAPS) and particle boundaries in the inner magnetosphere is extensively investigated by analyzing particle and field data obtained by the Arase satellite and ionospheric convection data obtained by Super Dual Auroral Radar Network (SuperDARN). The poleward E-field of ionospheric SAPS is thought to be applied by a pair of the field-aligned currents driven by a latitudinal gap between the ion and electron plasma sheets (PS). Indeed, the enhancement of electric field is frequently observed between the two PS in the ionosphere, as reported by past studies using low-altitude satellites. Arase also frequently observes a radially-outward E-field enhancement right on the earthward side of the electron PS in associated with a poleward E-field of ionospheric SAPS identified by SuperDARN. A close examination of the Arase observations, however, reveals that SAPS E-field is not confined in the PS gap, but rather is often located in the region of the outward pressure gradient of the ring current ions. Their inner edge locations match in some events, while in some other cases, they do not match closely and the ring current ions are extended further inward than the SAPS E-field. We discuss possible mechanisms that could explain the variety of the spatial relationship of SAPS with the PS and ring current populations.

R006-P23
ポスター１：11/4　PM1/PM2（13:45-18:15）

地上光学・電波機器とあらせ衛星・Van Allen Probes 衛星の同時観測に基づくサブオーロラ帯の３種類のオーロラの複数例解析

#椙村　怜[1)], 塩川　和夫[1)], 大塚　雄一[1)], 大山　伸一郎[1)],Connors　Martin[2)], 門倉　昭[3)],Shevtsov Boris[4)],Poddelsky Alexey[4)],Poddelsky　Igor[4)], 西谷　望[1)],Shepherd　Simon G.[5)],Ruohoniemi　John M.[6)],Smith Charles W.[7)],Macdowall　Robert J.[8)], スペンス　ハラン[7)], リーブス　ジェフ[9)],Funsten Herbert O.[9)], 三好　由純[1)], 篠原　育[10)], 笠原　禎也[11)], 土屋　史紀[1)], 熊本　篤志[12)], 中村　紗都子[1)], 新堀　淳樹[1)], 浅村　和史[13)], 横田　勝一郎[14)], 風間　洋一[15)], 田　采祐[1)],Wang　Shiang-Yu[15)],W. Y. Tam　Sunny[16)], 笠原　慧[17)]
([1] 名大 ISEE,[2]Athabasca University,[3]National Institute of Polar Research, Midori-cho 10-3, Tachikawa, Tokyo 190-8518, Japan,[4]Institute of Cosmophysical Research and Radiowave Propagation,[5]Thayer School of Engineering, Dartmouth College, Hanover, NH, USA,[6]Bradley Department of Electrical and Computer Engineering, Virginia Tech, Blacksburg, VA, USA,[7]Institute for the Study of Earth, Oceans, and Space, University of New Hampshire,[8]NASA Goddard Space Flight Center, Greenbelt, MD, USA,[9]Los Alamos National Laboratory, Los Alamos, NM, USA,[10]Institute of Space and Astronautical Science, Japan Aerospace Exploration Agency,[11]Graduate School of Natural Science and Technology, Kanazawa University,[12]Graduate School of Science, Tohoku University,[13]Japan Aerospace Exploration Agency,[14]Department of Earth and Space Science, Graduate School of Science, Osaka University,[15]Academia Sinica Institute of Astronomy and Astrophysics,[16]Institute of Space and Plasma Sciences, National Cheng Kung University,[17]Department of Earth and Planetary Science, School of Science, University of Tokyo,[18]Graduate School of Science, Tokyo University,[19 宇宙研,[20 大阪大,[21]ASIAA,[22 名大 ISEE 研,[23]Academia Sinica,[24]Los Alamos National Laboratory, Los Alamos, NM, USA

Multi-event analysis of three-types of auroras at subauroral regions using ground instruments and magnetospheric satellites

#Rei SUGIMURA[1)], Kazuo Shiokawa[1)], Yuichi Otsuka[1)], Shin ichiro Oyama[1)], Martin Connors[2)], Akira Kadokura[3)], Boris Shevtsov[4)], Alexey Poddelsky[4)], Igor Poddelsky[4)], Nozomu Nishitani[1)], Simon G. Shepherd[5)], John M. Ruohoniemi[6)], Charles W. Smith[7)], Robert J. Macdowall[8)], Harlan Spence[7)], Geoff Reeves[9)], Herbert O. Funsten[9)], Yoshizumi Miyoshi[1)], Iku Shinohara[10)], Yoshiya Kasahara[11)], Fuminori Tsuchiya[1)], Atsushi Kumamoto[12)], Satoko Nakamura[1)], Atsuki Shinbori[1)], Kazushi Asamura[13)], Shoichiro Yokota[14)], Yoichi Kazama[15)], ChaeWoo Jun[1)], Shiang-Yu Wang[15)], Sunny W. Y. Tam[16)], Satoshi Kasahara[17)]
([1]ISEE,Nagoya univ,[2]Athabasca University,[3]National Institute of Polar Research, Midori-cho 10-3, Tachikawa, Tokyo 190-8518, Japan,[4]Institute of Cosmophysical Research and Radiowave Propagation,[5]Thayer School of Engineering, Dartmouth College, Hanover, NH, USA,[6]Bradley Department of Electrical and Computer Engineering, Virginia Tech, Blacksburg, VA, USA,[7]Institute for the Study of Earth, Oceans, and Space, University of New Hampshire,[8]NASA Goddard Space Flight Center, Greenbelt, MD, USA,[9]Los Alamos National Laboratory, Los Alamos, NM, USA,[10]Institute of Space and Astronautical Science, Japan Aerospace Exploration Agency,[11]Graduate School of Natural Science and Technology, Kanazawa University,[12]Graduate School of Science, Tohoku University,[13]Japan Aerospace Exploration Agency,[14]Department of Earth and Space Science, Graduate School of Science, Osaka University,[15]Academia Sinica Institute of Astronomy and Astrophysics,[16]Institute of Space and Plasma Sciences, National Cheng Kung University,[17]Department of Earth and Planetary Science, School of Science, University of Tokyo,[18]Graduate School of Science, Tokyo University,[19]ISAS/JAXA,[20]Osaka Univ.,[21]ASIAA,[22]ISEE, Nagoya Univ.,[23]Academia Sinica,[24]Los Alamos National Laboratory, Los Alamos, NM, USA

Additional co-authors:
Kunihiro Keika (1), Tomoaki Hori (2), and Ayako Matsuoka (3)
(1) Graduate School of Science, Tokyo University
(2) Institute for Space-Earth Environmental Research (ISEE), Nagoya University
(3) Institute of Space and Astronautical Science, Japan Aerospace Exploration Agency

Strong Thermal Emission Velocity Enhancement (STEVE) is a latitudinally-narrow, purple band of emission seen at subauroral latitudes, which was discovered in 2016. Further, well-known Stable Auroral Red (SAR) arcs also occurs at subauroral latitude. Red and green arcs, which are similar in that they occur in the subauroral latitudes to SAR arcs with only red emission, have been reported. However, the characteristics of the magnetospheric plasma and electromagnetic field variations as a source of these three types of optical emissions have not fully been studied using conjugate observations between magnetospheric satellites and ground-based optical and radio instruments. In this study, we report the auroral morphology as seen in all-sky image data obtained at seven locations (Athabasca, Gakona, Husafell, Kapuskasing, Magadan, Nyrola and Tromso) during about four years from January 2017 to April 2021. By referring to the optical images as well as the ionospheric footprint of magnetospheric satellites (Arase and Van Allen Probes) calculated with the Tsyganenko magnetic field model (TS04), we have identified four cases of STEVE, four cases of SAR arc, three cases of green and red

arcs in which these satellites were located in the conjugate regions in the magnetosphere of the optical emissions. For all three types of optical emissions, satellite data showed that the plasmasphere and ring-current particles spatially overlapped in the conjugate regions of the magnetosphere. An increase in the low-energy (0.1 to a few keV) electron flux as also found for all types of arcs. No significant mHz to kHz electromagnetic waves, nor electrostatic waves from 0.01 Hz to 10 kHz, were observed for any of these 11 events. SuperDARN radar data showed a strong westward plasma flow in the ionosphere, especially during the STEVE events, while the plasma flows associated with SAR arcs and red and green arcs are relatively weak and variable. These analyses not only provide the first comparison of the magnetospheric particle and electromagnetic field characteristics of the three types of optical emissions in the subauroral latitudes, but also provide an important summary of the differences and similarities between these optical emissions.

R006-P24
ポスター 1 ：11/4　PM1/PM2 （13:45-18:15）

科学衛星あらせによって観測された低周波波動の自動分類プログラムの開発

#山下　航河 [1)], 三宅　壮聡 [2)]
([1] 富山県大,[2] 富山県大

Development of automatic classification program for low frequency waves observed by Arase satellite

#Koga Yamashita[1)], Taketoshi Miyake[2)]
([1]Toyama Pref. Univ.,[2]Toyama Pref. Univ.

Various types of low frequency waves are observed by Electric Field Detector (EFD) onboard Arase satellite. In this study, we are going to detect these low frequency waves from EFD data, and classify these waves into several types by using Machine learning method. At first, we applied SVM method to EFD spectrum data from 2017 to 2019, and detected 806 low frequency waves. Next, we try to classify these low frequency waves into several types by clustering method. We apply K-means method and hierarchical clustering method to the EFD spectrum data and the numerical data, which are the duration time and the center frequency, of low frequency waves, respectively. We found 5 types of low frequency waves with different characteristics. However, many artificial noises are included in the waves with narrow-band spectrum, therefore, we are going to distinguish natural waves from artificial noises. In addition, we are going to detect the characteristic low frequency waves, which were confirmed visually, by using Machine learning method.

本研究では、科学衛星あらせに搭載された電場観測器 (EFD) によって宇宙空間で観測された低周波波動の分類を行う。最初に目視による分類を行い、比較的広帯域なスペクトルを持つ 3 種類の特徴的な波動が観測されていることが確認できた。しかし、低周波波動のデータは膨大であり、また目視による個人の先入観を排除するために、機械学習を利用して低周波波動の分類を行った。まず、 EFD の観測データから SVM 法を用いて低周波波動の検出を行った結果、806 個の低周波波動データを検出し、それぞれの発生時間と周波数帯を特定した。次にクラスタリングを用いて低周波波動の分類を行った。スペクトル画像データに K-means 手法、低周波波動検出時に特定した数値データに階層型クラスタリングを用いて分類を行った結果、低周波波動のタイプを狭帯域なスペクトルを持つ波動 2 種類、広帯域なスペクトルを持つ波動 3 種類に分けられた。しかし、狭帯域なスペクトルを持つ波動には人工ノイズが多く含まれていることが明らかになったため、更に人工ノイズと自然波動に分類する必要がある。また目視で確認できていた広帯域なスペクトルを持つ波動が機械学習では抽出できなかったため、EFD の数値データを用いて広帯域なスペクトルを持つ波動をさらに細かく分類し、目視による分類で確認できた特徴的な波動を抽出することを目指す。

R006-P25
ポスター 1 ：11/4　PM1/PM2 （13:45-18:15）

インターフェロメトリ観測に基づく ECH 波動の分散関係と背景電子温度の推定

#滝　朋恵 [1)], 栗田　怜 [2)], 新城　藍里 [1)], 中村　紗都子 [3)], 小嶋　浩嗣 [2)], 笠原　禎也 [4)], 松田　昇也 [4)], 松岡　彩子 [5)], 三好　由純 [6)], 篠原　育 [7)]
([1] 京大・工・電気,[2] 京都大学 生存研,[3]IAR&ISEE,[4] 金沢大,[5] 京都大学,[6] 名大 ISEE,[7] 宇宙研／宇宙機構

Derivation of dispersion of ECH waves and electron temperature from the interferometry observation by the Arase satellite

#Tomoe Taki[1)], Satoshi Kurita[2)], Airi Shinjo[1)], Satoko Nakamura[3)], Hirotsugu Kojima[2)], Yoshiya Kasahara[4)], Shoya Matsuda[4)], Ayako Matsuoka[5)], Yoshizumi Miyoshi[6)], Iku Shinohara[7)]
([1]Engineering, Kyoto Univ.,[2]RISH, Kyoto Univ.,[3]IAR&ISEE,[4]Kanazawa Univ.,[5]Kyoto University,[6]ISEE, Nagoya Univ.,[7]ISAS/JAXA

Electron Cyclotron Harmonic Waves (ECH) are longitudinal waves oscillating perpendicular to the ambient magnetic field and characterized by a harmonic structure that appears at (n+1/2) times the electron cyclotron frequency fce. The dispersion of ECH waves strongly depends on the electron temperature. Thus it is possible to estimate the electron temperature by determining the dispersion of ECH waves based on the plasma wave observation. This method is important because the energy of the core electrons, which determines the temperature of electrons, can be below the lower limit of the energy range covered by plasma particle sensors.

In this study, the dispersion of ECH waves is estimated using interferometry observations by the Arase satellite. Interferometry is a method to calculate the velocity and spatial scale of an object by making observations at multiple points and cross-correlating the data. The interferometry performed by the Arase satellite uses only two of its four antennas, and the interferometry is achieved by recording the differential voltages between each antenna and the satellite ground.

The phase difference and phase velocity of ECH waves between fce and 2fce are calculated in the frequency domain. It is found that the phase difference is larger at lower frequencies and the phase velocity is faster at higher frequencies. This is thought to be due to the fact that the phase velocity is faster at higher frequencies in the same branch as expected from the dispersion of ECH waves.

In this presentation, we will show the dispersion curve of ECH waves and estimated electron temperature from the interferometry observation performed by the Arase satellite.

電子サイクロトロン高調波（ECH: Electron Cyclotron Harmonic Waves）は磁力線に垂直方向に振動する縦波であり、電子サイクロトロン周波数の (n+1/2) 倍の周波数付近にスペクトルのピークを持つ高調波構造が特徴である。ECH 波動の分散関係は背景電子温度に依存することが知られており、ECH 波動の分散関係を観測から推定することで、背景電子温度を推定可能である。内部磁気圏においては、背景電子温度を決定するコアとなる電子は、粒子観測器の観測下限以下のエネルギーに存在している場合があるため、プラズマ波動計測から背景電子温度を推定することは重要な意味をもつ。

本研究では、ECH 波動の分散関係をあらせ衛星のインターフェロメトリ観測を用いて推定する。インターフェロメトリ観測とは、複数点で観測を行いそのデータの相互相関を取ることで、対象の速度や空間スケール、波長を推定する手法である。あらせ衛星では、4 本のアンテナのうち 2 本のみを使用し、各アンテナと衛星グラウンドの差動を測定することでインターフェロメトリ観測を実現している。

あらせ衛星のインターフェロメトリ観測で得られた、fce から 2fce の間の ECH 波動の位相差・位相速度を算出すると、位相差は周波数が低いほど大きくなり、位相速度は周波数が高いほど大きくなる傾向が見られた。これは ECH 波動が、同一のブランチでは周波数が高いほど位相速度が大きくなることと調和的な結果である。

本研究では、この周波数ごとの位相速度の変化を利用して分散曲線を推定し、背景電子温度の推定を試みる。

R006-P26
ポスター 1 ：11/4　PM1/PM2 （13:45-18:15）

あらせ衛星で観測されたコーラスエレメントの特徴解析

#平塚　貴也 [1)], 松田　昇也 [1)], 笠原　禎也 [1)], 中村　紗都子 [2)], 北原　理弘 [3)], 三好　由純 [2)], 篠原　育 [4)]
([1] 金沢大,[2] 名大 ISEE,[3] 東北大,[4] 宇宙研／宇宙機構

Feature analysis of chorus elements observed by the Arase satellite

#Takaya Hiratsuka[1)], Shoya Matsuda[1)], Yoshiya Kasahara[1)], Satoko Nakamura[2)], Masahiro Kitahara[3)], Yoshizumi Miyoshi[2)], Iku Shinohara[4)]
([1]Kanazawa Univ.,[2]ISEE, Nagoya Univ.,[3]Tohoku Univ.,[4]ISAS/JAXA.,

Whistler-mode chorus waves are important plasma waves that contribute to the formation of terrestrial radiation belts. The Arase satellite aims to clarify particle acceleration processes in the inner magnetosphere. Particularly, the waveform capture (WFC), which is one of receivers of the plasma wave experiments (PWE) aboard Arase, measures electric and magnetic field waveforms. It is known that chorus waves are composed of fine-structures (also called “chorus elements”), whose frequency and intensity variations are important parameters which characterize the efficiency of the wave-particle interaction.

In this study, we propose a technique for quantitatively parameterizing the spectral features of chorus elements observed by the PWE. First of all, we perform fast Fourier transform analysis on the magnetic field waveform measured by the PWE/WFC. As a next step, we roughly extract chorus elements from the obtained power spectrum image using several image processing techniques (e.g., binarization, opening, and closing). Finally, we obtain a superposed spectral image (hereafter referred to as the ”averaged chorus element”) by shifting the original chorus elements’ spectra along time. We confirmed that this technique reduces the effects of noises and fluctuations in the original spectra. We successfully parameterized several features of chorus elements, such as frequency sweep rate, wave amplitude variation, and wave duration. We applied this method to the long-term plasma wave measurement data, and statistically analyzed the variation of these parameters along the orbit of Arase. In this presentation, we introduce several examples of the averaged chorus elements calculated from the waveform data observed by the PWE/WFC, and show the results of the quantitative parameterization of the averaged chorus elements.

地球周辺の宇宙空間には高エネルギー電子が充満した放射線帯が広がっており，その形成過程にはコーラスと呼ばれるプラズマ波動が寄与している．ジオスペース探査衛星「あらせ」は，その物理過程を観測的に明らかにすることを目的としており，搭載されたプラズマ波動・電場観測器（PWE）の波形捕捉受信器（WFC）によって，電磁界の精密波形観測が行われている．コーラス波動は，コーラスエレメントと呼ばれる微細なスペクトル構造で構成され，その周波数変化や強度変化は，波動粒子相互作用の効率を決定する重要なパラメータである．

本研究では，PWE によって観測された磁界波形データからコーラスエレメントを抽出し，それらの特徴を定量的に数値化する方法を提案する．まず，PWE/WFC によって観測された 8 秒間〜60 秒間の連続磁界波形データを高速フーリエ変換する．次に，得られたパワースペクトル画像からコーラスエレメントの概形を抽出する．最後に，抽出された複数のコーラスエレメントを時間方向にシフトして重ね合わせ，パワースペクトル密度の平均値を計算することで，観測イベントごとの平均的なコーラスエレメントのスペクトル（以下，平均描像）を求める．以上の処理によって，個々のコーラスエレメントの特徴の揺らぎや，雑音の影響等を低減する．得られた平均描像から，周波数変化率や振幅変化，継続時間などの特徴を数値化する．「あらせ」による長期観測データに対して本手法を適用することで，コーラスエレメントの特徴を定量的に統計解析することができる．本発表では，PWE/WFC で観測された実際の波形データからコーラスエレメントの平均描像を求め，コーラスエレメントの特徴を定量評価した結果を示す．

R006-P27
ポスター 1 ：11/4　PM1/PM2 （13:45-18:15）

あらせ衛星で観測されたホイスラーモード波の空間分布に関する統計解析

#林　京汰 [1)], 笠原　禎也 [1)], 松田　昇也 [1)], 土屋　史紀 [2)], 熊本　篤志 [2)], 北原　理弘 [2)], 松岡　彩子 [3)], 中村　紗都子 [4)], 三好　由純 [4)], 篠原　育 [5)],Malaspina　David[6)],Ripoll　Jean-Francois[7)]
[(1] 金沢大学,[(2] 東北大学,[(3] 京都大学,[(4] 名古屋大学,[(5]ISAS/JAXA,[(6]Colorado Boulder Univ.,[(7]CEA, DAM, DIF

Statistical analysis of the spatial distribution of whistler-mode waves observed by the Arase satellite

#Keita Hayashi[1)], Yoshiya Kasahara[1)], Shoya Matsuda[1)], Fuminori Tsuchiya[2)], Atsushi Kumamoto[2)], Masahiro Kitahara[2)], Ayako Matsuoka[3)], Satoko Nakamura[4)], Yoshizumi Miyoshi[4)], Iku Shinohara[5)], David Malaspina[6)], Jean-Francois Ripoll[7)]
[(1]Kanazawa Univ.,[(2]Tohoku Univ.,[(3]Kyoto Univ.,[(4]Nagoya Univ.,[(5]ISAS/JAXA,[(6]Colorado Boulder Univ.,[(7]CEA, DAM, DIF

In the inner magnetosphere, physical processes such as acceleration and loss of energetic particles are caused by various plasma waves. It is important to clarify the characteristics and spatial distribution of plasma waves in order to understand the plasma environment in the inner magnetosphere. Malaspina et al. (2016) revealed the spatial distribution of plasma wave activity around the magnetic equatorial region using the data observed by the Van Allen Probes for about 3 years. In the previous study, however, the analysis was limited within ± 20 degrees of magnetic latitude since the inclinations of the Van Allen Probes are about 10 degrees.

In this work, we analyze the plasma wave data observed by the Arase satellite for about 4 years to clarify the spatial distribution of electromagnetic field intensities of various plasma waves as functions of magnetic latitude and magnetic local time. As the inclination of the Arase is about 31 degrees, we are able to analyze the wider magnetic latitude range up to ± 40 degrees. We investigate the spatial distribution of plasma wave intensity using electromagnetic spectral data observed by PWE/OFA onboard the Arase satellite referring the orbit data of the Arase. In the current study, we focus on the frequency range below electron cyclotron frequency fc, and investigated the local time dependence and magnetic latitude dependence of chorus emissions.

In this presentation, we focus on the frequency range below the local electron cyclotron frequency and discuss the spatial distribution of the whistler-mode waves observed by Arase.

内部磁気圏では，様々なプラズマ波動によってプラズマ加速や消失といった物理過程が引き起こされており，内部磁気圏のプラズマ環境変動を理解するうえで，プラズマ波動の特徴や空間分布を把握することは重要である．Malaspina et al. (2016) は Van Allen probes 衛星で観測された約 3 年分の観測データを用いて磁気赤道面付近のプラズマ波動の空間分布を統計的に明らかにした．しかし，先行研究では衛星の軌道傾斜角が約 10 度であるため，磁気緯度± 20 度までの解析に留まっている．

これに対し，本研究ではあらせ衛星で観測された約 4 年分の観測データを用いて，内部磁気圏内で観測される様々なプラズマ波動の磁気緯度や磁気地方時に対する電磁界強度の依存性について明らかにする．あらせ衛星の軌道傾斜角は約 31 度であり，磁気緯度が± 40 度程度までの解析が可能である．解析にはあらせ衛星に搭載された PWE/OFA によって観測された電磁場スペクトルデータと，あらせ衛星の軌道を合わせて処理することでプラズマ波動の強度分布を調査した．

本講演では，特に電子サイクロトロン周波数以下の周波数帯域に着目して解析を行った結果を示し，ホイスラーモード波動の空間分布を統計的に議論する．

R006-P28
ポスター 1 ：11/4　PM1/PM2 （13:45-18:15）

あらせ衛星で観測されたコーラス波動に伴う電子フラックス変動現象の統計解析

#德田　晴哉 [1)], 頭師　孝拓 [2)], 栗田　怜 [3)], 小嶋　浩嗣 [4)], 笠原　慧 [5)], 横田　勝一郎 [6)], 笠原　禎也 [7)], 松田　昇也 [8)], 中村　紗都子 [9)], 熊本　篤志 [10)], 土屋　史紀 [11)], 松岡　彩子 [12)], 三好　由純 [13)], 篠原　育 [14)]
([1] 奈良高専,[2] 奈良高専,[3] 京都大学 生存研,[4] 京大・生存圏,[5] 東京大学,[6] 大阪大,[7] 金沢大,[8] 金沢大学,[9]IAR&ISEE,[10] 東北大・理・惑星プラズマ大気,[11] 東北大・理・惑星プラズマ大気,[12] 京都大学,[13] 名大 ISEE,[14] 宇宙研／宇宙機構

Investigation of deformation of electron pitch angle distributions associatedasso-ciated with chorus waves observed by Arase

#Seiya Tokuda[1)], Takahiro Zushi[2)], Satoshi Kurita[3)], Hirotsugu Kojima[4)], Satoshi Kasahara[5)], Shoichiro Yokota[6)], Yoshiya Kasahara[7)], Shoya Matsuda[8)], Satoko Nakamura[9)], Atsushi Kumamoto[10)], Fuminori Tsuchiya[11)], Ayako Matsuoka[12)], Yoshizumi Miyoshi[13)], Iku Shinohara[14)]
([1]NITNC,[2]National Institute of Technology , Nara Col,[3]RISH, Kyoto Univ.,[4]RISH, Kyoto Univ.,[5]The University of Tokyo,[6]Osaka Univ.,[7]Kanazawa Univ.,[8]Kanazawa Univ.,[9]IAR&ISEE,[10]Planet. Plasma Atmos. Res. Cent., Tohoku Univ.,[11]Planet. Plasma Atmos. Res. Cent., Tohoku Univ.,[12]Kyoto University,[13]ISEE, Nagoya Univ.,[14]ISAS/JAXA

In the Earth's inner magnetosphere, wave-particle interaction plays an important role in the acceleration and loss of energetic electrons. Kurita et al. (2018) reported a deformation of electron pitch angle distribution caused by the upper band chorus observed by the Arase satellite. In this event, it is shown that the deformation appears where effective wave-particle interaction is expected in the velocity space and the electron flux changes along the resonant ellipses. In this study, we analyzed the deformation of electron pitch angle distribution associated with chorus waves from the observation result of MEP-e and PWE onboard the Arase satellite in order to understand this phenomenon. We extracted events showing a sudden increase in electron flux in association with the activation of chorus waves from observation data of MEP-e and PWE. In the period from March 2017 to May 2018, 73 events were obtained. Many of the events were intensively observed from March 2017 to May 2017, the period when the Arase satellite was conducting observations on the morning side of the Earth's magnetosphere. Of the chorus waves of events obtained, about 70% had a peak of wave amplitude in the upper band chorus frequency range, like those reported in Kurita et al. (2018). On the other hand, about 30% of the events are found to have a peak of the wave amplitude in the lower band chorus frequency range. In this presentation, we will report the results of an analysis comparing the resonant energy calculated from chorus waves and the pitch angle and energy ranges where the increase in electron fluxes are observed.

地球内部磁気圏では、波動粒子相互作用によって高エネルギー電子が加速・消失することが知られている。Kurita et al. (2018) では、あらせ衛星で観測された upper band chorus によって、電子のピッチ角分布が変動する現象が報告されている。このイベントでは、速度空間において有効な波動粒子相互作用が期待される領域で、ピッチ角分布の変動が発生し、resonant ellipses に沿って電子フラックスが増加していることが示されている。本研究では、このような現象の更なる理解に向けて、あらせ衛星で取得された長期間のデータを用いて、コーラス波動に伴う電子フラックスの変動現象を解析した。あらせ衛星に搭載された中間エネルギー電子分析器 (MEP-e) 及びプラズマ波動・電場観測器 (PWE) の観測データから、コーラス波動に対応して電子フラックスが急激に変動を起こしているイベントを抽出した。その結果、2017 年 3 月から 2018 年 5 月までの期間において、73 件のイベントが得られた。また、このような現象は、あらせ衛星が地球の朝側で観測を行っていた期間である、2017 年 3 月から 2017 年 5 月に集中して観測されていることが分かった。得られたイベントのコーラス波動のうち、70% 程度は Kurita et al. (2018) で報告されたものと同様に upper band chorus の帯域に波動強度のピークをもつものであったが、30% 程度は lower band chorus の帯域に波動強度のピークをもつことが明らかになった。発表においては、コーラス波動から計算される共鳴エネルギーと電子のピッチ角分布を各イベントで比較し、解析した結果を報告する。

R006-P29
ポスター 1 ：11/4　PM1/PM2 （13:45-18:15）

#小路　真史 [1)], 三好　由純 [1)],Kistler　Lynn[2)], 浅村　和史 [3)], 笠羽　康正 [4)], 松岡　彩子 [5)], 笠原　禎也 [6)], 松田　昇也 [7)], 土屋　史紀 [8)], 熊本　篤志 [8)], 中村　紗都子 [9)], 田　采祐 [10)], 篠原　育 [11)]
([1 名大 ISEE,([2University of New Hampshire,([3 宇宙研,([4 東北大・理,([5 京都大学,([6 金沢大,([7 金沢大学,([8 東北大・理・惑星プラズマ大気,([9IAR&ISEE,([10 名大 ISEE 研,([11 宇宙研／宇宙機構

Statistical analyses on low energy ion heating by EMIC waves via WPIA: Arase observations

#Masafumi Shoji[1)], Yoshizumi Miyoshi[1)], Lynn Kistler[2)], Kazushi Asamura[3)], Yasumasa Kasaba[4)], Ayako Matsuoka[5)], Yoshiya Kasahara[6)], Shoya Matsuda[7)], Fuminori Tsuchiya[8)], Atsushi Kumamoto[8)], Satoko Nakamura[9)], ChaeWoo Jun[10)], Iku Shinohara[11)]
([1ISEE, Nagoya Univ.,([2University of New Hampshire,([3ISAS/JAXA,([4Tohoku Univ.,([5Kyoto University,([6Kanazawa Univ.,([7Kanazawa Univ.,([8Planet. Plasma Atmos. Res. Cent., Tohoku Univ.,([9IAR&ISEE,([10ISEE, Nagoya Univ.,([11ISAS/JAXA

Electromagnetic ion cyclotron (EMIC) waves are generated through the cyclotron wave-particle interaction, affecting the plasma environment in the magnetosphere. Heating of the ions by EMIC waves in the inner magnetosphere has also been investigated by spacecraft observations by comparing variations of ion distribution and waves. The energy transfer between the plasma waves and ions can be quantitatively evaluated by calculating the inner product between the wave electric field vector and the ion velocity vector, so-called WPIA (wave-particle interaction analysis). We apply the WPIA method to the Arase spacecraft data and investigate the spatial distribution of the positive qV・E region in the inner magnetosphere. Using 4.5 years data, we choose EMIC wave events associating ion flux enhancement between 10 eV/q to 100 eV/q of which the WPIA analysis can be applied for the necessary data sets observed by the Arase satellite. The occurrence peaks of the proton and helium heating events appear in the dayside and post noon regions. We classify the enhancements of low energy ion flux by their formation mechanism. Most of the ion flux enhancements are generated through the ion heating by the EMIC waves while some others are formed by the sloshing motion of the ions. We also perform test particle simulations to understand the ion heating process in the perpendicular direction by the parallel propagating EMIC waves.

R006-P30
ポスター 1 ：11/4　PM1/PM2 （13:45-18:15）

あらせ衛星観測に基づく地球内部磁気圏における VLF 帯人工電波の伝搬経路の可視化

#野田　周英 [1)], 栗田　怜 [2)], 小嶋　浩嗣 [2)], 笠原　禎也 [3)], 熊本　篤志 [5)], 土屋　史紀 [4)], 三好　由純 [6)], 篠原　育 [7)], 中村　紗都子 [8)], 北原　理弘 [9)]
([1] 京都大学,[2] 京大・生存圏,[3] 金沢大,[4] 東北大・理・惑星プラズマ大気,[5] 東北大・理・地球物理,[6] 名大 ISEE,[7] 宇宙研／宇宙機構,[8] 京大・理・地球惑星,[9] 東北大・理・地球物理

Visualization of the propagation path of signals from the VLF transmitters in the inner magnetosphere observed by Arase

#Shuei Noda[1)], Satoshi Kurita[2)], Hirotsugu Kojima[2)], Yoshiya Kasahara[3)], Atsushi Kumamoto[5)], Fuminori Tsuchiya[4)], Yoshizumi Miyoshi[6)], Iku Shinohara[7)], Satoko Nakamura[8)], Masahiro Kitahara[9)]
([1]Kyoto University,[2]RISH, Kyoto Univ.,[3]Kanazawa Univ.,[4]Planet. Plasma Atmos. Res. Cent., Tohoku Univ.,[5]Dept. Geophys, Tohoku Univ.,[6]ISEE, Nagoya Univ.,[7]ISAS/JAXA,[8]Dept. of Geophys., Kyoto Univ.,[9]Dept. Geophys., Grad. Sch. Sci., Tohoku Univ.

In the Earth's inner magnetosphere, various kinds of electromagnetic waves propagate and interact with charged particles trapped by the earth's magnetic fields. The interaction results in acceleration and loss of the trapped particles. It is known that man-made signals from the ground-based VLF transmitters can propagate into the magnetosphere through the ionosphere. Low altitude satellite measurements show that the VLF signals cause the precipitation loss of the radiation belt electrons into the atmosphere through pitch angle scattering. Thus it is important to understand the propagation characteristics of the signals from the VLF transmitters in the inner magnetosphere. For this purpose, we statistically investigated the VLF signals from the transmitters to identify the propagation path of these waves in the magnetosphere based on the plasma wave measurement performed by High Frequency Analyzer (HFA) onboard the Arase satellite. The statistical map of the VLF signal intensity was derived using the data obtained by HFA for three years. We successfully identified the geomagnetic longitude and altitude range where the VLF signals propagate in the magnetosphere and electric field intensities along the propagation paths. The propagation paths are the plausible location where pitch angle scattering by the VLF signals takes place. In the presentation, we show the propagation path and electric field intensities of the signals from the VLF transmitters in the inner magnetosphere.

地球内部磁気圏では様々な電磁波が伝搬しており、それらは地磁気に束縛された荷電粒子と相互作用を起こす。この相互作用により荷電粒子は加速、消失する。地上の VLF 送信局から放たれる電波は電離圏を通り抜けて磁気圏へと伝搬することは知られている。低高度を周回する科学衛星による観測では、この VLF 帯電波により放射線帯の電子がピッチ角散乱を受け、大気へ消失していることが示唆されている。このことから、VLF 送信局からの信号が、磁気圏内を伝搬する経路を明らかにすることは、放射線帯電子の消失を理解する上で重要な意味をもつ。この VLF 帯電波の磁気圏内における伝搬経路を明らかにするため、あらせ衛星に搭載されたプラズマ波動観測器から得られたデータを用いて、磁気圏内で観測される VLF 送信局の信号を統計的に調査した。この VLF 送信局の信号の強度の統計解析では、2017 年から 2019 年の 3 年間にわたるあらせ衛星の High Frequency Analyzer (HFA) による観測データを用いた。この統計解析により、VLF 送信局の信号が磁気圏内を伝搬する経路と、その経路沿いの電界強度を明らかにすることができた。VLF 送信局の信号によって放射線帯電子のピッチ角散乱が引き起こされるのは、この伝搬経路上であると考えられる。本発表では、VLF 送信局が磁気圏内を伝搬する経路をそれぞれの送信局に対して示す。

R006-P31
ポスター１：11/4　PM1/PM2（13:45-18:15）

#プテリ　デシプルナミシンギー [1)], 笠原　禎也 [1)], 松田　昇也 [1)], 土屋　史紀 [2)], 熊本　篤志 [2)], 松岡　彩子 [3)]
[(1] 金沢大学,[(2] 東北大学,[(3] 京都大学

Electron density profile approximation technique by using lightning whistler propagation characteristic

#Desy Purnami Singgih Putri[1)], Yoshiya Kasahara[1)], Shoya Matsuda[1)], Fuminori Tsuchiya[2)], Atsushi Kumamoto[2)], Ayako Matsuoka[3)]
[(1]Kanazawa University,[(2]Tohoku University,[(3]Kyoto University

A lightning whistler wave is an electromagnetic plasma wave originated by the lightning flush in the VLF. It propagates through the ionosphere into the Earth's magnetosphere as a whistler mode wave. It generally propagates from the southern hemisphere along the Earth's magnetic field lines to the northern hemisphere or vice-versa. At the source point, it is simultaneously emitted in a wide frequency range, but the propagation velocity is larger in the higher frequency range and becomes slower in the lower frequency resulting in a dispersive spectrum property. The propagation velocity depends on the electron density along the propagation path. Thus the dispersive property strongly depends on the length of the propagation path and the total electron content along the path. To obtain the lightning stroke location, we refer to the world wide lightning location network (WWLLN). It locates lightning globally using sparsely distributed VLF detection stations[1]. Due to the propagation characteristics of the lightning whistlers, it is possible to estimate a density profile along the propagation path. We further expect to derive a global density profile accumulating the lightning whistler events. In the present study, we propose a technique to reconstruct the global density profile using ray tracing by scrutinizing the dispersion analysis of a lightning whistler. Ray tracing program numerically calculates the propagation path of whistler mode waves calculating the refractive index referring to the background magnetic field vector and the electron density[2]. In other words, we expect a reliable propagation path that gives an appropriate magnetic field and electron density models in the ray tracing program.

The international geomagnetic reference filed (IGRF-12) model and the Tsyganenko (TS05) were used to approximate the background magnetic field. The global density profile was generated first separately from the main ray tracing program using the global core plasma model (GCPM), and the international reference ionosphere (IRI). GCPM provides derived core plasma density as a function of geomagnetic and solar conditions. Plasmasphere observed by Gallagher et al. only extends inward until ˜2RE , then IRI can be used up to ˜600 km[3]. The ray paths of whistler mode signals calculation in the frequency range 1-10 kHz initiating from a region near the candidate lightning stroke from the WWLLN database (around ˜1000 km from the source) and try to reconstruct the spectrum shape of the lightning whistler detected by the spacecraft orbiting in the inner magnetosphere. Therefore, we also approximate the region of the lightning whistler source. In this work, we propose modifications in the generated density profile model that satisfies the lightning dispersion characteristics measured by the satellites in the magnetosphere, including delay time and dispersion direction. First, we showed the straightforward modification method by multiplying the global density profile with a constant. Then the modification uses a linear function: keep the density profile on the lower altitude and change the higher one.

We applied our method to a lightning whistler event on August 14, 2017, measured by PWE/WFC aboard the Arase satellite and analyzed the dispersion of the observed lightning whistler. We show how the density modification affects the ray path dispersion characteristics. The first modification can approach the appropriate dispersion, but the propagation time is slower than the observation. The second modification can better approximate the propagation time and get a good agreement in the direction. In the presentation, we will introduce our method and tentative results applied to the observation data.

R006-P32
ポスター１：11/4　PM1/PM2（13:45-18:15）

脈動オーロラに伴う高エネルギー電子の中層大気への降り込み：あらせ衛星-EISCAT 同時観測

#尾林　佑哉[1)], 三好　由純[1)], 高橋　一輝[1)], 中村　紗都子[2)], 細川　敬祐[3)], 小川　泰信[4)], 齋藤　慎司[5)], 大山　伸一郎[1)], 浅村　和史[6)], 栗田　怜[7)], 笠原　禎也[8)], 松田　昇也[8)], 土屋　史紀[9)], 熊本　篤志[9)], 松岡　彩子[10)], 篠原　育[11)]
([1] 名大 ISEE,[2]IAR&ISEE,[3] 電通大,[4] 極地研,[5] 情報通信研究機構,[6] 宇宙研,[7] 京都大学 生存研,[8] 金沢大,[9] 東北大・理・惑星プラズマ大気,[10] 京都大,[11] 宇宙研／宇宙機構,[12] 東北大・理・惑星プラズマ大気,[13] 京都大,[14] 宇宙研／宇宙機構

Precipitation of high-energy electrons into the mesosphere accompanying pulsating aurorae: Arase and EISCAT conjugate observation

#Yuya Obayashi[1)], Yoshizumi Miyoshi[1)], Kazuteru Takahashi[1)], Satoko Nakamura[2)], Keisuke Hosokawa[3)], Yasunobu Ogawa[4)], Shinji Saito[5)], Shin ichiro Oyama[1)], Kazushi Asamura[6)], Satoshi Kurita[7)], Yoshiya Kasahara[8)], Shoya Matsuda[8)], Fuminori Tsuchiya[9)], Atsushi Kumamoto[9)], Ayako Matsuoka[10)], Iku Shinohara[11)]
([1]ISEE, Nagoya Univ.,[2]IAR&ISEE,[3]UEC,[4]NIPR,[5]NICT,[6]ISAS/JAXA,[7]RISH, Kyoto Univ.,[8]Kanazawa Univ.,[9]Planet. Plasma Atmos. Res. Cent., Tohoku Univ.,[10]Kyoto Univ.,[11]ISAS/JAXA,[12]Planet. Plasma Atmos. Res. Cent., Tohoku Univ.,[13]Kyoto Univ.,[14]ISAS/JAXA

Pulsating aurora (PsA) is caused by intermittent precipitations of 1 to few tens of keV from the magnetosphere. The PsA is caused by the interaction of electrons with chorus waves near the equator. On the other hand, recent studies have shown that sub-/relativistic electrons are scattered by chorus waves that propagate to high latitudes and electrons precipitate into the mesosphere at an altitude of 60-80 km (Miyoshi+ [2015, 2020, 2021]). In this study, we investigate the energetic electron precipitation during pulsating auroral events that occurred at Tromso from 02:00 to 06:00 UT on March 12, 2022, using data from the Arase satellite and EISCAT radar. At that time, the Arase satellite observed intense chorus waves near the equator, and strong precipitations into the mesosphere was observed with the EISCAT radar. Using the plasma wave data observed by Arase, the pitch angle scattering coefficient was derived, which suggests that the energy range of precipitating electrons is mostly around 10 keV. The EISCAT observations showed intense ionization below an altitude of 80 km, indicating that energetic electrons of several hundred keV were precipitated along with electrons of 10 keV level. It is unlikely that such high-energy electron precipitation can be generated by wave-particle interactions at the equator, and it is expected that the energetic electrons are scattered at the off-equator, as shown by Miyoshi+[2020].

脈動オーロラ（PsA）とは、宇宙空間から 1~数十 keV のエネルギーを持つ電子が降りこみ、高度 100km 付近の大気が数秒から数十秒の周期で明滅する現象である。この脈動オーロラは、赤道面におけるコーラス波と電子の相互作用によって生じることが明らかになっている。一方で、これと同時に高緯度へ伝搬したコーラス波が数 MeV の高エネルギー電子を加速させ、高度 60~80km の中間圏に降りこませていることが明らかになってきている（Miyoshi+[2015、2020、2021]。この脈動オーロラ時の高エネルギー電子降りこみに関して、本研究では、2022 年 03 月 12 日の 02:00-06:00UT、Tromsøにて発生したイベントについて、あらせ衛星と EISCAT の観測データを用いて調査を行った。このとき、あらせ衛星は赤道面付近で活発なコーラスを観測し、また EISCAT において中間圏への強い降り込みが観測されていた。あらせ衛星が観測したプラズマ波動データから、ピッチ角散乱係数を導出したところ、約 10keV 付近の電子の降りこみを引き起こすことができると判明した。一方、EISCAT の観測からは、高度 80km 以下でも顕著な降り込みが観測され、数 100keV のエネルギーを持つ高エネルギー電子も同時に降りこんでいたことが示された。このような高エネルギーの電子の降りこみは、赤道面での波動粒子相互作用だけでは説明することができず、Miyoshi+[2020] が示したようなコーラスが高緯度に伝搬することによって引き起こされた可能性が考えられる。

R006-P33
ポスター 1 ：11/4　PM1/PM2 （13:45-18:15）

#岩瀬　智哉 [1)], 寺本　万里子 [1)], 片岡　龍峰 [2)], 三好　由純 [3)], 笠原　禎也 [4)], 松岡　彩子 [5)], 鳥居　祥二 [6)], 尾崎　光紀 [4)], 松田　昇也 [4)], 中村　紗都子 [3)], 北原　理弘 [8)], 小路　真史 [3)], 今城　峻 [5)], 篠原　育 [7)], 三宅　晶子 [9)], 中平　聡志 [7)]
([1] 九工大,[2] 極地研,[3] 名大 ISEE,[4] 金沢大,[5] 京都大学,[6] 早稲田大学理工総研,[7] 宇宙研,[8] 東北大・理・惑星プラズマ大気,[9] 茨城高専

Relativistic electron precipitation and plasma waves observed by the International Space Station and the Arase satellite

#Tomoya Iwase[1)], Mariko Teramoto[1)], Ryuho Kataoka[2)], Yoshizumi Miyoshi[3)], Yoshiya Kasahara[4)], Ayako Matsuoka[5)], Shoji Torii[6)], Mitsunori Ozaki[4)], Shoya Matsuda[4)], Satoko Nakamura[3)], Masahiro Kitahara[8)], Masafumi Shoji[3)], Shun Imajo[5)], Iku Shinohara[7)], Shoko Miyake[9)], Satoshi Nakahira[7)]
([1]Kyutech,[2]NIPR,[3]ISEE, Nagoya Univ.,[4]Kanazawa Univ.,[5]Kyoto University,[6]WISE, Waseda U.,[7]ISAS/JAXA,[8]Planet. Plasma Atmos. Res. Cent., Tohoku Univ.,[9]NIT(KOSEN), Ibaraki College

Relativistic Electron Precipitation (REP) is a phenomenon of MeV electron precipitation into the atmosphere from the outer radiation belt. Previous studies (e.g., Kataoka et al., 2016) suggest that electromagnetic ion cyclotron (EMIC) waves cause REP during magnetic storms when they resonate with and scatter energetic electrons in the radiation belt. Meanwhile, Kataoka et al. (2020) have reported three different types of REP events associated with different types of plasma waves (chorus, electrostatic whistler, and EMIC waves). While different types of plasma waves can play important roles as drivers of REP, the relative importance between the different types of plasma waves and REP events have not been statistically clarified. In this study, we identified plasma waves which were associated with many REP events from conjugate observations between the International Space Station (ISS) and the Arase satellite. First, we identified REP events from data observed by CALorimetric Electron Telescope (CALET) /Charge Detector (CHD) onboard ISS in the period from March 2017 to December 2021. Then, we detected 31 REP-related conjunction events, in which the ionospheric footprints of Arase were close to the ISS locations when the CALET/ISS observed REP events. Finally, we identified the plasma waves by visual inspection from the REP-related conjunction events, using the electric and magnetic field spectra data observed by Plasma Wave Experiment (PWE)/Onboard Frequency Analyzer (OFA) and Magnetic Field Experiment (MGF) onboard the Arase satellite. We identified chorus waves in 9 events out of the 31 conjunction REP events dominantly in the post-midnight sector (23-03MLT) near the magnetic equator. The second largest population is the 7 REP events associated with electrostatic whistler waves, which were mostly observed in the pre-midnight sector (20-24MLT). The last 3 events were associated with EMIC waves. Besides these waves, hiss waves were also seen in 7 events. These results suggest that various types of plasma waves other than EMIC waves can drive REP events.